CE 16/94

LIBRARY
UNIVERSITY OF MORATUWA, SRI LANKA
MORATUWA

LB/DON/72/2015
DCE 23195

GEOSYNTHETIC REINFORCED PILE SUPPORTED EMBANKMENTS

Jayasundara Mudiyanselage Pradeep Kumara

(09/8919)

Thesis submitted in partial fulfillment of the requirements for the degree of Master of Engineering in Structural Engineering Design

624"15"
624.01(043)

Department of Civil Engineering

University of Moratuwa

Sri Lanka

July 2015

University of Moratuwa
109272

109272

109272
+
CD-ROM

TH2921

Declaration

"I declare that this is my own work and this thesis does not incorporate without acknowledgement any material previously submitted for a Degree or Diploma in any other University or institute of higher learning and to the best of my knowledge and belief it does not contain any material previously published or written by another person except where the acknowledgement is made in the text.

Also, I hereby grant to University of Moratuwa the non-exclusive right to reproduce and distribute my thesis, in whole or in part in print, electronic or other medium. I retain the right to use this content in whole or part in future works (such as articles or books)."

Signature: … ***UOM Verified Signature*** Date: 17/07/2015

The above candidate has carried out research for the Masters thesis under my supervision.

UOM Verified Signature

Signature of the supervisor: ……/……/…… Date: 17/07/2015

Abstract of Thesis

The design of embankments on weak foundation soils is a challenge to the geotechnical Engineer. There are several issues related to bearing capacity failures, intolerable settlements and slope instability that need to be addressed. The piled embankments with the inclusion of a geosynthetic layer have proved to be one of the economic and effective techniques to handle such problems.

The inclusion of the geosynthetic reinforcement eliminates the need for inclined piles used in conventional piled embankments for resisting large lateral pressures. The geosynthetic layer enhances the load transfer mechanism and considerably minimizes the differential and maximum settlements.

This study attempts to analyze the various methods available today for the design of these structures. A numerical study is carried out. The effects of certain factors like pile modulus, stiffness of the geosynthetic reinforcement, height of the embankment, effect of the soil layer directly below the geogrid which are not considered by other available methods are studied using a finite element program – Plaxis 2D.

The results from two design methods are evaluated and compared with the results from Plaxis. It is found that numerical analysis was able to address many factors that were neglected by all the other available methods. It was also found to be more reliable than currently used methods. The German Draft Standard (EBGEO) approaches the numerical Plaxis calculations better than British Standard 8006

Acknowledgements

I would like to acknowledge the Department of Civil Engineering of University of Moratuwa, to provide me the opportunity for studying the Master of Engineering Degree Program in Structural Engineering.

I would like to express my sincere appreciation to all the staff members of this M Eng program for their encouragement and excellent guidance to complete this work in successful manner.

I am very grateful to my supervisors Professor M.T.R.Jayasinghe and Dr. L.I.N.De Silva of University of Moratuwa and Dr. Asiri Karunawardena, Director General of NBRO for their valuable support, guidance and encouragements.

Furthermore I like to express my sincere thanks and appreciation to Eng N Rupasinghe, the chairman of the Central Engineering Consultancy Bureau (CECB) for granting permission to carry out my Master of Engineering Degree Program.

Finally, I would like to extend my grateful thanks and appreciation to all who supported time to time, to achieve my goals.

TABLE OF CONTENTS

Page

DECLARATION i
ABSTRACT ii
ACKNOWLEDGMENTS iii

TABLE OF CONTENTS iv
List of Figures vi
List of Tables ix

1. INTRODUCTION 1
   1.1. Background 1
   1.2. Significance of research Work. 4
   1.3. Aim of This M Eng Thesis. 4
   1.4. Statement of the Problem 5
   1.5. Methodology. 5
2. LITERATURE REVIEW 7
   2.1. Theory of Soil Arching 7
      2.1.1. Stress Concentration Ratio 10
   2.2. Design of Geosynthetic Reinforcement 11
      2.2.1. Stress Reduction Factor 12
      2.2.2. Tension in Reinforcement 14
      2.2.3. Soil Resistance 16
      2.2.4. Tension in Reinforcement due to Lateral Sliding 17
      2.2.5. Limits of Strain in Reinforcement 18
   2.3. Pile Design 18
      2.3.1. Pile Group Extent 19
      2.3.2. Pile Cap Punching Capacity 20
   2.4. Lateral Movement of Embankment 20
   2.5. Slope Stability 22
      2.5.1. BS8006 22
      2.5.2. Modified Boundary Element Method 23
   2.6. Settlements 31
3. VALIDATION OF NUMERICAL ANALYSIS 33
   3.1. Methods for estimation of Axial bearing capacity 33
   3.2. Case Study 35
   3.3. Numerical Analaysis 37
   3.4. Methods for estimation of tensile capacity of Geo Reinforcement 41
   3.5. Validation 42

4. THE BRITISH STANDARD & THE GERMAN STANDARD (EBGEO).....43
4.1. BS 8006.....43
4.2. The load transferred directly to the pile cap (*P'c:* Marston).....44
4.3. German Draft Standard (EBGEO).....46
4.4. Conclusions.....47
5. MODELING IN PLAXIS.....49
5.1. PLAXIS.....49
5.2. Numerical Modeling of the Geosynthetic Reinforced Pile Supported Embankments.....49
5.3. The Purpose of this Study.....49
5.4. Cases.....49
5.4.1. How to choose the cases.....50
5.4.2. Study.....50
5.4.3. Varieties Studies had to be carried out.....50
5.5. Axisymmetric Model.....51
5.5.1. Embankment Soil.....52
5.5.2. Pile Concreting.....53
5.5.3. Foundation Soil.....54
5.6. Plain Strain Model.....55
5.6.1. Embankment Soil.....56
5.6.2. Pile Concreting.....56
5.6.3. Foundation Soil.....57
5.7. Methodology.....59
5.7.1. The phases of construction.....62
5.8. Results and Comparison.....62
6. COMPARISON OF VARIOUS METHODS.....63
6.1. Introduction.....63
6.2. Two Cases.....63
6.2.1. Calculations with EBGEO.....63
6.2.2. Calculations with Plaxis.....63
6.2.3. Calculations with BS8006.....64
6.2.4. Case 1 Thin Embankment.....65
6.2.5. Case2 Thick Embankment.....71
6.3. Analysis.....79
6.4. Discussion.....81
7. ANALYSIS OF OUTCOMES FROM PLAIN STRAIN METHOD.....86
7.1. Introduction.....86
7.2. Output from Plain strain analysis.....87
7.2.1. Effect of Change of Pile sizes.....87
7.2.2. Effect of Change of Pile spacing.....90
7.2.3. Effect of Change of Traffic Load over the Embankment.....93
7.2.4. Effect of Change of Embankment Height.....96
7.2.5. Effect of Change of Spacing between Geo Reinforcement layers.....99
7.3. Discussion.....102

8. CONCLUSIONS AND RECOMMENDATIONS.....106
8.1. Conclusions.....106
8.2. Recommendations.....107

9. APPENDIX 1 109
9.1. Calculation Example for BS8006 (Friction Pile and End Bearing Pile) and EBGEO 109
9.2. BS8006-Friction Pile (KLEEF) 110
9.2.1. Specimen Calculation 110
9.3. BS8006-End Bearing (STUIT) 114
9.3.1. Specimen Calculation 114
9.4. EBGEO Specimen Calculation 116
9.4.1. Specimen Calculation 116
9.5. PLAXIS 8.2 120
9.5.1. Specimen Calculation 120
10. APPENDIX 2 – STRUCTURAL DESIGN OF A PILE 121
10.1. Code Requirements 121
11. List of References 127

List of Figures

Figure 1.1 Conventional pile-supported systems 2
Figure 1.2 Piled Embankment with Concrete Slab (CPS) 2
Figure 1.3 Pile embankment with a geogrid reinforcement platform 3
Figure 2.1 The soil mass overlying a potential void 7
Figure 2.2 The formation of a true arch (Void under soil mass) 8
Figure 2.3 Soil mass collapses to form an inverted arch 8
Figure 2.4 Load Transfer Mechanism 9
Figure 2.5 Unit Cell Utilization 12
Figure 2.6: Tensile force in the reinforcement under embankment of medium dense soil 16
Figure 2.7 Lateral Sliding stability at the interface of fill and reinforcement 18
Figure 2.8 Outer limit of pile caps 20
Figure 2.9 Variable required for the analysis of GRPS embankments 23
Figure 2.10 Effect of pile position on the homogenous slope 25
Figure 2.11 Effect of pile diameter on the homogenous slope 25
Figure 2.12 Effect of pile spacing on homogenous slope 26
Figure 2.13 Effect of pile spacing on homogenous slope 26
Figure 2.14 Effect of pile position on two –layer slope 27
Figure 2.15 Effect of pile diameter on a two –layer slope 28
Figure 2.16 Effect of pile spacing on the two layer slope 28
Figure 2.17 Effect of pile soil limiting pressure multiplier on the two-layer 29
Figure 2.18 Force on slope without piles 30
Figure 2.19 Forces acting on a slope reinforced with piles 31
Figure 3.1 Static load test 34
Figure 3.2 PDA test 34
Figure 3.3 Soil profile according to site investigation 35
Figure 3.4 Load-displacement curve of static load test 36
Figure 3.5 Global geometry of the reference pile 38
Figure 3.6 Deformed mesh of the reference pile 39
Figure 3.7 Load-displacement behavior of reference pile under empirical load (Soil body collapsing) 40
Figure 3.8 Load-displacement curve for ultimate load obtained from last analysis 40

Figure 3.9 Estimated axial capacity (kN) using different methods.....41
Figure 4.1 All design models for piled embankments divide the load into portions 45
Figure 4.2
Figure 4.3 Left: realistic values for *a/H* give very similar values for *p'c/σ'v*. Right: for extreme values of a/H (thin embankments), the ratio *p'c/ σ'v* does not approach the expected value of 1.0.....46
Figure 5.1 Case 1 Thin Embankment Case 2 Thick Embankment 50
Figure 5.2 Axi-Symmetric Finite Element Model.....60
Figure 5.3 Axi-Symmetric Finite Element Model Connectivity 60
Figure 5.4 Plain Strain Finite Element model 61
Figure 5.5 Plain Strain Finite Element model – Connectivities 61
Figure 6.1 Thin Embankment.....65
Figure 6.2 (Plaxis model diagram) h=1.25m, pile diameter =0.5m 65
Figure 6.3 The influence of variation of the embankment height on the load on the pile head.....66
Figure 6.4 The influence of variation of the embankment height on the tensile force on the Geogrid.....66
Figure 6.5 The influence of variation of the centre to centre distance on the load on the pile head. 67
Figure 6.6 The influence of variation of the centre to centre distance on the tensile force on the Geogrid.....68
Figure 6.7 The influence of variation of the pile head area on the load on the pile head 68
Figure 6.8 The influence of variation of the pile head area on the tensile force on the Geogrid.....69
Figure 6.9 The influence of variation of the internal friction angle on the load on the pile head.....69
Figure 6.10 The influence of variation of the internal friction angle on the tensile force on the geogrid.....70
Figure 6.11 The influence of variation of the surcharge load on the load on the pile head....70
Figure 6.12 The influence of variation of the surcharge load on the tensile force on the geogrid.....71
Figure 6.13 Thick Embankment.....71
Figure 6.14(Plaxis model diagram) h=6.0m, pile diameter =0.3m.....72
Figure 6.15 The influence of variation of the embankment height on the load on the pile head.....72
Figure 6.16 The influence of variation of the embankment height on the tensile force on the Geogrid.....73
Figure 6.17 The influence of variation of the centre to centre distance on the load on the pile head 74
Figure 6.18 The influence of variation of the centre to centre distance on the tensile force on the Geogrid.....74
Figure 6.19 The influence of variation of the pile head area on the load on the pile head.....75
Figure 6.20 The influence of variation of the pile head area on the tensile force on the Geogrid.....75
Figure 6.21 The influence of variation of the internal friction angle on the load on the pile head.....76
Figure 6.22 The influence of variation of the internal friction angle on the tensile force on the geogrid.....76
Figure 6.23 The influence of variation of the surcharge load on the load on the pile head....77
Figure 6.24 The influence of variation of the surcharge load on the tensile force on the geogrid.....78

Figure 6.25 Arching: the vertical stress in the soil at point *A* is less than ($\gamma H + p$).....83
Figure 6.26 Incomplete arching: the height of the fill, H, is smaller than the critical height H_c. For this case, part of the surface load *p* is not transferred to the pile caps. Therefore, the displacement of point A can be larger than in Figure 3.2..... 84
Figure 7.1 Geometry of Embankment used for Plaxis 2D – Plain strain model analysis.....86
Figure 7.2 The influence of variation of pile size on Axial load on piles.....87
Figure 7.3 The influence of variation of pile size on Maximum Shear force on piles.....87
Figure 7.4 The influence of variation of pile size on Maximum Bending Moment on piles .88
Figure 7.5. The influence of variation of pile size on Tension in Geogrid.....88
Figure 7.6. The influence of variation of pile size on Total deformation of Embankment profile.....89
Figure 7.7. The influence of variation of pile size on Total deformation of Embankment profile.....89
Figure 7.8. The influence of variation of pile size on Axial load on piles.....90
Figure 7.9. The influence of variation of pile size on Shear Force on piles.....90
Figure 7.10. The influence of variation of pile spacing on Maximum Bending Moment on piles 91
Figure 7.11. The influence of variation of pile spacing on Tension in Geogrid.....91
Figure 7.12. The influence of variation of pile spacing on Total deformation of Embankment profile.....92
Figure 7.13. The influence of variation of pile spacing on Factor of Safety of Embankment profile.....92
Figure 7.14. The influence of variation of Traffic load on Axial load on piles.....93
Figure 7.15. The influence of variation of Traffic load on Maximum Shear Force on piles..93
Figure 7.16. The influence of variation of Traffic load on Maximum Bending Moment on piles.....94
Figure 7.17. The influence of variation of Traffic load on Tension in Geogrid.....94
Figure 7.18. The influence of variation of Traffic load on Total deformation of Embankment profile 95
Figure 7.19. The influence of variation of Traffic load on Factor of Safety of Embankment profile.....95
Figure 7.20. The influence of variation of Embankment Height on Axial load on piles.....96
Figure 7.21. The influence of variation of Embankment Height on Maximum Shear Force on piles.....96
Figure 7.22. The influence of variation of Embankment Height on Maximum Bending Moment on piles.....97
Figure 7.23 The influence of variation of Embankment Height on Tension in Geogrid.....97
Figure 7.24 The influence of variation of Embankment height on Total deformation of Embankment profile.....98
Figure 7.25. The influence of variation of Embankment Height on Factor of Safety of Embankment profile.....98
Figure 7.26. The influence of variation of spacing between GR Layers on Axial load on piles.....99
Figure 7.27. The influence of variation of spacing between GR Layers on Maximum Shear Force on piles.....99
Figure 7.28. The influence of variation of spacing between GR on Maximum Bending Moment on piles.....100
Figure 7.29. The influence of variation of Space between GRL on Tension in GRL.....100

Figure 7.30. The influence of variation of space between GRL on Total deformation of Embankment profile.....101
Figure 7.31. The influence of variation of space between GRL on Factor of Safety of Embankment.....101
Figure 7.32. The failure mode for 40kN/m^2 traffic load.....103
Figure 7.33. The failure modes of embankments having different GR spacing.....104
Figure 9.1. Case 1 & 2 Thin and thick Embankment.....109

List of Tables

Page

Table 3.1 Axial capacity of reference pile based on analytical and empirical methods styles.....35
Table 3.2 Pile capacity based on PDA.....36
Table 3.3 Material properties and input parameters.....37
Table 3.4 Tensile force on Geo Reinforcement using different calculation methods.....42

Table 5-1 Materials Properties Embankment Soil 52
Table 5-2 Materials Properties Concrete (Pile).....53
Table 5-3 Materials Properties Foundation Soil. 54
Table 5-4 Input variation used for Plaxis models. 55
Table 5-5 Materials Properties Embankment Soil (for plain strain model).....56
Table 5-6 Materials Properties of Piles with the variation of pile size (for plain strain model) 57
Table 5-7 Materials Properties of Piles with the variation of pile spacing (for plain strain model) 57
Table 5-8 Materials Properties of Peat (for plain strain model) 58
Table 5-9 Materials Properties of Sand (for plain strain model) 58
Table 5-10 Materials Properties of Dense Sand (for plain strain model) 59
Table 6-1 Analysis of the results-case1.....79
Table 6-2 Analysis of results – case2.....80
Table 9-1 BS8006-End Bearing File (British Standard) Specimen Calculation.....110
Table 9-2 Calculation Table1 BS8006 End Bearing Pile.....112
Table 9-3 Calculation Table2 BS8006 End Bearing Pile.....112
Table 9-4 Result Bs8006 End Bearing Pile.....113
Table 9-5 Calculation Table1 Friction Pile 114
Table 9-6 Calculation Table2 Friction Pile 114
Table 9-7 Results Friction Pile.....115
Table 9-8 German Draft Standard (EBGEO) Calculation. 117
Table 9-9 EBGEO Calculation Tensile Force on the Geogrid Results.-EBGEO 118
Table 9-10 Results German Draft Standard (EBGEO) 119
Table 9-11 Results Plaxis 8.2.....120
Table 10-1 Summary of Code requirements.....123
Table 10-2 Summary of Current UK Design Codes.....123

1. INTRODUCTION

1.1. Background

With the rapid development of the economy, the demand for infrastructures for the community was increased rapidly. Due to the scarcity of land for such development, Engineers started to utilize the unusable marshy lands and other weak grounds using various construction techniques. The main factors that had to be concern for the design over such weak foundation soils, bearing capacity, slope stability, lateral pressures and movements and differential settlement etc. the following are the available techniques to address these issues.

1. Preloading
2. Deep mixing columns
3. Stone columns
4. Use of light weight fill
5. Soil replacement
6. Pilling with solid cover slab

Geosynthetic reinforced pile supported (GRPS) embankments, the subject of this thesis is a method which is closer to the last method of above, but much economical and very successful.

Out from the above methods, first five techniques required specialized skills and consume longer construction period. The 6th method, the conventional pile-supported system (CPS) required larger pile caps and closely spaced piles. This method is also required inclined pile to assist the lateral loads. These are required to avoid differential settlement and to transfer the loads to stable soil strata. The pile embankment with a concrete slab need a larger amount of reinforcement steel making itself uneconomical solution.

Geotechnical Engineers found that it is much economical to replace this concrete slab with Geosynthetic, which have high tensile strength. Use of several Geosynthetic layers avoid differential settlement and provide resistance to lateral pressure preventing the necessity of inclined piles of the edge of the embankment. This property of the Geosynthetic can be used to minimize the differential settlement, increase the bearing capacity and slope stability when use in embankment construction over soft

soil. This GRPS system (Figure 1.3) has a geosynthetic reinforced platform or mat which increases the efficiency of transferring the load from the soil to the piles without giving rise to deflections between the pile caps.

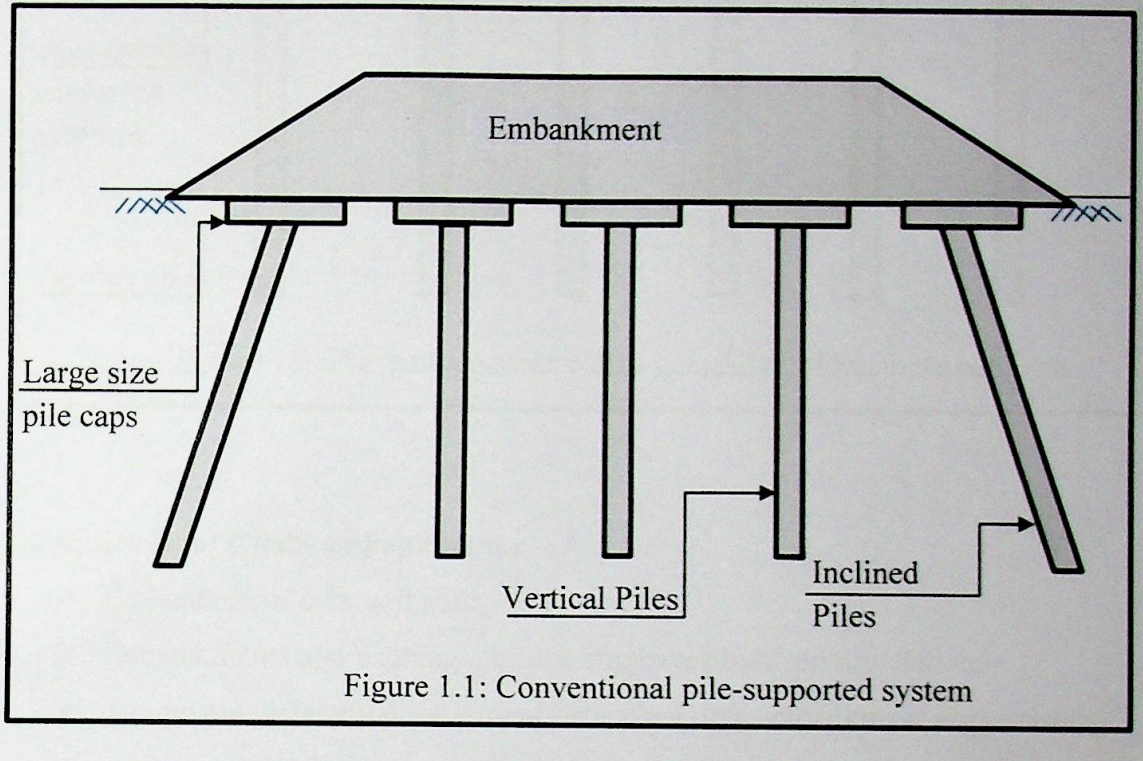

Figure 1.1: Conventional pile-supported system

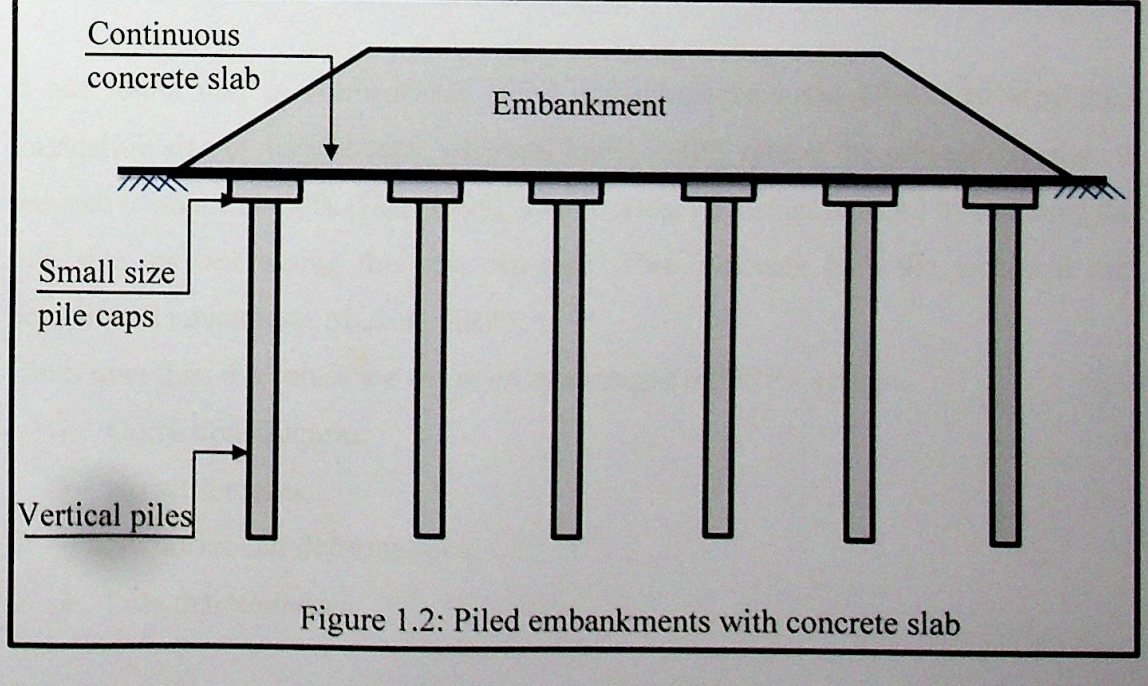

Figure 1.2: Piled embankments with concrete slab

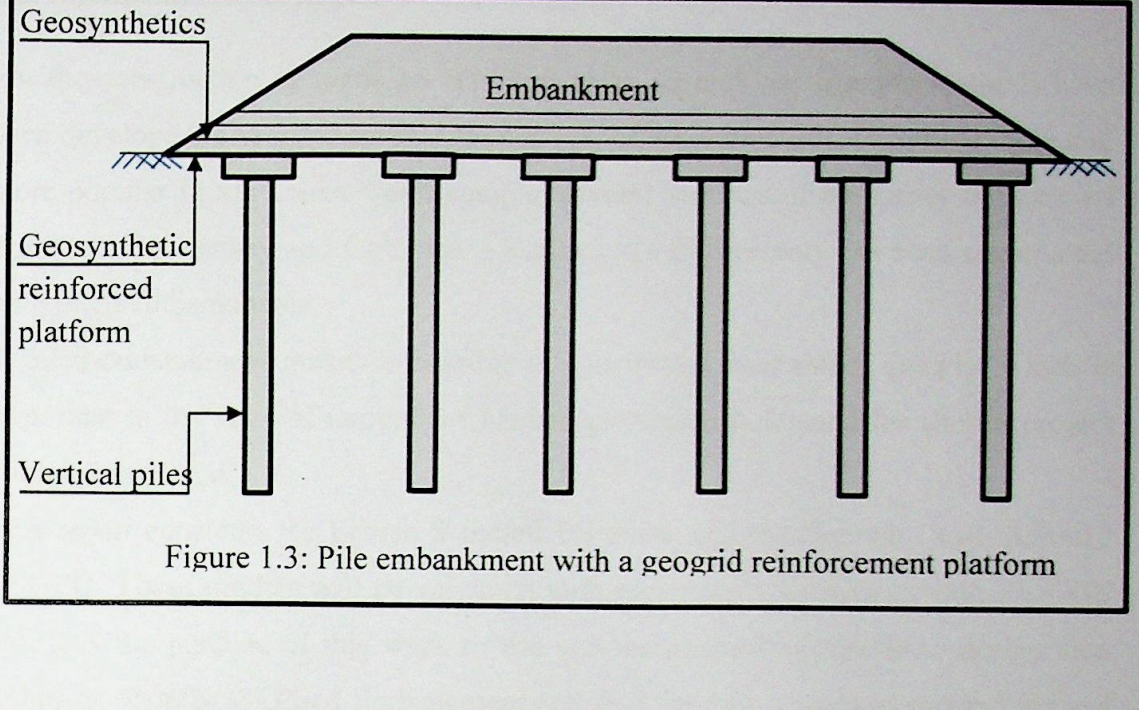

Figure 1.3: Pile embankment with a geogrid reinforcement platform

Applications of GRPS embankments:

- Embankments over soft soils,
- Embankments approaching a bridge supported by deep foundations,
- To prevent differential settlement between a new embankment near existing
- structures or existing embankment where settlement has ceased,
- Sub-grade improvement.

It has found that in conventional piled embankments cover 60% - 70% of total foundation area by its pile caps, whereas, in the GRPS system the percent coverage is reduced to about 10-20% (Han, 1999). The cost can be further reduced by reducing the pile size and increasing the pile cap size. This indicates both the technical and economical advantages of using GRPS.

Other than this, the below are the main advantages of GRPS system.

- Quick construction,
- No settlements,
- No horizontal deformations,
- Less maintenances.

UNIVERSITY OF MORATUWA
LIBRARY
SRI LANKA

1.2. Significance of research Work.

For the construction of roads on very soft soils, several construction methods have been developed. The piled embankment is one of these methods, becoming more and more popular in Sri Lanka. For Example, several sections of the newly constructed Southern Expressway and Colombo – Katunayaka Expressway has been constructed with piled embankments.

A piled embankment makes it possible to construct a road rather quickly, which is important in the view of current Sri Lankan government demand for shorter project completion period.

This report considers the British Standard BS 8006, and the German Draft-Standard EBGEO. These models will be validated with numerical calculations with PLAXIS 2D. It is the purpose of this work to use various methods available to design Geo Synthetic Reinforced Piled Embankment and find the best analytical method for real life use by comparing the results.

1.3. Aim of This M Sc Thesis.

The aim of this reports is to validate the analytical design models EBGEO and BS8006 with numerical calculation and to summarize several aspects on the design of piled embankments.

This report considers only the calculation of the tensile force in the geosynthetic reinforcement (GR) and force on the pile head due to the vertical loads and the fill arching on the piles. The (often significant) tensile forces in the GR due to the horizontal stresses in the embankment ("spreading") are beyond the scope of this study.

Other than the comparison of design of above three methods, effect on;

- Load on piles,
- Settlement of embankment
- Maximum Bending moment & Shear Force on pile
- Tension in Geosynthetic Reinforcement

UNIVERSITY OF MORATUWA LIBRARY SRI LANKA

Due to variation of several parameters that has to consider during design will be compared in graphical form. This was carried out using finite element models developed using Plaxis 2D. The considered cases are;

- Variation of pile size
- Variation of Traffic Load
- Variation of No.of geo-reinforcement layers
- Variation of spacing between geo-reinforcement layers
- Variation of pile spacing
- Variation of embankment height.

1.4. Statement of the Problem

A number of methods are available for the design of GRPS embankment systems. Limited guidelines are also available for GRPS systems. For the Dutch Code a choice will be made among the three methods (BS8006-End Bearing Pile, BS8006-Friction Pile, and German Draft Standard). An evaluation based on the results of finite element method (PLAXIS 8.2) is needed to support this choice.

1.5. Methodology.

1. In order to achieve the research objectives, the following approach will be followed. Literature review on Geosynthetic Reinforced Pile Supported Embankment, Pile Foundation in the Sri Lanka and World. Empirical method and theoretical considerations
2. Three design models which are BS8006 (STUIT & KLEEF), EBGEO & PLAXIS 2D are selected to considered here.
3. Two cases have been calculated with finite element method and three design methods.

   Case 1 has a thin embankment and case 2 has a thick embankment. The center to center distance of the piles and diameter of the piles are different, and other parameters are identical.

For both cases a number of sensitivity analysis has been carried out, where always one parameter is varied whereas the remaining parameters are constant.

4. Compare the results of numerical analysis with calculation results of 2D analytical design procedures.
5. Analysis, discussion.
6. Conclusion and recommendations.

2. LITERATURE REVIEW

2.1. Theory of Soil Arching

McNulty (1965) defined the concept Soil Arching as "the ability of a material to transfer loads from one location to another in response to a relative displacement between the locations. A system of shear stresses is the mechanism by which the loads are transferred." Figure 2.1 to 2.3 below illustrate this concept.

Consider soil on a rigid base, there is no tendency for differential movement and hence no soil arching. The stress acting at a point **a** in Figure 2.4 is the overburden stress γH, where γ is the unit weight of the soil and H is the height of the soil prism. When one of the local supports at the point **a** is removed, the point **a** is in tension and a roof tension arch is formed. The true arch collapses as the soil is not in equilibrium. The soil settles in an inverted arch, the adjacent soil develops the required shear strength and the soil reaches equilibrium state. The transfer of pressure from the yielding portion to the stationary portion is called arching.

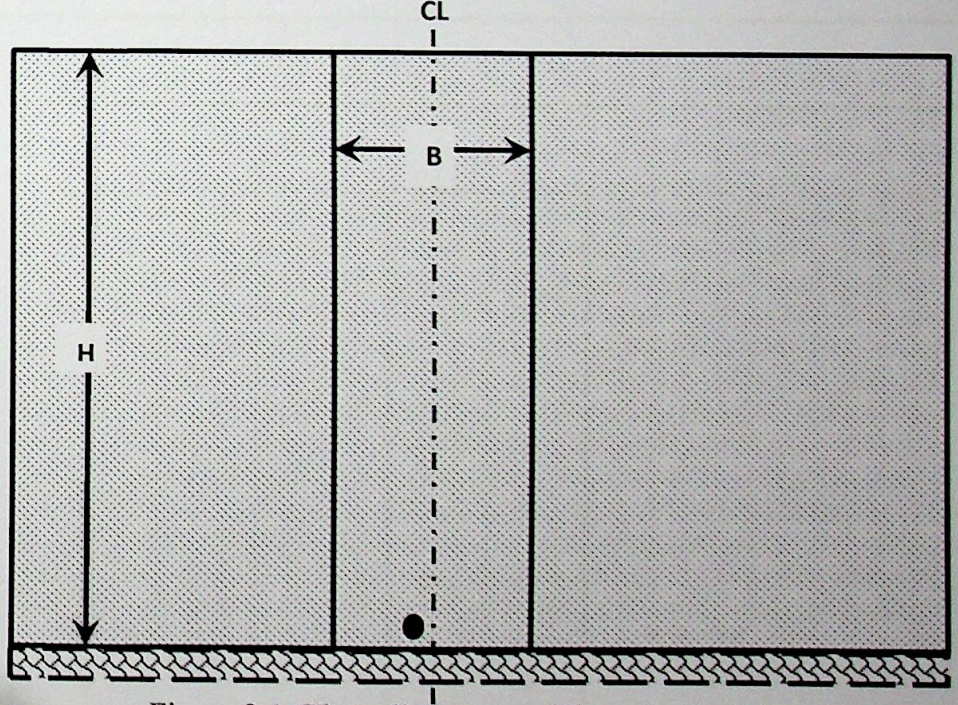

Figure 2.1: The soil mass overlying a potential void
(McKelvey, 1994 – cited in Li et al., 2002)

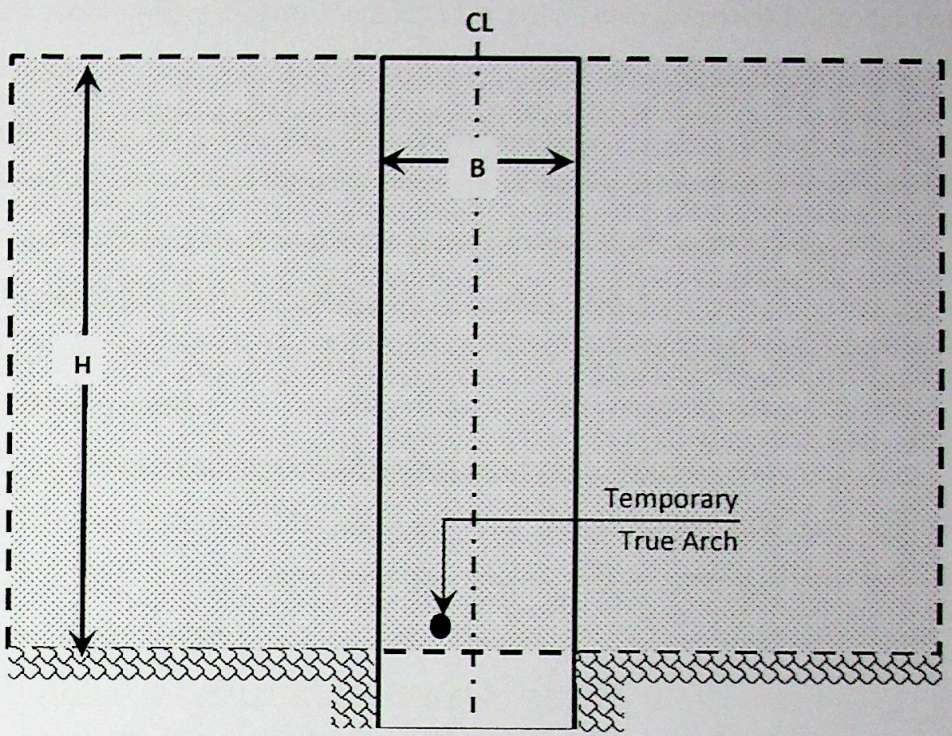

Figure 2.2: The formation of a true arch (Void under soil mass)
(McKelvey, 1994 – cited in Li et al., 2002)

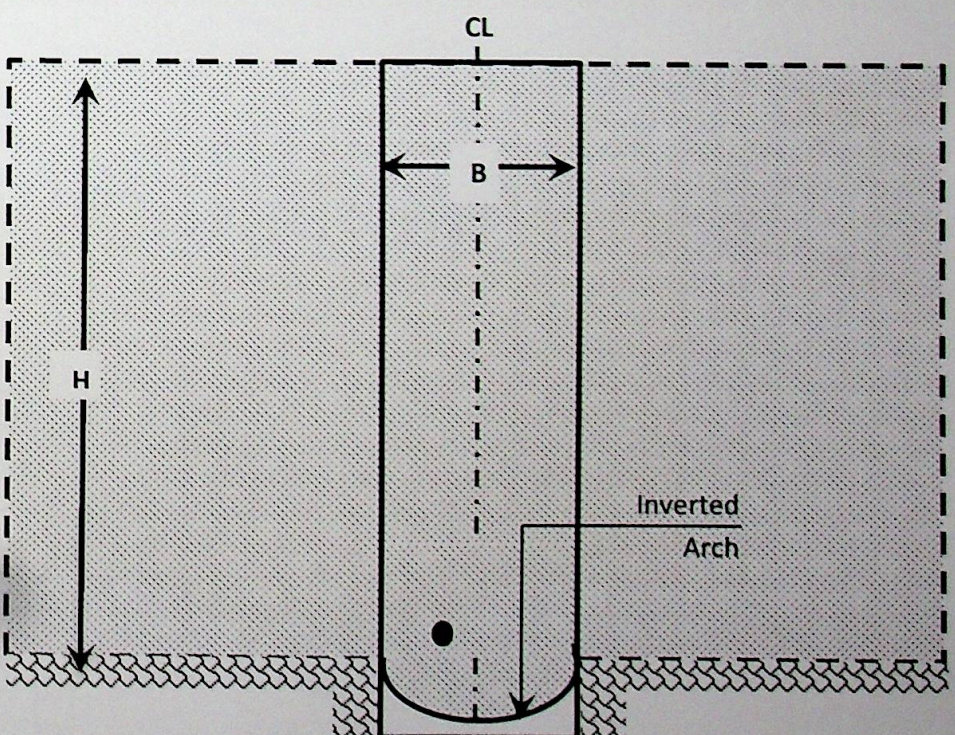

Figure 2.3: Soil mass collapses to form an inverted arch
(McKelvey, 1994 – cited in Li et al., 2002)

The below mentioned different methods also have been proposed to model the soil arching effect.

- Terzaghi (1936) (cited in Han and Gabr, 2002)

  Terzaghi considered the shear strength along the soil prism which is mobilized to a certain height, at which the plane of equal settlement exists.

- Giroud et al. (1990) (cited in Han and Gabr, 2002)

  Applied McNulty's model to deal with soil layer-geosynthetic systems overlying voids.

- Hewlett and Randolph (1988) (cited in Li et al., 2002)

  Considered limit equilibrium in a domed region for the sand between the two piles. Most of the load above the crown was transferred onto the support through the crown.

- Schmertmann (1991) (cited in Han and Gabr, 2002)

  Proposed that all the load within the triangular prism (plane strain) or conical prism (axisymmetric) is transferred directly onto the adjoining support.

In all the above cases, it is assumed that all the pressure is to be carried by the geosynthetic; i.e., there is a cavity below the geosynthetic layer as shown in Figure 2.3.

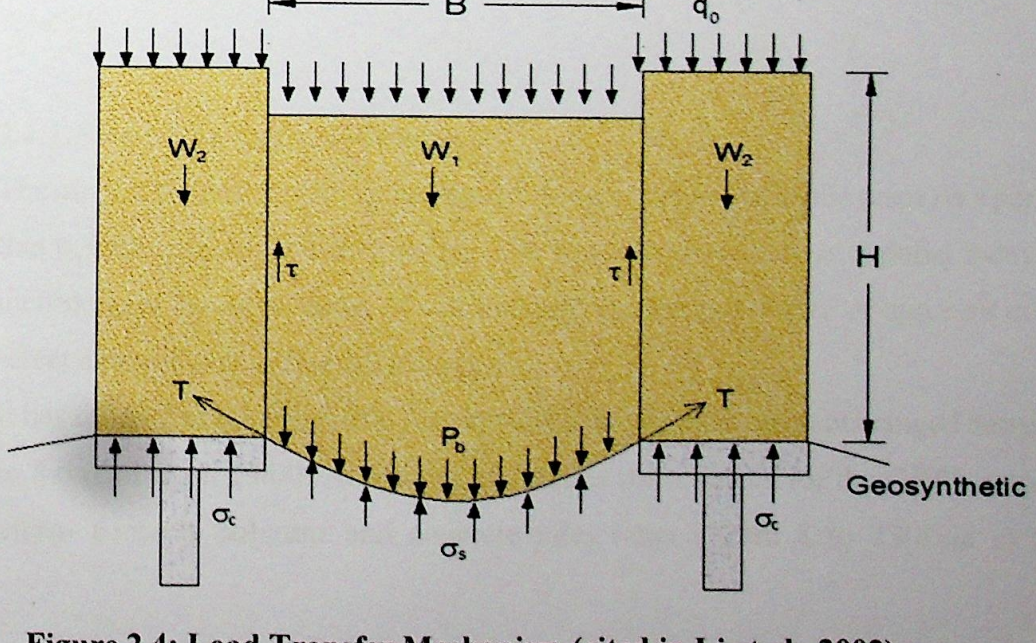

Figure 2.4: Load Transfer Mechanism (cited in Li et al., 2002)

Soil Arching $P_b=\rho(\gamma H+q)$ Eqn. 2.1

Where,

ρ-Density of the water. (kg/m^3)

γ-Soil unit weight. (kN/m^3)

H-Height of the embankment (m)

q-Surcharge (kPa)

Stress concentration ratio $n=(\sigma_c/\sigma_s)>1$

The weight of the fill tends to move downward due to the presence of soft soil below the geosynthetic layer. This downward motion is resisted by the shear resistance provided by the fill on the pile caps. The shear resistance reduces the pressure acting on the geosynthetic but increases the load acting on the caps. The geosynthetic layer and the embankment fill form a stiffened fill platform that supports load transfer mechanism. To improve the interaction between soil and piles a high quality filling material is used. The differential settlement between pile caps is expected to be lower due to the inclusion of the geosynthetic layer. The reduction of the displacement reduces the shear stresses induced by soil arching. Hence, the load transfer by soil arching is reduced. This also reduces the load transferred to the pile caps. The vertical component of the tension forces in the reinforcement(s) is however, transferred to the pile caps. A single geosynthetic layer acts as a tension membrane while a multi-layer system can interlock better with the surrounding soil and act as a stiffened "beam" or "plate".

2.1.1. Stress Concentration Ratio

The ratio of the stress on the pile (caps) to the soil between the pile (caps) is a parameter that is used to quantify load transfer. The stress concentration is a global index which incorporates the mechanism of soil arching, tension membrane or apparent cohesion effect and pile-soil stiffness difference.

It has found that the value of n for conventional pile embankments ranged between 1.0 to 8.0 (Ooi et al. 1987). According to studies the n values for the GRPS systems on vibro- concrete columns and concrete piles ranged from 8 to 25(Reid et al. and

Maddison et al), which is much higher than the conventional piled embankments. This increase in n is due to the inclusion of the geosynthetic layer.

The n value is a parameter of stiffness or rigidity of the foundation. It equals to one for a fully flexible foundation resting on a pile-soil composite foundation and become a very high value for a rigid conventional foundation. The GRPS system has n values in between these two types.

2.2. Design of Geosynthetic Reinforcement

The flexible geosynthetic reinforcement layer or mat with soil layer over the pile caps replaces the conventional rigid concrete slab. This layer provide the required tensile resistance. And due to the flexibility of the geosynthetic layer, load transfer due to soil arching is observed.

The design of the reinforcement should consider:

- Vertical stress transferred to the geo-reinforcement after soil arching effect has taken place
- The tensile force generated in geo-reinforcement due to the vertical pressure of the embankment
- The tensile force developed in the reinforcement due to lateral spreading of the embankment.

The design methods that will be discussed here are:

- BS 8006,
- Terzaghi's theory,
- Finite element method using Plaxis-finite element program (this will be discussed in Chapter 4.)

Most of the current design methods ignore the soil resistance below the geosynthetic layer; i.e., a void is considered below the geosynthetic layer. This makes the design conservative. Here we are considering piles arranged in a rectangular pattern.

UNIVERSITY OF MORATUWA LIBRARY

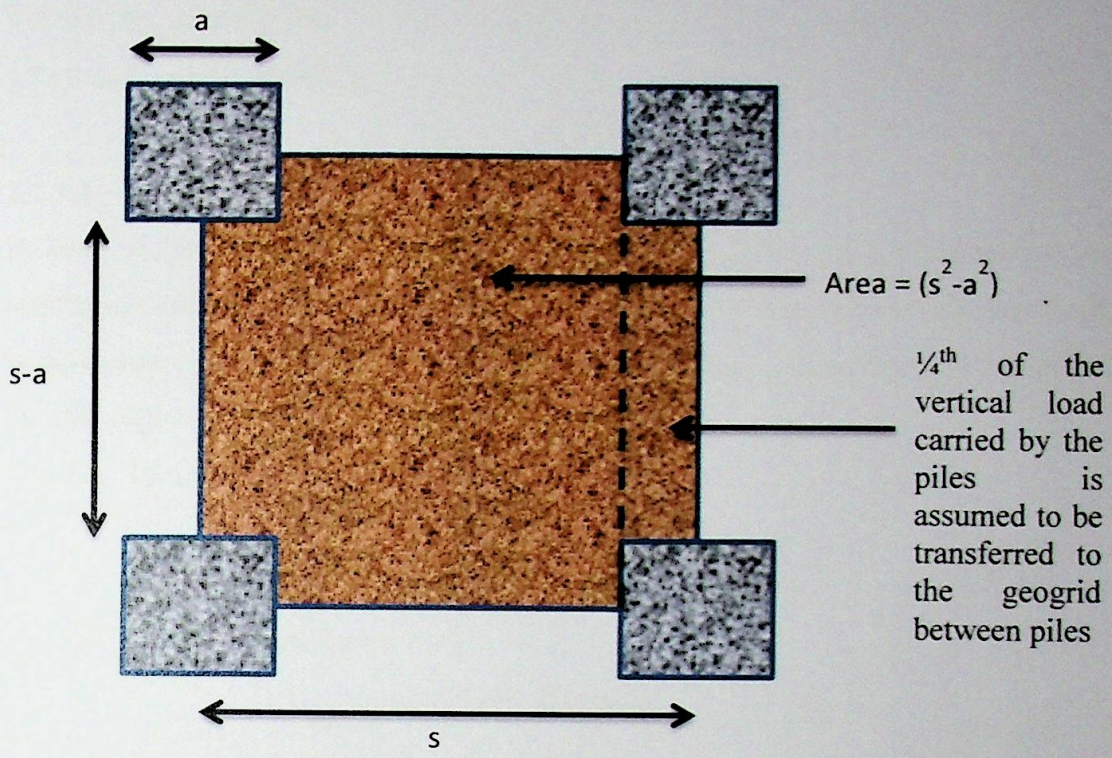

Figure 2.5: Unit Cell Utilization (Russell and Pierpoint, 1997 – cited Li et al., 2002)

A unit cell supported at four ends on piles is considered (Figure 2.5) - (Russell and Pierpoint, 1997 - cited in Li et al., 2002). The area of the cell is s^2 and the area not supported by the pile is (s^2-a^2). A quarter of the load is assumed to be transferred to the reinforcement.

2.2.1. Stress Reduction Factor.

The stress reduction factor S_{3D} is defined in order to compare the various methods. It is defined as the ratio of the average vertical stress acting on the reinforcement to the overburden pressure due to the embankment fill.

$$S_{3D} = \frac{2W_T(s-a)}{\gamma H(s^2-a^2)} \qquad \text{Eqn. 2.2}$$

Where,

S_{3D} The stress reduction ratio

W_T distributed vertical load acting on the geogrid between adjacent pile caps (kN)

s spacing between adjacent pile cap (m)

H height of the embankment (m)

a size of the pile cap (m)

γ Soil unit weight (kN/m3)

2.2.1.1. BS8006(1995)

BS8006 is the British Standard method used for design of embankments with reinforced soil foundations on poor ground. This is a is very conservative and most widely used method. The distributed vertical load acting on the reinforcement between the pile caps is W_T

For H>1.4 x (s-a)

$$W_T = \frac{1.4s\, f_{fs}\gamma(s-a)x}{s^2-a^2}\left(s^2-a^2\frac{p'_c}{\sigma'_v}\right) \qquad \text{Eqn.2.3}$$

For $0.7(s-a) \le H \le 1.4(s-a)$

$$W_T = \frac{s(\,f_{fs}\gamma H + f_q ws)}{s^2-a^2}\left(s^2-a^2\frac{p'_c}{\sigma'_v}\right) \qquad \text{Eqn.2.4}$$

But,

$$W_T = 0\ if\ \frac{S^2}{a^2} \le \frac{p'_c}{\sigma'_v} \qquad \text{Eqn.2.5}$$

Where,

s the spacing between the piles

a the size of the pile caps

w_s the uniformly distributed surcharge loading

p`c the vertical stress on pile caps

σ`v the factored average vertical stress at the base of the embankment

$$\sigma'_v = f_{fs}\gamma H + f_q w_s \qquad \text{Eqn.2.6}$$

Where,

f_{fs} the partial load factor for soil unit weight

f_q the partial load factor for applied external loads

γ the unit weight of the soil

H the height of the embankment fill

This method considers the piles as buried rigid conduits. The vertical stress is given using Marston's formula for positive projecting conduits.

$$P'_c = \sigma'_v \left[\frac{C_c H}{H}\right]^2$$ Eqn.2.7

BS8006 gives empirical equations for arching coefficient as follows

$C_c = 1.95\frac{H}{a} - 0.18$ for end-bearing piles (unyielding) Eqn.2.8

$C_c = 1.5\frac{H}{a} - 0.07$ for friction and other piles Eqn.2.9

Where,

C_c the arching coefficient in BS8006-1995

Based on the above equations the stress reduction ratio is given by

$$S_{3D} = \frac{2.8s}{(s+a)^2 H} x \left[s^2 - a^2\left(\frac{P_c}{\gamma H}\right)\right]$$ Eqn.2.10

2.2.1.2. Terzaghi Method

Terzaghi's (1943) (cited in Li et al., 2002) method was based on results from trap door tests at large displacement. Terzaghi considered the problem as three dimensional.

He considered the shear strength along a soil prism which is mobilized to a certain height where there exists a plane of equal settlement. The stress reduction ratio is given as

$$S_{3D} = \frac{(s^2 - a^2)}{4HaK.Tan(\emptyset)} x \left[1 - e^{\frac{-4HaK.Tan(\emptyset)}{(s^2-a^2)}}\right]$$ Eqn.2.11

K is the ratio of the horizontal to vertical pressure. Terzaghi has taken K=1.

2.2.2. Tension in Geosynthetic Reinforcement

For the calculation of tensile force in the geo-reinforcement the British Standard BS8006 (1995) suggests the below formula. The tensile force T_{rp} per metre "run" generated due to the distributed load W_T is given by

$$T_{rp} = \frac{W_T(s-a)}{2a}\sqrt{1 + \frac{1}{6\epsilon}}$$ Eqn.2.15

Where,

T_{rp} the tension in the reinforcement

ε the strain in the reinforcement.

The tension in the reinforcement is calculated taking into consideration the maximum allowable strain in the reinforcement. Six percent strain is considered the upper limit for transferring the load to the piles. The upper limit should be reduced for shallow embankments to prevent differential movements on the surface of the embankment. A maximum creep strain of 2% is permitted for permanent construction. This tensile load is developed only if the foundation is settled.

Giroud et al. (1990) (cited in Li et al., 2002) proposed a membrane theory for a geosynthetic layer overlying an infinitely long void. This was also used to determine the tension in the reinforcement.

The formula can be stated as

$$T_{rp} = \sigma_s(s - a)\Omega \qquad \text{Eqn.2.16}$$

Where,

σ_s the stress placed on the geosynthetic reinforcement

Ω a dimensionless factor relating the geosynthetic strain to the geosynthetic deflection.

Ω can be defined as

$$\Omega = \frac{1}{4}\left[\frac{2y}{(s - a)}\right] + \frac{(s - a)}{2y} \qquad \text{Eqn.2.17}$$

Where,

y the geosynthetic deflection.

Normally all the geosynthetic are anisotropic in nature. They have more strength in the machine or cross-machine direction. In general practice, there are two theories to determine the strength of the geosynthetic layer that is to be used.

1. Strength of the geosynthetic in the weak direction is assumed for the strength in all directions.
2. Limit the applied tension to half of the strength in the strong direction.

The more conservative approach is generally used in all designs. The actual value is generally close to the less conservative approach.

2.2.3. Soil Resistance

Most of the design methods available ignore the support of the soil pressure on the geo-reinforcement layer. However, if this resistance is adopted in the design, it will considerably reduce the tension in the reinforcement.

As a result of studying the support from below soil on the geo-reinforcement, the below theories were merged.

- Reid and Buchman (1984) (cited in Han, 2003) found from their study that the resistance from the soil below the GRPS platform is $0.18\gamma H$ where γ is the unit weight of the embankment fill and H is the height of the embankment.
- John (1987) (cited in Han, 2003) found the soil resistance to be $0.15\gamma H$.
- The finite element model by Jones et al. (1990) (cited in Han, 1999) proved that partial support from the reinforcement reduced the tensile force in the reinforcement significantly (Figure 2.6). This can be seen in the Plaxis model developed in Chapter 5.

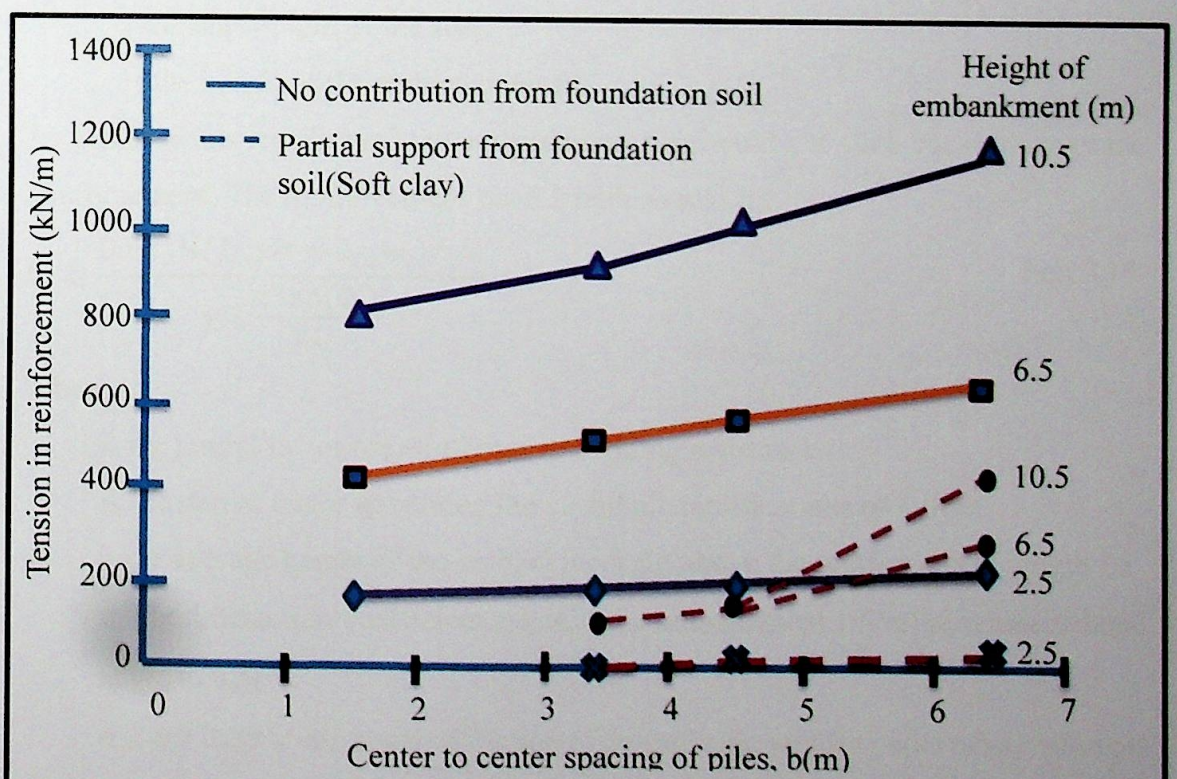

Figure 2.6: Tensile force in the reinforcement under embankment of medium dense soil (Jones et al. (1990)- cited in Han, 1999)

UNIVERSITY OF MORATUWA LIBRARY SRI LANKA

The settlement of the below soil platform can be due to consolidation or under-consolidation of the soil, liquefaction, lowering of ground water, etc. Therefore, in such situations it is reasonable to consider a cavity under the GRPS platform as the settlement below the platform is caused by factors other than the embankment loads.

2.2.4. Tension in Reinforcement due to Lateral Sliding

The need for raking of the piles is eliminated with the use of geo-reinforcement. Therefore, the reinforcement should resist the horizontal force generated due to lateral sliding (Figure2.7) while limiting the strain of reinforcement and lateral pile movements. The reinforcement tensile load needed to resist the outward thrust on the embankment in accordance to BS8006 (1995) is

$T_{ds} = 0.5K_a (f_{fs}\gamma H + 2f_q w_s)H$ Eqn.2.18

Where,

K_a the active earth pressure coefficient ($Ka=\tan^2(45-ø/2)$).

w_s the uniformly distributed surcharge loading

f_{fs} the partial load factor for soil unit weight

f_q the partial load factor for applied external loads

γ the unit weight of the soil

H the height of the embankment fill.

To generate this tensile load the embankment fill should not slide outwards over the reinforcement. The reinforcement bond length should be

$$L_e \geq \frac{0.5k_aH(f_{fs}\gamma H + 2f_q w_s)f_s f_n}{\gamma H \frac{\alpha \tan(\emptyset')}{f_{ms}}}$$ Eqn.2.19

Where,

f_s the partial factor for reinforcement sliding resistance

f_n the partial factor governing the economic ramifications of failure

h the average height of the embankment fill above the reinforcement length Le

α' the interaction coefficient relating the embankment fill/reinforcement bond angle to $\tan\phi'_{cv}$

ϕ'_{cv} the large strain angle of friction of the embankment fill under effective stress conditions

f_{ms} the partial material factor applied to tan ϕ'_{cv}

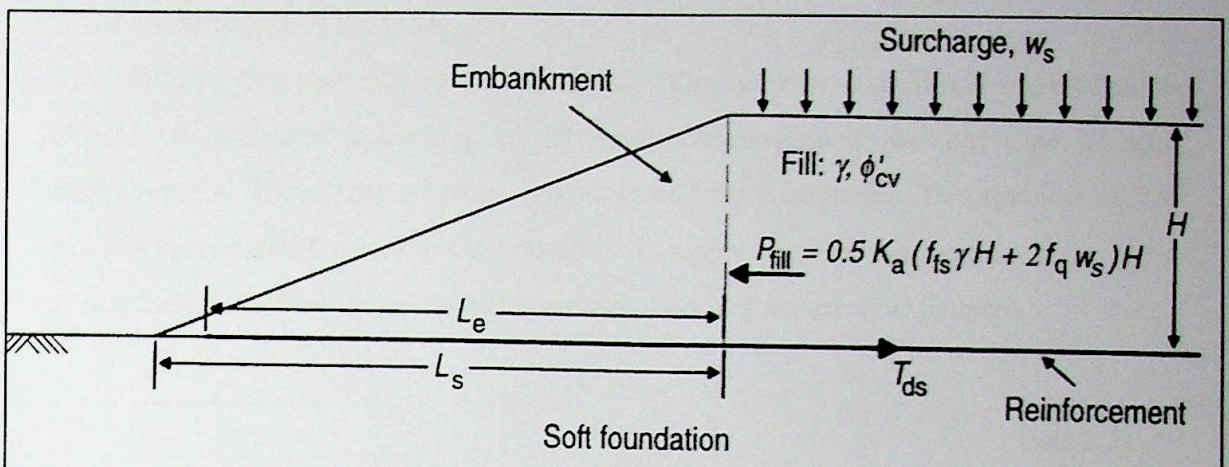

Figure 2.7: Lateral Sliding stability at the interface of fill and reinforcement (BS 8006, 1995)

2.2.5. Limits of Strain in Reinforcement

The soil arch is formed only if there is a settlement in the embankment. However, in order to avoid the differential settlement at the surface of the embankment, BS 8006 suggest limitations to the maximum strain. An upper limit of about 6% is imposed to ensure that all the load is transferred to the piles. As the shallow embankments sometimes cannot form the full arching action, this upper limit can be reduced to prevent differential movements. The long term maximum creep strain of 2% is generally allowed over the design life of the reinforcement to ensure long term localized settlements are limited to an acceptable value.

2.3. Pile Design

In geosynthetic reinforced pile supported embankments, the term pile is used not only for conventional piles but also for other soil improvement columns like stone columns, vibro concrete columns, soil-cement columns, etc. In the GRPS, the geosynthetic membrane is laid on the pile caps to provide support and prevent the lateral sliding of the embankment. This eliminate the necessity of raked piles that are used in conventional pile supported embankments. The pile design incorporates,

- Lateral movement of the pile

LIBRARY
UNIVERSITY OF MORATUWA, SRI LANKA
MORATUWA

- Bending moment developed in the pile due to lateral movement
- Axial bearing capacity of the pile
- Settlement of the pile

The load carrying capacity of the pile or any other column used in soil improvement should be evaluated according to the methods developed for that type of soil improvement. The effect of group action should be considered. The spacing of the piles is maximized for economical reasons. An upper limit on the spacing of the piles is imposed (BS 8006) when the piles are installed in a square grid pattern.

$$S = \sqrt{\frac{Q_p}{(f_{fs}\gamma H + f_q w_s}} \qquad \text{Eqn.2.21}$$

Where,

Q_p allowable load carrying capacity of each pile/column in pile group

f_{fs} partial factor for soil unit weight

g unit weight of the soil

H height of the embankment

f_q the partial load factor for external applied loads

w_s the external surcharge loading

2.3.1. Pile Group Extent

In order to ensure that any differential movement/settlement or instability outside the piled area does not affect the crest of the embankment BS 8006(1995) suggest that the piled area should extend beyond the edge of the shoulder of the embankment. The outer edge limit for the outer pile cap can be given as

$$L_p = H\,(n - \tan\theta_p) \qquad \text{Eqn.2.22}$$

Where,

L_p the horizontal distance between the outer edge of the outer pile cap & the toe of the embankment

109272

H the height of the embankment

n the side slope of the embankment

θ_p the angle to the vertical between the shoulder of the embankment and the outer edge of the outer pile cap

$$\theta_p = 45° - \frac{\varphi_{cv}}{2} \qquad \text{Eqn.2.23}$$

Where

φ_{cv} Describes the embankment fill

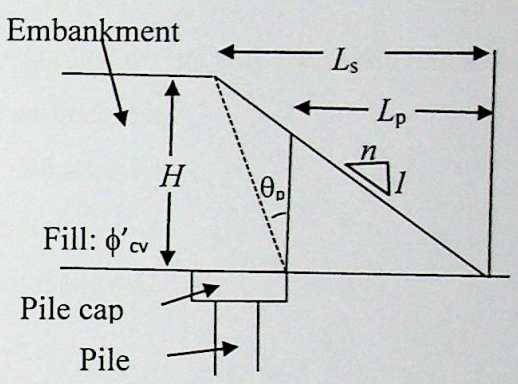

Figure 2.8 Outer limit of pile caps

2.3.2. Pile Cap Punching Capacity

The pile caps can punch through the embankment fill if there is a concentration of stresses on the pile caps and if the embankment height is very low. The inclusion of a geosynthetic layer decreases the stress concentration on the pile caps (cited in Han and Gabr, 2000). This reduction of the stress on the pile cap can result in a smaller probability of punching failure of the pile caps. There is currently no design available for designing the punching failure of the pile caps. However, it can be simulated numerically.

2.4. Lateral Movement of Embankment

Lateral movement of the GRPS system is an area that need more attention. This causes excessive settlements in the system and the foundations or structures in the adjacent areas can be greatly affected. Therefore, this is more dangerous than vertical

settlements. However, there are no methods available to estimate the lateral movements of geosynthetic reinforced pile supported embankments.

However it is essential to get an initial estimate of the lateral movements. This can be done by prototype testing. But this is a very uneconomical method. Initial predictive methods should be used to determine lateral ground movements. The design method used will depend on the sensitivity of the structure to the soil movements.

Seaman (1994) (cited in Li et al., 2002) investigated the effects of various factors on lateral movements. The increase in certain factors that tend to increase the lateral movements are:

- Vertical stress applied on the soil due to the embankment fill
- Length of the embankment
- Width of the embankment
- Embankment slope
- Poisson's ratio of the soil

The increase in certain factors that tend to decrease the lateral movements are

- Thickness and stiffness of the fill
- The distance from the embankment toe
- Stiffness of the soil
- Strength of the soil
- Adhesion between the soil and the fill

The lateral movements caused by application of the embankment load can be estimated using

- Empirical relations with the soil properties and the observed behavior of the soil on the site.
- Theoretical Analysis
- Prototype testing

The methods listed above do not consider the effect of piles and geosynthetic reinforcement.

The prototype testing method is one of the best and most reliable methods.

However, it is not an economical method for initial estimation. Empirical methods seem to be the simplest for estimation for the lateral movements.

2.5. Slope Stability

There are number of methods available for evaluation of slope stability of GRPS systems.

2.5.1. BS8006

BS 8006 recommended to use conventional slip circle method to check the stability of GRPS embankments. However, the presence of piles and geo reinforcement should be taken into consideration (Figure2.9).

According to BS8006, the analysis can be performed using effective stress parameters taking account for the pore water pressures. An analysis for short term stability should assume undrained conditions.

In order to ensure stability the following formula is needed to be satisfied.

$$M_D \leq M_{RS} + M_{RP} + M_{RR} \qquad \text{Eqn.2.32}$$

Where,

M_D the factored distributing moment at all locations along the base of the embankment

M_{RS} the factored restoring moment due to the soil at all locations along the base of the embankment

M_{RP} the resisting moment due to the axial load in the piles along the base of the embankment

M_{RR} the restoring moment due to the reinforcement at all locations along the base of the embankment

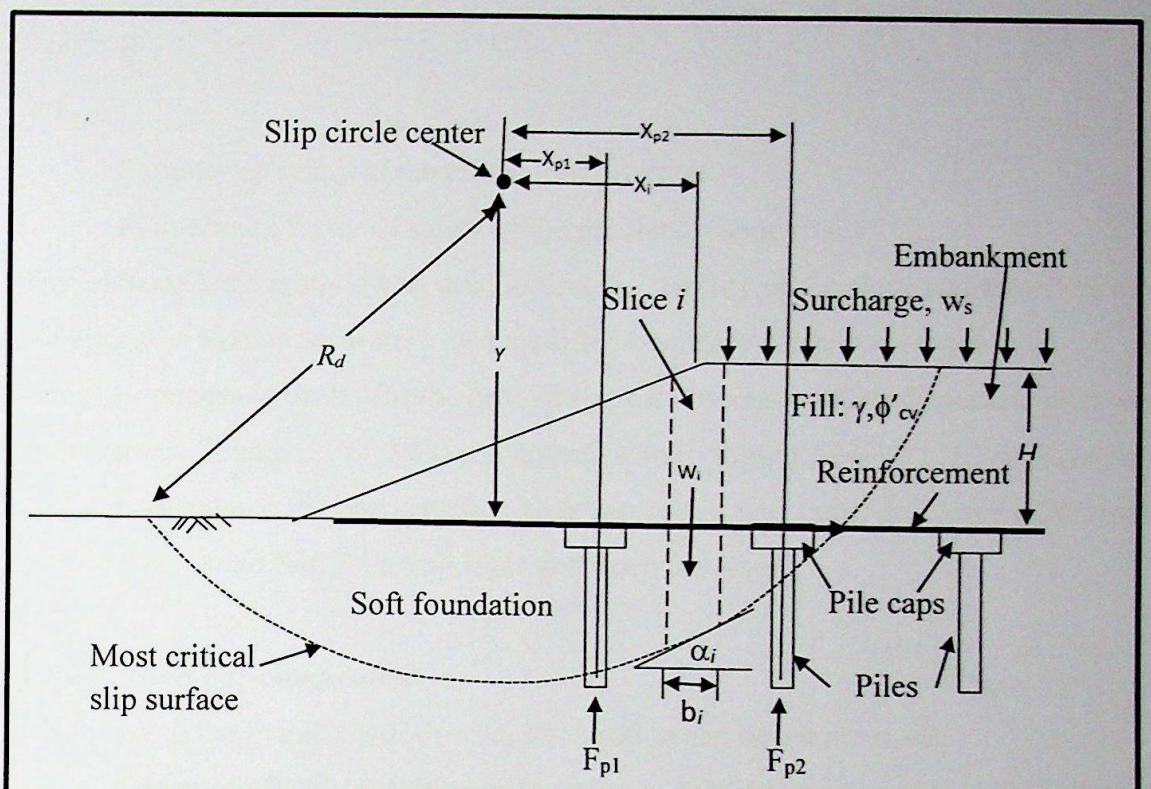

Disturbing moment due to soil and loading:

$$M_D = \left[\Sigma\{f_{fs}W_i + f_q b_i w_{si}\}\sin\alpha_i\right]R_d$$

Restoring moment due to soil:

$$M_{RS} = \left[\Sigma\left\{\frac{c'_i}{f_{ms}}b_i\sec\alpha_i + \left((W_i + b_i w_{si})\cos\alpha_i - u_i b_i \sec\alpha_i\right)\frac{\tan\phi'_{cvi}}{f_{ms}}\right\}\right]R_d$$

Restoring moment due to piles:

$$M_{RP} = F_{p1}X_{p1} + F_{p2}X_{p2}$$

Restoring moment due to reinforcement:

$$M_{RR} = T_1 Y$$

Figure 2.9. Variable required for the analysis of GRPS embankment slopes (Cited in Bs 8006, 1995)

2.5.2. Modified Boundary Element Method

The effect of piles on slope stability was studied by Lee et al. (1995) (cited in Li et al., 2002). The improvement ratio was defined by Lee et al. for the comparison of the ground improvement due to piles.

$$N_{ps} = \frac{F_p}{F_s}$$ Eqn.2.33

Where,

F_p factor of safety of the pile-sloped problem

F_s minimum factor of safety of the problem without piles

The Bishop Circle method was used to find the stability of the slope and the effect of the piles was studied separately by a modified boundary element method.

Lee et al. presented charts for the behavior of cast-in-situ reinforced concrete piles in homogenous (Figure 2.10 – 2.13) and layered slopes (Figure 2.14 – 2.17). Two layered soil was considered for later situation with two cases; Soft upper soil layer with hard founding layer and Soft founding layer with hard top layer.

2.5.2.1. Homogenous Slopes

According to the graphs the following information can be summarized.

- The most effective position of the piles is near the crest or near the toe. If the pile is close to middle of the slope the improvement ratio is reduced to 1.0. If the pile head is fixed against rotation it has no effect on the stability of the slope.
- As the pile spacing increases the improvement ratio reduces.
- The larger the diameter of the pile, the greater is the improvement ratio. In this case, when d/ds is greater than 1.0 toe piles are more effective.
- The soil modulus and the pile stiffness have little or no effect on the stability of the slope.
- The piled-slope improvement ratio increases linearly with increase in pile – soil limiting pressure

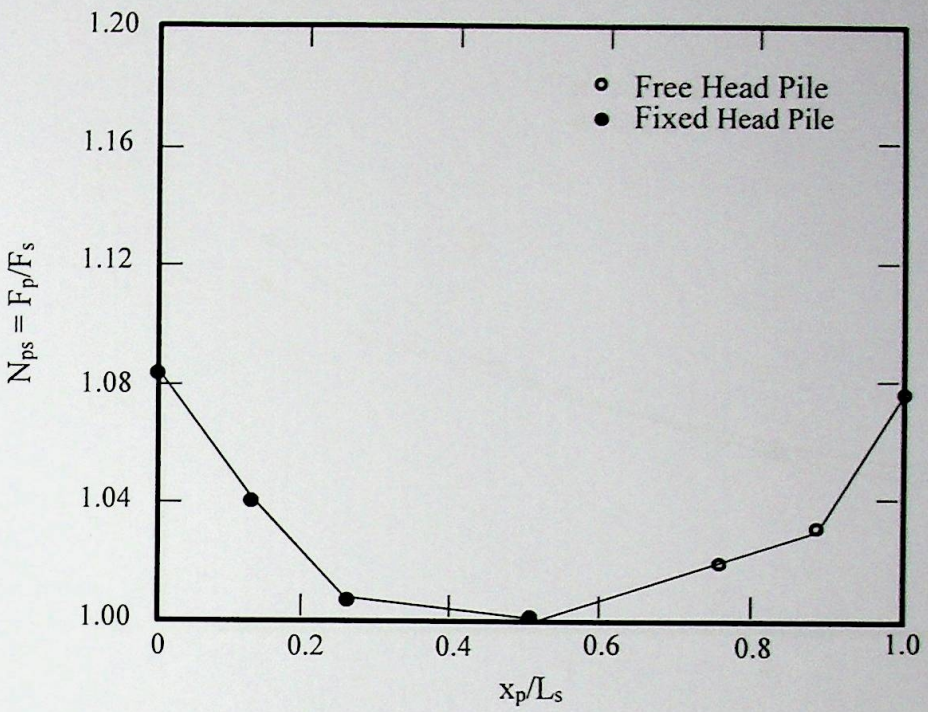

Figure 2.10: Effect of pile position on the homogenous slope (lee et al., 1995-cited in Li et al., 2002)

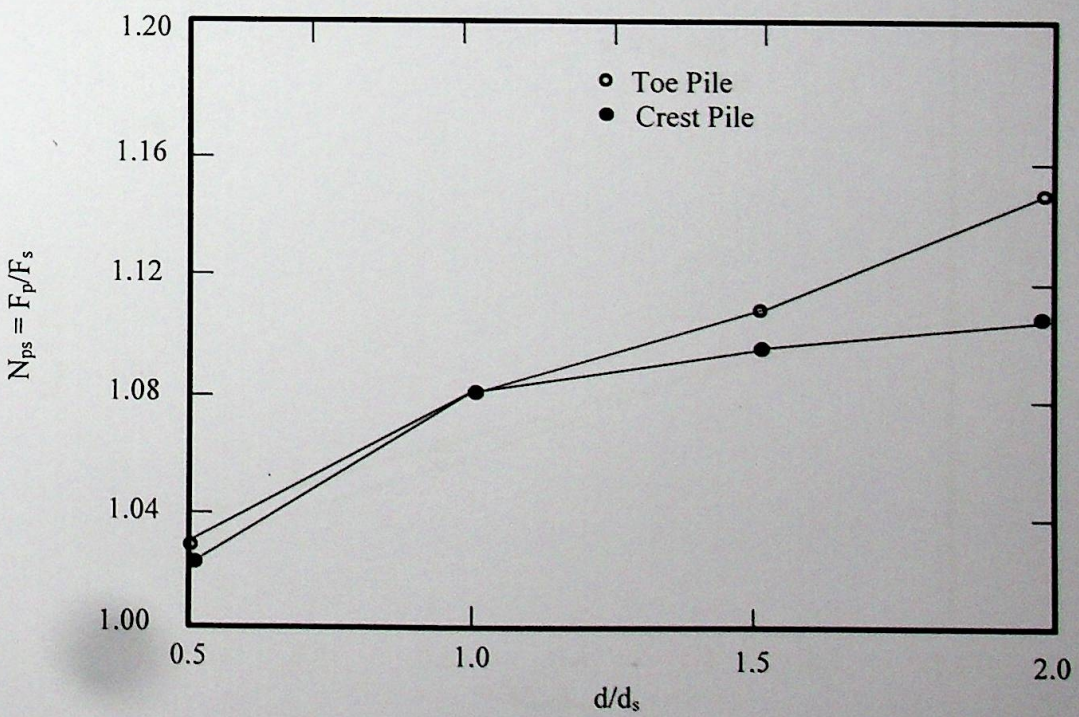

Figure 2.11: Effect of pile diameter on the homogenous slope (lee et al., 1995-cited in Li et al., 2002)

UNIVERSITY OF MORATUWA
LIBRARY
SRI LANKA

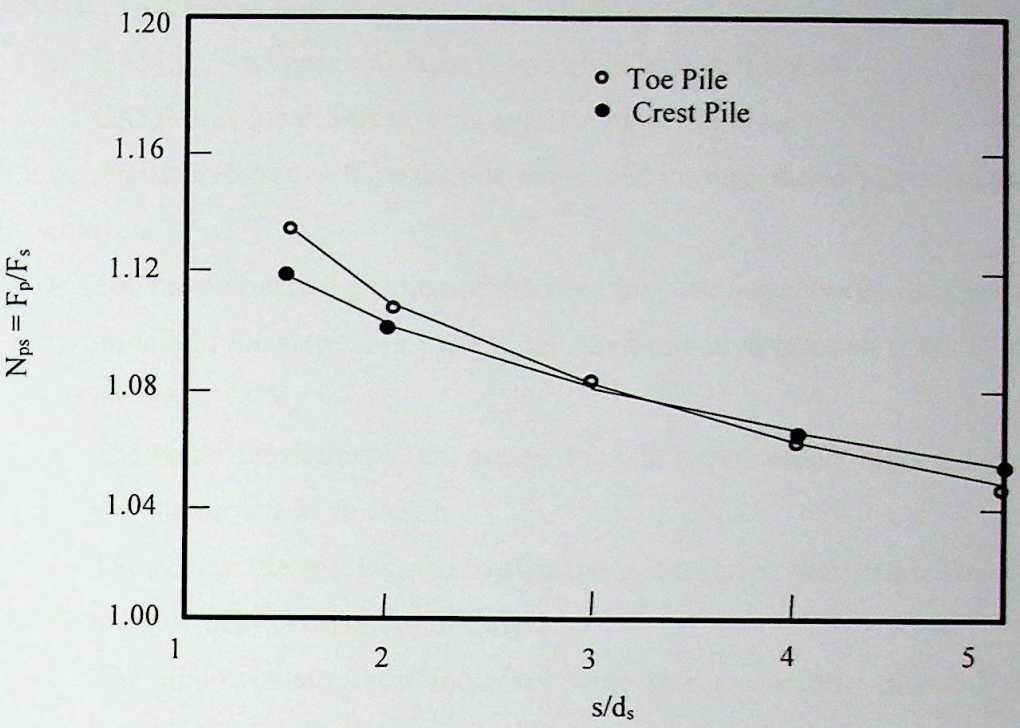

Figure 2.12: Effect of pile spacing on homogenous slope (Lee et al., 1995- cited in Li et al., 2002)

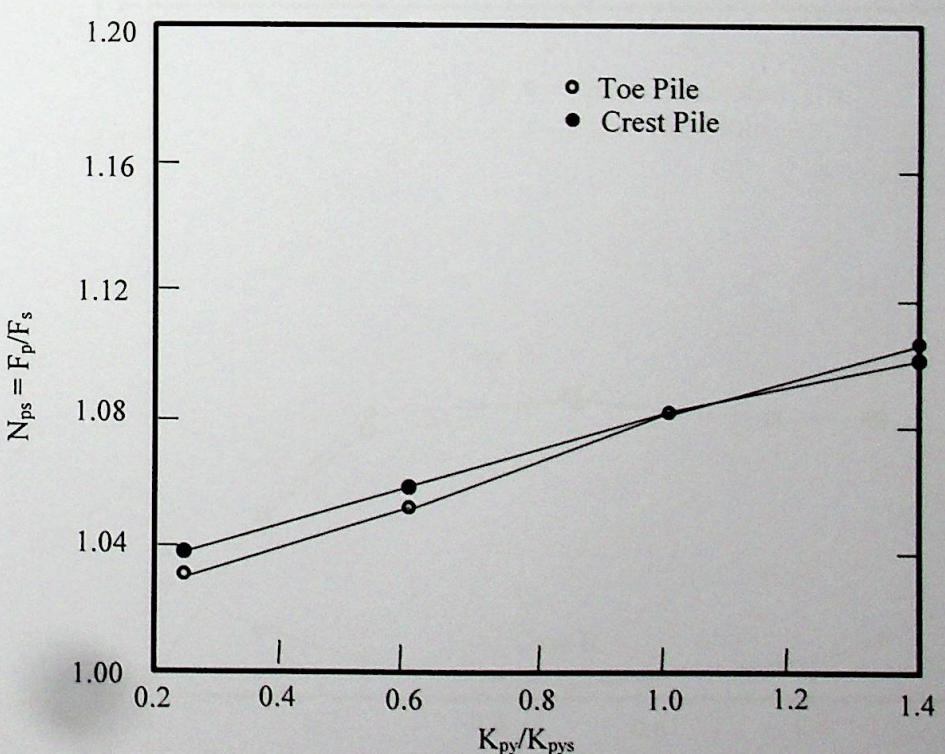

Figure 2.13: Effect of pile spacing on homogenous slope (Lee et al., 1995- cited in Li et al., 2002)

2.5.2.2. Two Layer Soil Slope

CASE 1: An upper soft layer is underlain by a stiff layer

CASE 2: A lower soft layer is overlain by a stiff layer

It is generally preferred to have the pile embedded through the soft layer into the firm lower layers.

- The most effective position of the piles for Case1 is between the crest and the middle of the slope. For Case 2, the most effective position is at the toe or at the crest.
- The larger the diameter, the greater the pile improvement ratio. This effect is seen more vividly in Case1.
- The greater the spacing, the smaller the pile improvement ratio. This effect is more evident in Case 1 than Case 2.
- The improvement ratio increases with increase in the pile-soil limiting pressure. This ratio is higher in Case1 than in Case 2.

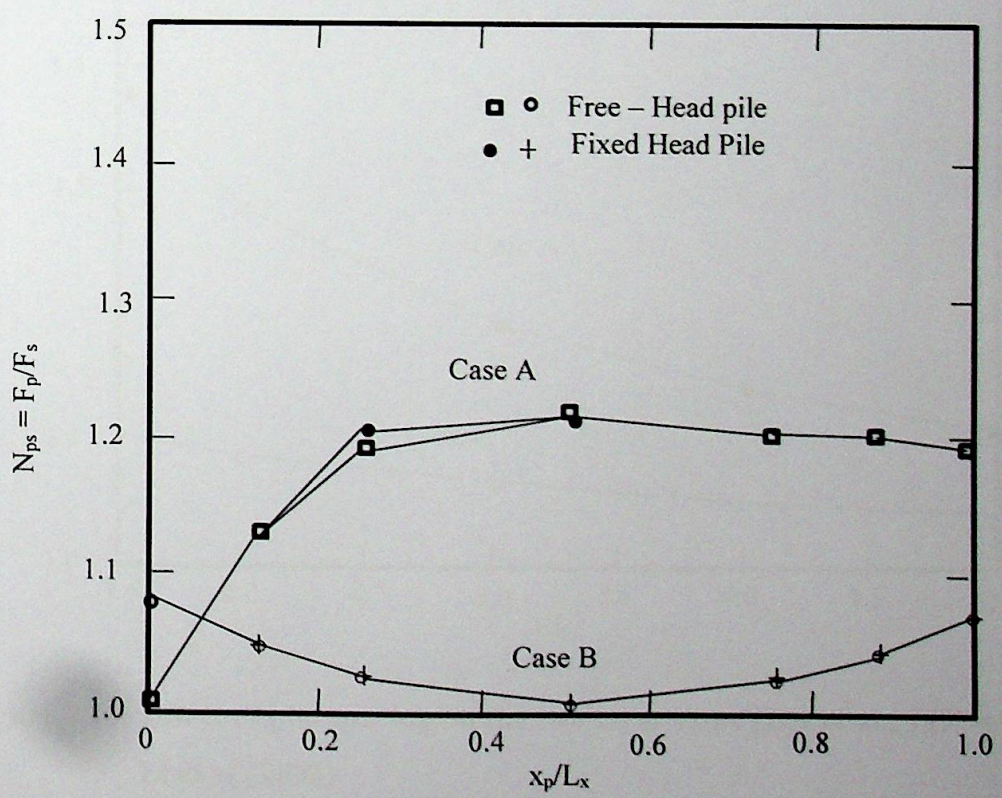

Figure 2.14: Effect of pile position on two –layer slope (lee et al., 1995-cited in Li et al., 2002)

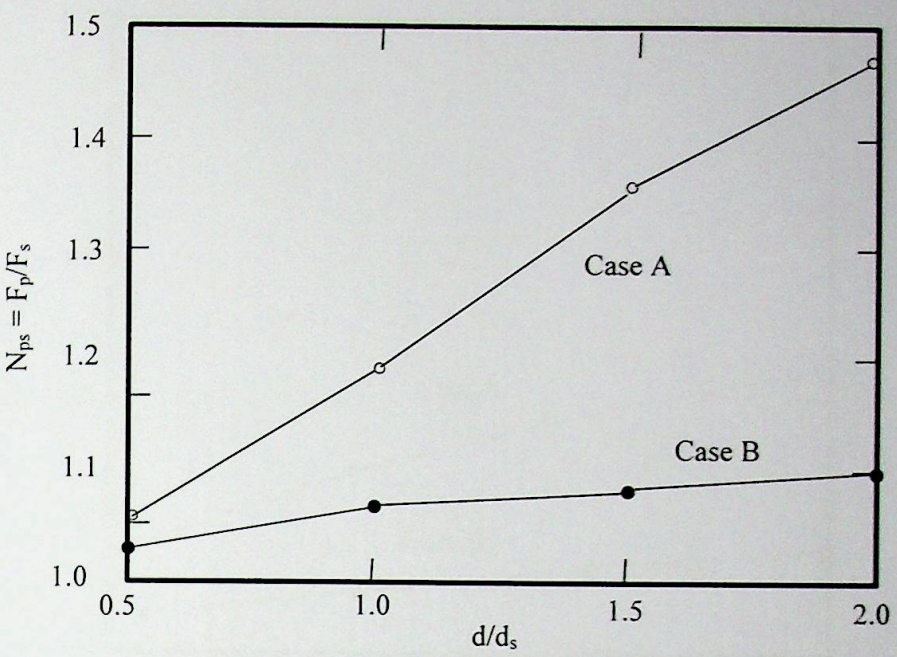

Figure 2.15: Effect of pile diameter on a two –layer slope (Lee et al., 1995-cited in Li et al., 2002)

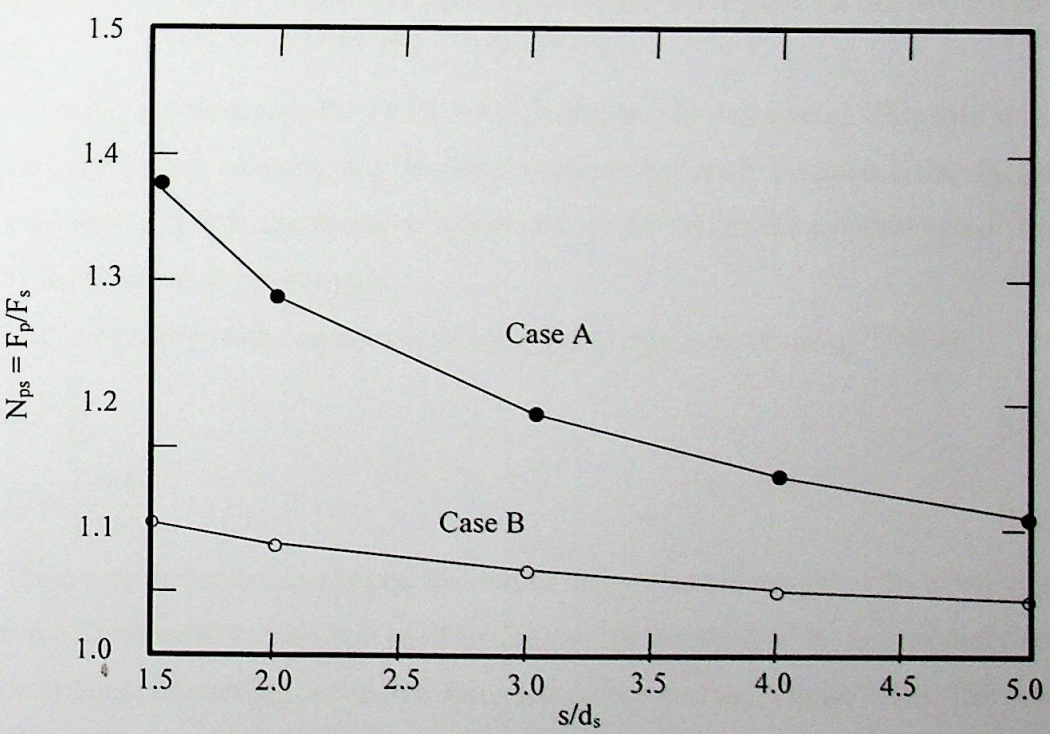

Figure 2.16: Effect of pile spacing on the two layer slope (Lee et al., 1995-cited in Li et al., 2002)

UNIVERSITY OF MORATUWA
LIBRARY
SRI LANKA

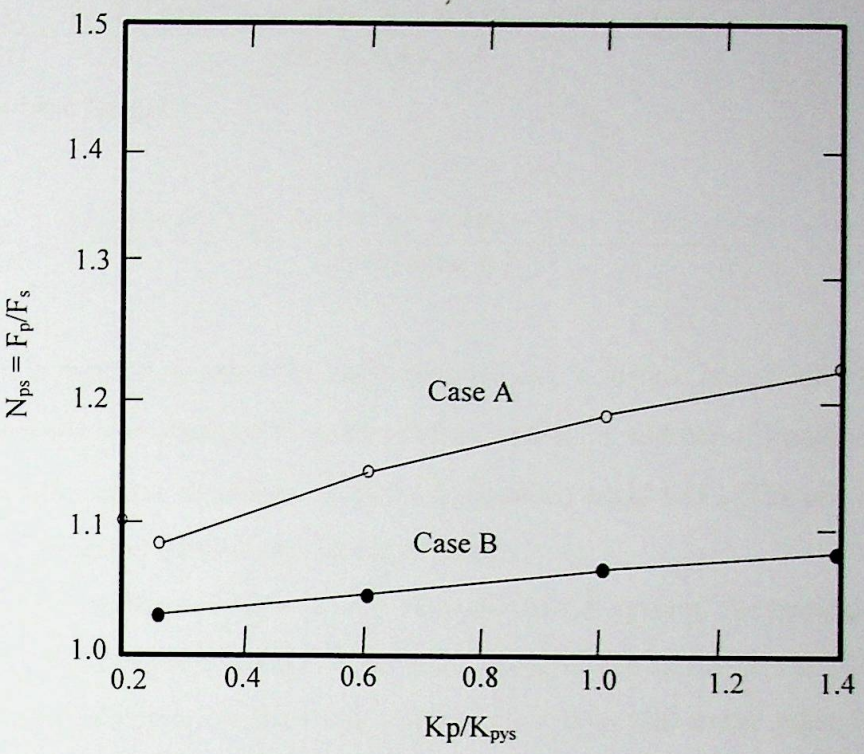

Figure 2.17: Effect of pile soil limiting pressure multiplier on the two-layer (Lee al., 1995-cited in Li et al., 2002)

For homogenous slopes the Friction Circle method is very useful. This method can be used when both cohesive and frictional components are to be used. Using the Mohr – Coulomb criterion, the factor of safety can be defined as the available shear strength to the required shear strength.

Factor of safety with respect to friction Fϕ and cohesion Fc are as follows:

$$F_c = \frac{C_a}{C_r} \qquad \text{Eqn.2.34}$$

$$F_\phi = \frac{Tan\phi_a}{Tan\phi_r} \qquad \text{Eqn.2.35}$$

The forces that maintain the equilibrium of the system are weight of the mass, cohesion force Cr required to maintain equilibrium and the resultant of the normal and frictional component of strength mobilized along the failure surface (Figure 2.18). The direction of the resultant corresponds to the line that forms a tangent to the friction circle, with a radius,

$R_f = R.Sin\ \phi_m$

Taylor (1937) (cited in Li et al., 2002) derived two expressions for the stability number for toe failure:

$$\frac{C_a}{F_c \gamma H} = \frac{(1/2)Cosec^2 x(y.Cosec^2 y - \cot y) + \cot x - \cot i}{2\cot x.\cot v + 2} \qquad \text{Eqn.2.36}$$

For base failure:

$$\frac{C_a}{F_c \gamma H} = \frac{(1/2)Cosec^2 x(y.Cosec^2 y - \cot y) + \cot x - \cot i - 2\eta}{2\cot x.\cot v + 2} \qquad \text{Eqn.2.37}$$

In this method, a value for Fϕ is assumed and a surface is defined by angles x and y. The angle v is obtained from its relation with ϕ_r. A number of iterations are carried out using the above equations, until Fc is obtained equal to F_ϕ. The critical surface is the one which has a minimum factor of safety.

When a number of piles are introduced into the system, the critical surface and the factor of safety will change. The forces acting in this system are similar to those above with the exception of the force acting on the slope due to the piles, Fp (Figure 2.19). This resulting force Fp can be incorporated into the system. This results in two new expressions for toe failure and base failure.

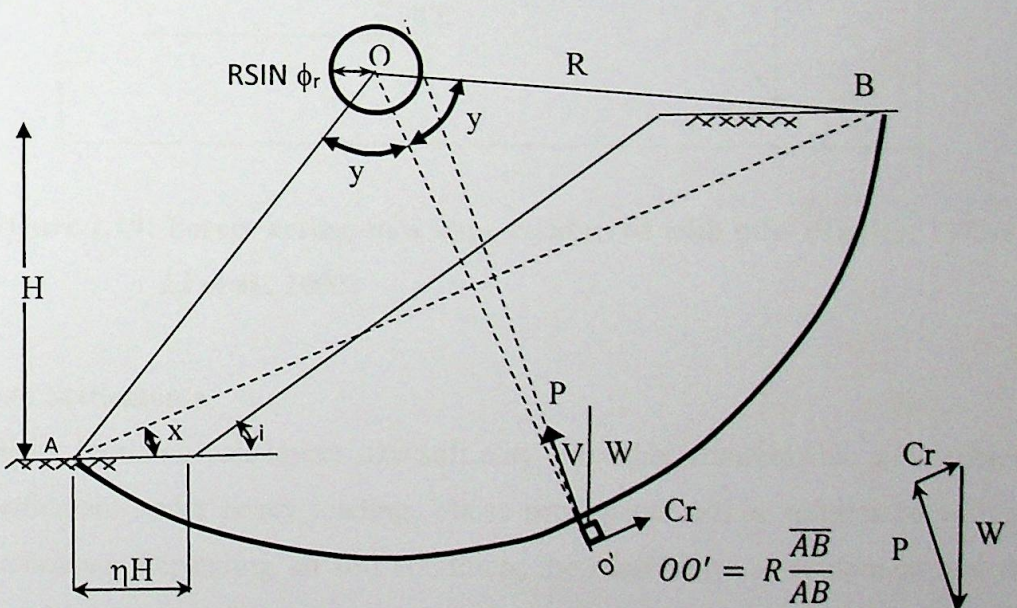

Figure 2.18 Force on slope without piles (Taylor, 1937-cited in Li et al., 2002)

$$E = 1 - 2\cot i + 3\cot i \times \cot x - 3\cot i \times \cot y + \cot x \times \cot y \qquad \text{Eqn.2.38}$$

Where,

CEO is the angle formed by Fp and horizontal, OG is the moment of Fp. The above equations can be used for calculation of factor of safety of the slope.

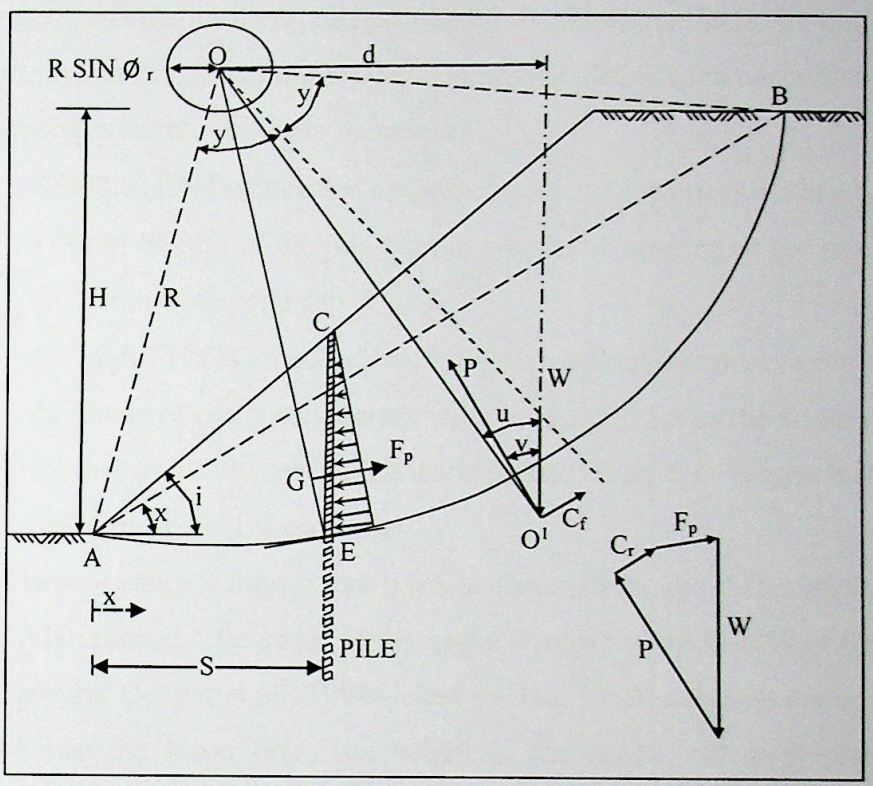

Figure 2.19: Forces acting on a slope reinforced with piles (Taylor, 1973-cited in Li et al., 2002)

2.6. Settlements

Weak founding soil layers like soft clay and other compressible soils subjected to settlement under heavy loading. Those settlements can be minimized with various techniques depending on soil condition, the availability of equipment and the cost involved for each method.

The GRPS system is more popular in embankment construction over soft ground. Some of the common techniques that used with GRPS system are piles, stone columns, vibroconcrete columns, deep mixed columns. Settlement is greatly reduced with the inclusion of a geosynthetic layer. The greater the stiffness of the geosynthetic

reinforcement, the smaller the settlement. The settlement also decreases with an increase in the stiffness of the piles.

The settlement analysis is carried out as for the unreinforced case. In the case of rigid piles, it is assumed that the entire load of the embankment is taken by the piles. Settlement calculations are carried out by available methods. In the case of other ground improvement techniques, settlement calculations are carried out on the basis of methods available for those techniques.

- BS8006 (1995) states that a plane of equal settlement exists at a height of 1.4(s-a) from the top of the pile caps in which s is spacing of the pile caps and a is the width of the pile cap.
- Terzaghi (1943) (cited in Han, 1999) carried out laboratory tests and found that the plane of equal settlements exists at 1.5-2.5 times the width of the void. If the height of the embankment is greater than this height then there is no problem of local depressions.

When two or more geogrids are used in the system, the differential settlement is effectively reduced. The strain in the upper reinforcement is 30% of the strain in the lower geogrid (Jenner et al., 1998 - cited in Han, 1999) although the upper geogrid is weaker than the lower one. The height of the equal settlement plane is reduced significantly by soil resistance. Soil resistance when increased to a certain limit can result in the equal settlement plane being lowered to the top of the upper geosynthetic layer in a multilayer system.

Finite element or finite difference methods provide a measure of the settlement expected in a GRPS embankment. This can be seen in the Plaxis models developed and discussed in Chapter 5.

3. VALIDATION OF NUMERICAL ANALYSIS

Estimation of axial bearing capacity plays an essential role in pile design. A part from semi-empirical and numerical methods, axial bearing capacity of piles can be either predicted by means of a maintain load test or dynamic load test. The latter test is based on wave equation analysis and it is provided by Pile driving analyzer (PDA). This chapter compares the axial capacity of pile obtained from PDA records and static load test with predicted axial capacities obtained using analytical, empirical and finite element analysis. From the results it can be observed that the use of Plaxis to estimate the capacity of a pile is in a good agreement with other estimation methods such as analytical and empirical methods.

3.1. Methods for estimation of Axial bearing capacity

3.1.1. Analytical Method

For the estimation of pile capacity, analytical methods were proposed by Vesic, Meyerhof and Coyle and Castello. The below equation has been recommended in most of the literatures.

$$P = q' N_q^* + \Sigma p \, \Delta l \, (K \, \sigma_v' \, \tan \delta) \qquad \text{Eqn.3.1}$$

Where,

- q' - Effective vertical Stress at the pile tip
- N_q^* - Bearing capacity factor
- K - Lateral earth pressure coefficient
- σ_v' - Average effective overburden pressure
- δ - Soil-pile friction angle
- P - Perimeter of the pile
- Δl - Incremental pile length
- A_p - Cross sectional area of the pile.

3.1.2. Empirical Method

Empirical correlations have been developed between the results of insitu test and the bearing capacity of piles. Meyerhof proposed correlations based on SPT (N) for which ultimate axial capacity (Equation 3.2) in homogeneous soil.

$$Q_u = A_p q_p + pl\, f_{ave}$$ Eqn.3.2

Where, $q_p(kN/m^2) = 40N\ L/D \leq 400\ N$ Eqn.3.3

$f_{ave}(kN/m^2) = 2\tilde{N}$ Eqn.3.4

Q_u - Ultimate axial capacity,

A_P - Area of the pile,

q_p - Ultimate stress,

D,L - Diameter and length of the pile respectively,

N - Average SPT (N) value almost 10D above and 4D below tip of the pile.

f_{ave} - Average unit skin resistance,

$\tilde{N}$ - Average SPT (N) value,

P - Perimeter of the pile.

3.1.3. Static Load Test (SLT) and Pile Dynamic Analysis Test (PDAT) Method

The objective of SLT is to develop a load- displacement curve. The load is applied in increment and allows the foundation to move under each increment, the increments of loads usually are 25, 50, 75, 100, and 200 percent of the design load. Failure load can be estimated from load displacement curve.

Pile Driving Analyzer (PDA) is relatively cost efficient, faster and easy to perform. The PDA test (Figure 3.2) is a quick test, hence; can be performed on more piles providing a bigger numbers of samples.

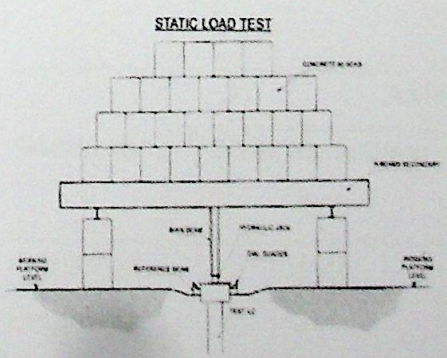

Figure 3.1 Static load test

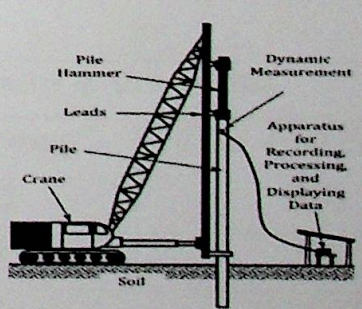

Figure 3.2 PDA test

UNIVERSITY OF MORATUWA
LIBRARY
SRI LANKA

3.2. Case Study

For this study SLT & PDAT data was selected from a study carried out for an 8 storied building for which driven piles were used as foundation. The pile diameter is 350mm and the piles were embedded about 10 to 12m depth. The Figure 3.3 shows the soil investigation data and other material properties in the above site.

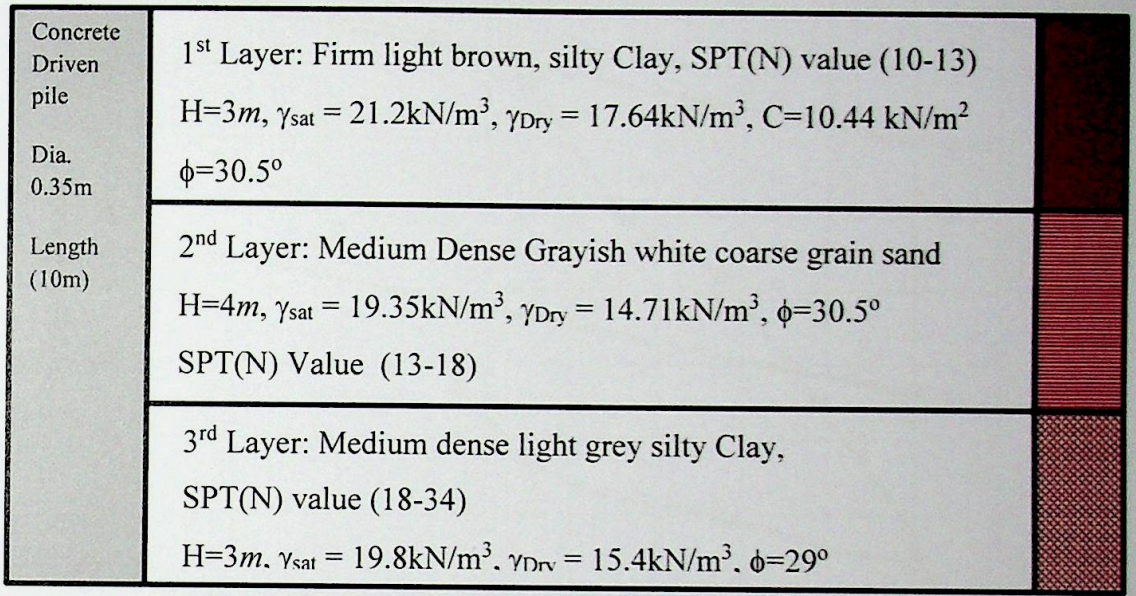

Figure 3.3 Soil profile according to site investigation (Used for Plaxis model as well)

The analytical and empirical analyses were performed by substituting the input data from Figure 3.3 into equations 3.1 through 3.4. The axial capacity obtained from analytical and empirical methods are tabulated in Table 3.1, however by picking up a value in between total axial bearing capacity can be considered to be 920.29 kN

Methods	**Axial Bearing Capacity of Driven Piles**		
	Skin Resistance (kN)	***End-Bearing (kN)***	***Total Axial Capacity (kN)***
Analytical	140	418	558
Empirical	360	923	1282.59

Table 3.1 Axial capacity of reference pile based on analytical and empirical methods styles

The result obtained from SLT is shown in Figure 3.4 below. According to that the Axial capacity of the pile is 780kN (obtained using Davisson's method). This load has taken by loading a 200% of an estimated design load of 450 kN

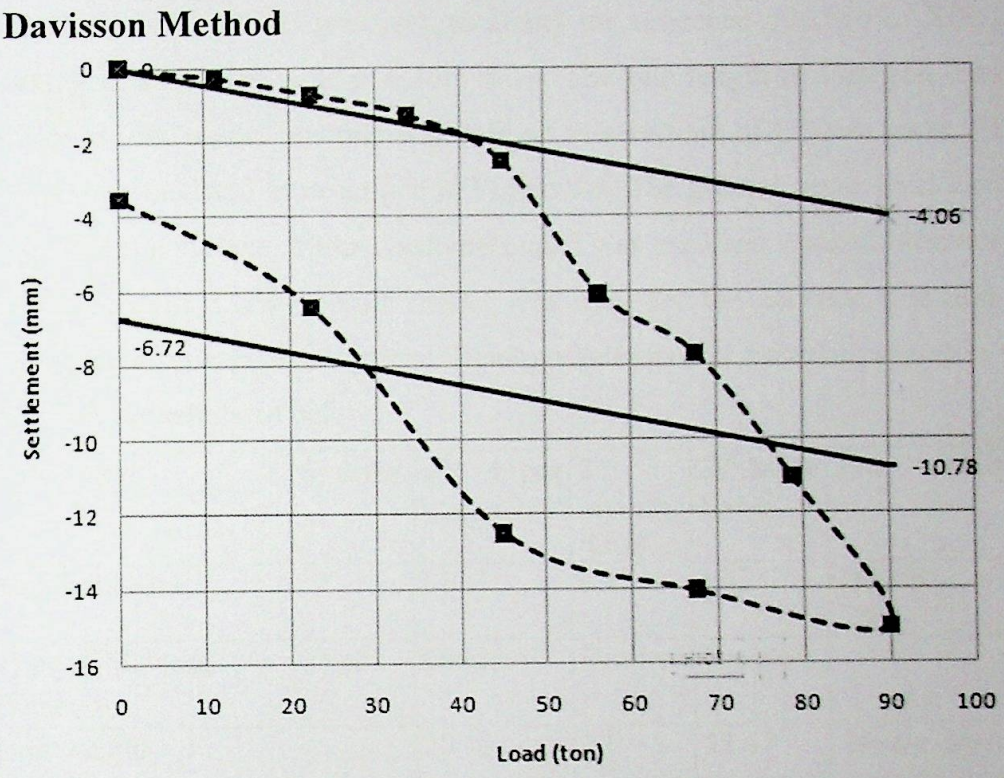

Figure 3.4 Load-displacement curve of static load test

7 nos of PDA tests has been carried out and results were shown in Table 3.2 below.

Pile No	Axial Bearing Capacity of Driven Piles			
	Length (m)	*Total Axial Capacity (kN)*	*Skin Resistance (kN)*	*End-Bearing (kN)*
Pile No.1	10.3	500	485	15
Pile No.2	8.8	452	438	14
Pile No.3	10	585	556	29
Pile No.4	10	603	576	27
Pile No.5	10.3	811	768	44
Pile No.6	10	770	733	36
Pile No.7	10	748	700	48

Table 3.2 Pile capacity based on PDA

In order to carry out the numerical analysis pile no. 06 can be selected due to the closeness of result from SLT and PDAT.

3.3. Numerical Analysis

An axisymmetric model was used to model the reference pile in PLAXIS 2D in a working area of 17m wide and 17m deep. The pile length is 10m and diameter is 350mm. In the model, the pile was defined as a column of 175mm width. The soil layers were modeled as described in Figure 3.3. The ground water level located 1m below the soil surface. Mohr-Coulomb model was used and drained behavior of soil was considered. Linear elastic model was used for the concrete pile and it was considered as non-porous material. Input parameters and material properties used in this study are tabulated below.

Parameter	**Symbol**	**1st layer Silty Clay**	**2nd layer Sand**	**3rd layer Sand**	**Pile**	**Unit**
Material Name		MC	MC	MC	Linear Elastic	-
Type of Material Behavior	Type	Drained	Drained	Drained	-	-
Unit weight	γ_{Unsat}	20.19	18	18.17	24	kN/m^3
Saturated unit weight	γ_{Sat}	21.2	19.5	19.63	24	kN/m^3
Horizontal Permeability	K_x	0.0001	1	1	0	m/Day
Vertical Permeability	K_y	0.0001	1	1	0	m/Day
E_{ref}		12060	15990	25860	-	kN/m^2
ν		0.2	0.2	0.2	0.15	-
Interface Reduction Factor	R_{inter}	1	1	1	-	-
Cohesion(Constant)	C_{ref}	10.44	0.06	0.08	-	kN/m^2
Friction Angle	ϕ	12	30.5	29	-	^{0}
ψ		0	0.5	0	-	^{0}
Earth pressure coefficient	$K_{0\,NC}$	0.79	0.49	0.51	-	-

Table 3.3 Material properties and input parameters

The plastic analysis was selected as type of analysis the load was applied by means of distributed load approach.

In load distribution approach, usually a load which is guessed to be more than failure load should be applied. Hence ultimate load obtained from empirical approach i.e. 1283 kN was considered as initial load for finite element analysis in PLAXIS. Using stage construction option, analysis was performed. Deformed mesh is shown in Figure 3.6.

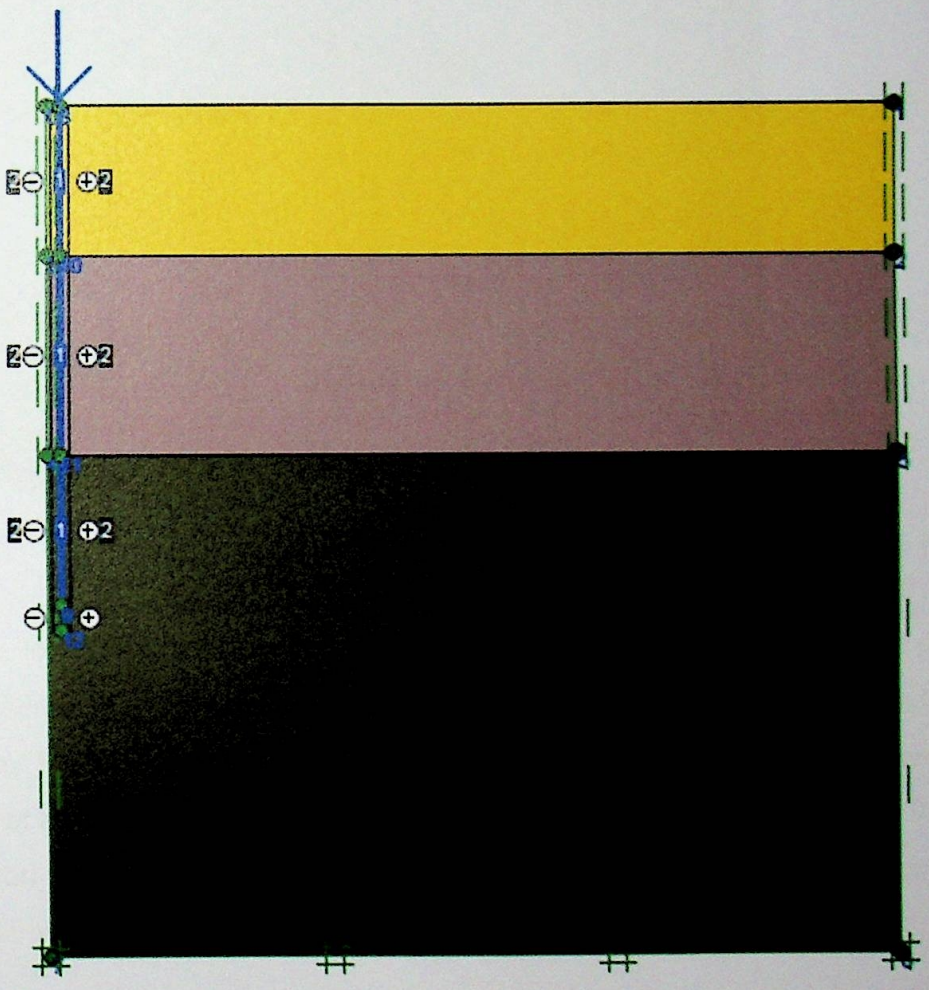

Figure 3.5 Global geometry of the reference pile

Along the length of the pile an interface had been modeled. In order to prevent stress oscillation in this stiff corner area, the interface was extended to 0.5 m below the pile`s tip inside the soil body. The strength reduction factor ($R_{inter}$) was considered to be equals to 1 as recommended by PLAXIS experts. Coefficient of earth pressure, Ko, was approximated by considering Jacky`s estimate of $K_o = 1\text{-}sin\Phi$.

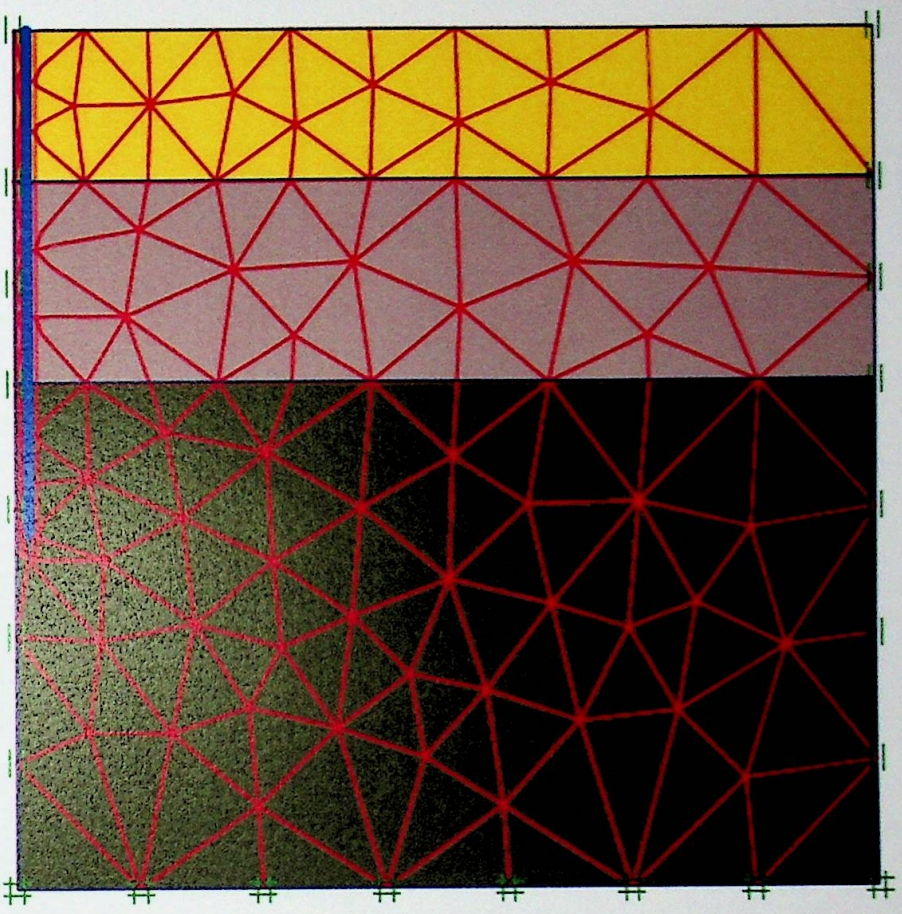

Figure 3.6 Deformed mesh of the reference pile

However, load displacement curve (Figure 3.7) plotted for the node point located at the top right side of the pile shows that soil body is collapsed under this load. The maximum load obtained from Figure 3.7 which is 919kN was considered for subsequent analysis. The result of final analysis confirms that the pile can carry 919kN and the soil will resist as shown schematically in Figure 3.8. Hence the total capacity of the pile was obtained to be 919kN.

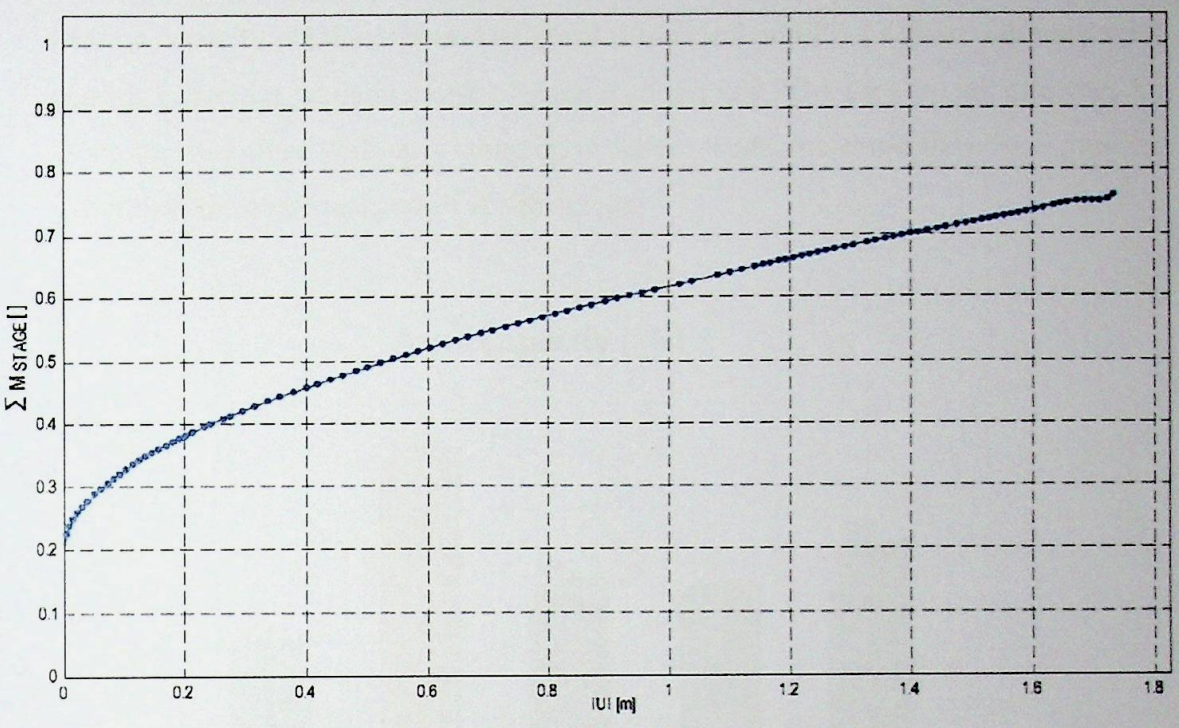

Figure 3.7 Load-displacement behavior of reference pile under empirical load (Soil body collapsing)

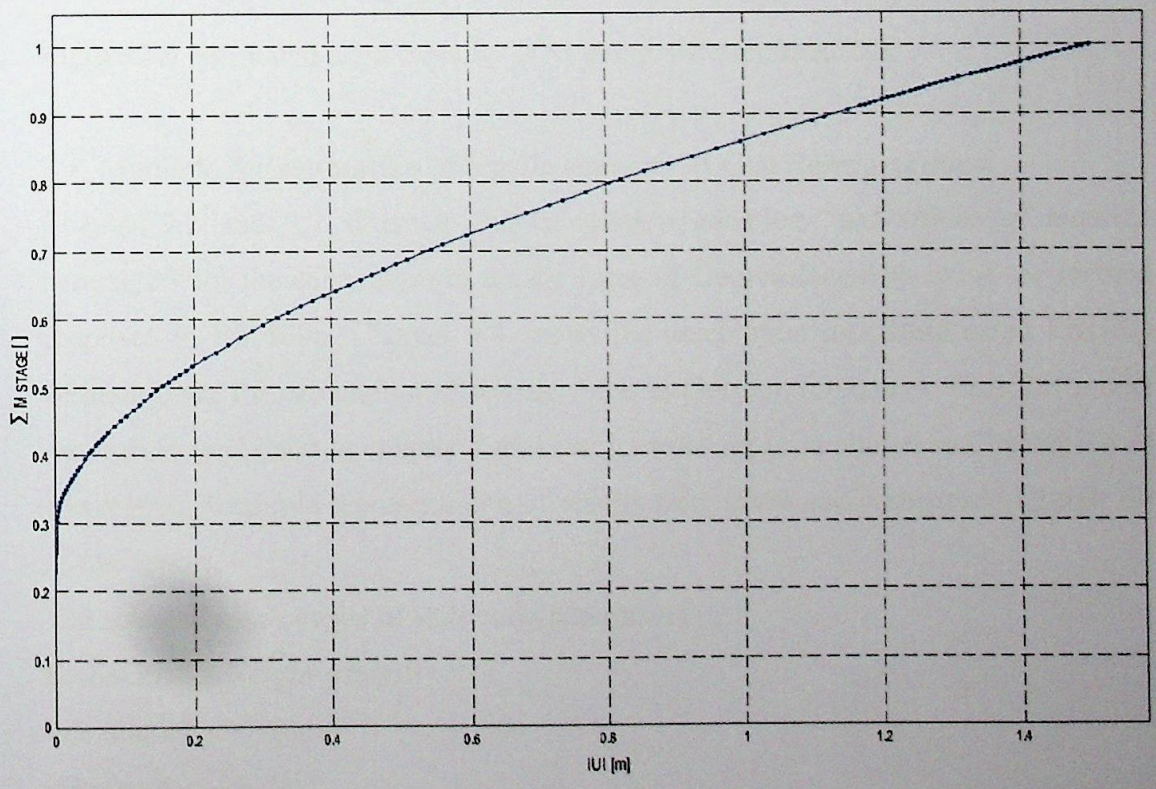

Figure 3.8 Load-displacement curve for ultimate load obtained from last analysis

The results of axial capacities were compared and plotted as in Figure 3.9. The axial bearing capacity obtained from Analytical, Empirical and PLAXIS are ultimate axial bearing capacities while in a case of static load test and PDA they are not ultimate. As this tests were done without loading up to failure loads, the result from SLT must be lower than the empirical and PLAXIS results.

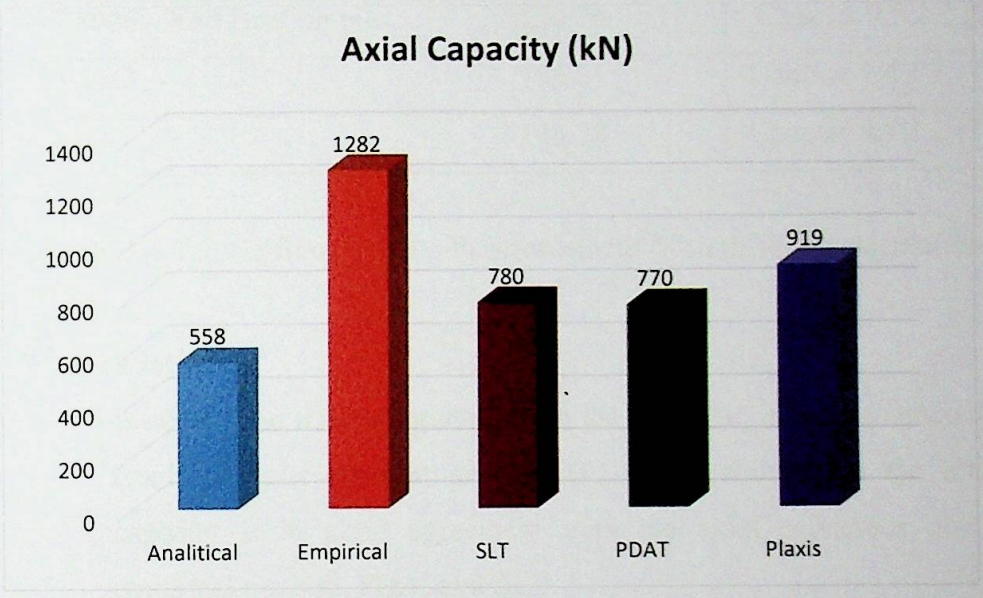

Figure 3.9 Estimated axial capacity (kN) using different methods

3.4. Methods for estimation of tensile capacity of Geo Reinforcement.

Chapter 9.2 and 9.3 illustrate the calculation equations and values of required parameters for the calculation of tensile force of Georeinfocement using the method proposed in BS 8006. Chapter 9.4 shows the calculation procedure using EBGEO German code for calculation of tensile force in Geo reinforcement. PLAXIS model was run as explained in chapter 5 and results were taken as shown in Chapter 9.5 of this report. A sample representation of results were taken and compared in Table 3.4 of this report.

The selected case consist of following parameters.

Embankment Height – 6.0 m

Pile diameter – 500mm

Pile spacing – 1.75m

Traffic Load – 30kPa

Asphalt Load – 6kPa

Stiffness of Geo reinforcement – 1500kN/m

Methods	Tensile force in Geo-reinforcement(kN/m)	Reference
BS 8006 – Friction pile	143.23	Chapter 9.2.1.4 (Table 9-4)
BS 8006 – End Bearing pile	130.76	Chapter 9.3.1.2 (Table 9-7)
EBGEO	185.21	Chapter 9.4.1.3 (Table 9-10)
Plaxis	146.58	Chapter 9.5.1.2 (Table 9-11)

Table 3.4 Tensile force on Geo Reinforcement from different calculation methods

3.5. Validation

- Based on the results obtained from the analyses, it can be concluded that the result of finite element analysis (PLAXIS) shows that the ultimate axial capacity is in good agreement with the axial capacities obtained using empirical method, PDA, and SLT.
- The tensile force calculated using BS 8006 (for both friction pile and End bearing piles) and Germen code is in a good agreement with output taken from Plaxis 8.2 for the same load case as shown.

4. THE BRITISH STANDARD & THE GERMAN STANDARD (EBGEO).

4.1. BS 8006

The British code BS8006 makes four assumptions to calculate the load on the geosynthetic reinforcement in a piled embankment (Figure 4.1):

1. The direct load on the pile caps may be calculated by using the equation of Marston for pipes, adapted for a piled embankment,
2. No support of soft soil
3. The load on the reinforcement (p'_r) is transferred into line-loads W_T on the strips of reinforcement between adjacent pile caps. BS8006 gives equations for this line-load W_T
4. The relation between the line-load W_T, the strain ε and the tensile stress in the geosynthetic reinforcement is given by the catenary equation:

$$T_{rp} = \frac{W_T(s-a)}{2a}\sqrt{1+\frac{1}{6\varepsilon}} \qquad \text{Eqn.4.1}$$

Where,

T_{rp} is the tensile stress in the reinforcement in kN/m', W_T is the line-load in kN/m' on the reinforcement strip between two adjacent piles, a is the size of a pile cap side in m, s the centre to centre distance between two piles in m (see Figure 2.5) and ε is the average strain in the reinforcement.

This report considers mainly the first three assumptions. First the load directly transferred to the piles, calculated with the equation of Marston (assumption 1) is considered, including the assumption of no support of soft soil (assumption 2). Then the load transferred to the Geosynthetically reinforcement (p'_r in kPa and W_T in kN/m', assumption 3) is calculated from both the assumption of vertical equilibrium and the equations of the British Standard. Finally the two resulting expressions for W_T are compared.

UNIVERSITY OF MORATUWA LIBRARY SRI LANKA

4.2. The load transferred directly to the pile cap (*P'c*: Marston)

As in most models for the design of a piled embankment, BS8006 starts with dividing the total load into two parts. The first part is the load p'_c (kPa) transferred directly to the piles. This load is larger than $\sigma'_v = \gamma H + p$, the average vertical load caused by then embankment and the surcharge load, due to the arching effect. In this equation, γ is the weight of the fill in kN/m^3, p is the surcharge load in kPa and H is the thickness of the embankment in m. The second part of the load, p'_r (kPa) is the load carried by the reinforcement in between the piles. This p'_r has not been worked out explicitly in the British Standard.

To derive p'_c, the load transferred directly to the piles, BS8006 bases itself on the 2D equations of Marston for a load on an infinitely long pipe (see for example Love et al 2003). Marston found:

$$\frac{p'_c}{\sigma'_v} = \frac{C_c a}{H} \qquad \text{Eqn.4.2}$$

Where,

C_c is the arching coefficient. For the 3D case of a piled embankment, BS8006 assumes that it is a good approach to square the right part of this equation of Marston (BS8006 page 105, in accordance with Jones et al, 1990):

$$\frac{p'_c}{\sigma'_v} = \left(\frac{C_c a}{H}\right)^2 \qquad \text{Eqn.4.3}$$

For this adapted Marston equation, BS8006 gives the following arching coefficients:

End-bearing piles

$$C_c = 1.95\frac{H}{a} - 0.18 \qquad \text{Eqn.4.4}$$

Friction and other piles

$$C_c = 1.5\frac{H}{a} - 0.07 \qquad \text{Eqn.4.5}$$

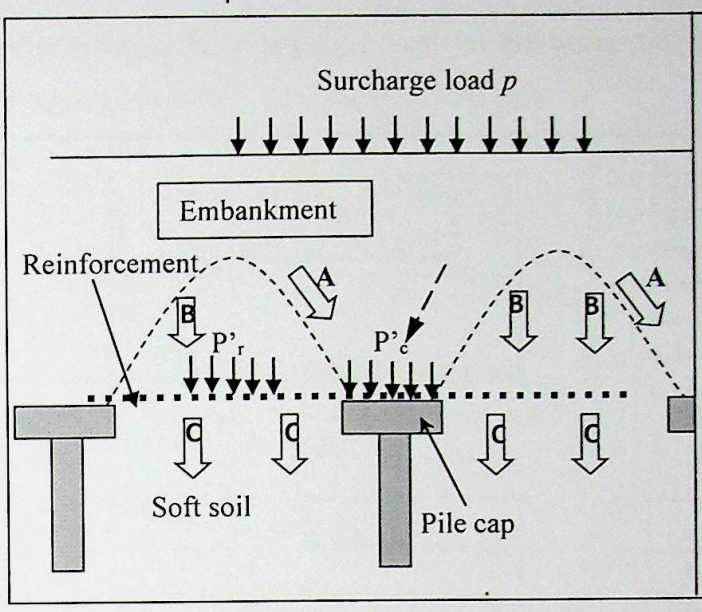

- Load portion A is transferred to piles gives p'_c (kPa) on pile caps,
- Load portion B (weight of soil below the virtual arch) gives load p' (kPa) working on the reinforcement. This load p', is transferred by the reinforcement to the piles. BS8006 does not calculate P'_r directly, but works with the line load W_r on the reinforcement strip just between two adjacent pile caps.

Figure 4.1 all design models for piled embankments divide the load into portions

In reality the ranges for a and H will be $0.3 < a < 1.25$ and $0.90 < H < 10.00$ leading to $0.03 < a/H < 1.39$. We observe:

- It is inconsistent to distinguish a C_c for end-bearing piles and for friction piles, while it is also assumed that the soft soil does not give any support. Assuming no soft soil support (a gap below the mattress), the geosynthetic reinforcement 'should not feel' whether a pile is end-bearing or frictional.
- For realistic values for a/H, there is not much variation in the values of p'_c/σ'_v (see Figure 4.2, left bottom graph)
- For a really thin embankment, (say H = 0.1 m, so a/H = 3 to 12.5), we should expect that p'_c/σ'_v approaches 1.0. This is not the case, as shown in the right bottom graph of Figure 4.2. We conclude that the adapted Marston equation and its values for C_c are not valid over the whole range of possible values of a/H in a piled embankment. Since it was derived for pipes in the soil, it is likely that the original Marston equation and the resulting values of C_c only apply to

We conclude that the adapted equations are disputable. However, the value of pc calculated with the adapted Marston equations is only used as an input parameter for the calculation of the load on the reinforcement. The load on the pile itself will be the

entire load, namely both the load on the geotextile (transferred to the pile by the geotextile) and the load directly on the pile.

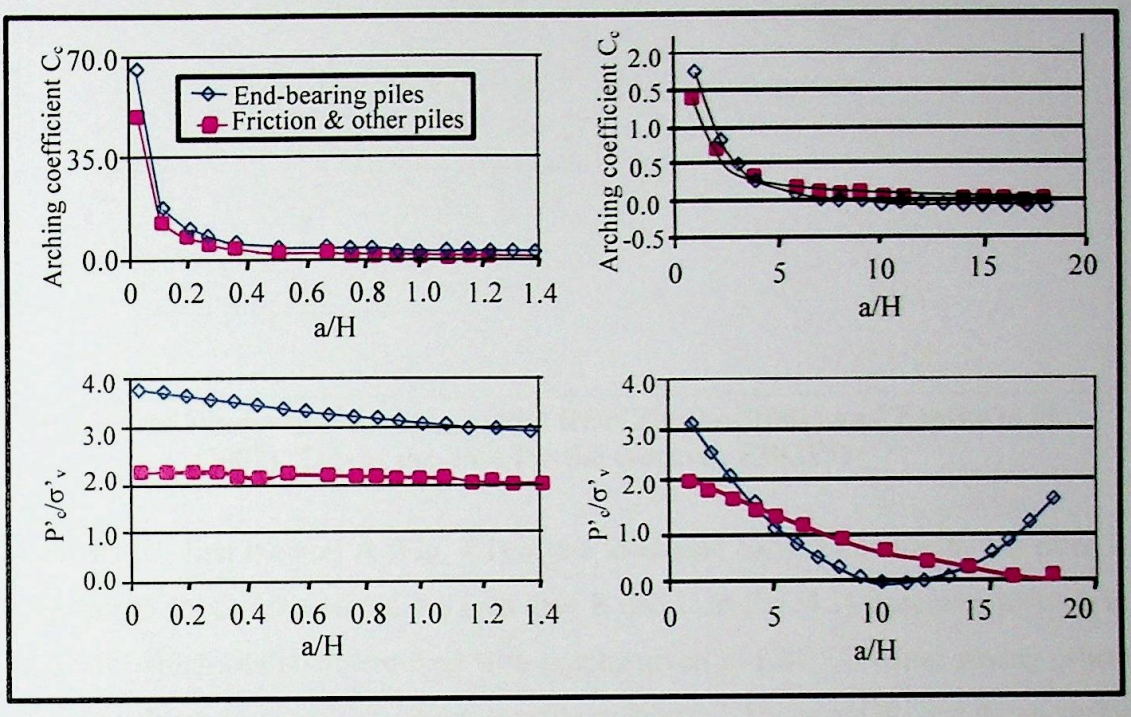

Figure 4.2: Figure 4.3 Left: realistic values for *a/H* give very similar values for p'_d/σ'_v. Right: for extreme values of a/H (thin embankments), the ratio p'_d/σ'_v does not approach the expected value of 1.0

4.3. German Draft Standard (EBGEO)

The design concept in the German EBGEO-Draft (Chapter 6.9 - EBGEO) is based on the work of Zaeske, 2001. The tensile force in the reinforcement due to vertical load and "arching" are dependent not only on the parameters in the BS 8006, but also on the internal friction angle of the fill material and the modulus of subgrade reaction k, kN/m³ of soft soil.

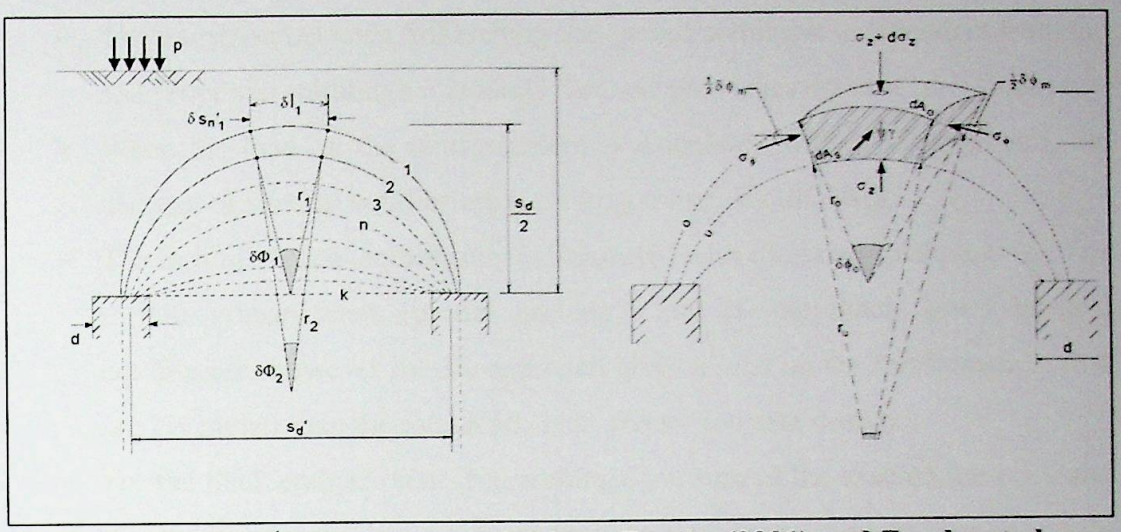

Figure 4.2a Theoretical arching model from Zaeske (2001) and Zaeske et al (2002). This is the base for the German EBGEO

In EBGEO, first the part A (Fig. 4.1) of the total load carried directly by the piles is calculated. Part of the rest of the load (say B and C in Fig. 4.1) generates a strain in the GR, which can be determined with graphs given in EBGEO using among others the time-dependent tensile modulus (tensile stiffness) J, kN/m of GR, and the modulus k, kN/m³ of soft soil in the sense of Winkler. Then, using J, the tensile force F, kN/m can be determined. The rest of the load (say part C in Fig. 4.1), which is not specifically calculated, is supposed to be carried by the soft subsoil.

The EBGEO-graphs mentioned above are given numerically by Heitz, 2006.

4.4. Conclusions

The British Code BS8006 shows some fundamental inconsistencies because of:

- The coefficients Cc presented in Marston's equations distinguish arching on end-bearing piles (unyielding) and on friction- or other piles, while the assumption of no support of soft soil is being made. These assumptions do not agree with each other.
- BS8006 is basically a 2D approach
- BS8006 makes the choice to consider a sort of arch. Load from above the arch is not 'felt' by the reinforcement (full arching). This top load is just ignored by putting it to zero. This is implemented in a way that the demand of vertical equilibrium is no longer met (for full arching).

- The transition between full arching and partial arching is independent from the soil properties, although it is likely that soil properties do have an influence.
- When the load on the reinforcement is calculated with a 3D approach, the demand of vertical equilibrium is no longer met, for all cases.
- The lack of vertical equilibrium is illustrated with illustrative calculations. For a thin embankment (partial arching), the 2D approach gives vertical equilibrium, however the 3D approach gives a load on the reinforcement that is 37% higher than the total load. This gives a too safe design.
- For the thick embankment (full arching), the sum of the load on the piles and the reinforcement is always lower than the total load. This can give an unsafe design.

❖ (The Majority of this chapter was copied from Van Eekelen et al (2008a and 2008b)

UNIVERSITY OF MORATUWA
LIBRARY
SRI LANKA

5. MODELING IN PLAXIS

5.1. PLAXIS.

PLAXIS is a range of finite element packages intended for 2D and 3D analysis of deformation, stability and groundwater flow in geotechnical engineering. Geotechnical applications require advanced constitutive models for the simulation of the non-linear and time-dependent behavior of soils. In addition, since soil is a multiphase material, special procedures are required to deal with hydrostatic and non-hydrostatic pore pressures in the soil. Although the modeling of the soil itself is an important issue, many geotechnical engineering projects involve the modeling of structures and the interaction between the structures and the soil. Plaxis 8.2 is equipped with special features to deal with the numerous aspects of complex geotechnical structures.

5.2. Numerical Modeling of the Geosynthetic Reinforced Pile Supported Embankments.

Numerical modeling of the geosynthetic reinforced pile supported embankments was performed in PLAXIS 8.2 – finite element software. Numerical modeling enables the designer to study the effects of embankment loading, the soil behavior in various conditions without resorting to simplified assumptions.

5.3. The Purpose of this Study.

In chapter 4, the study attempts to analysis the British Standard (BS8006) and German Draft Standard (EBGEO) available today for the design of Geosynthetic Reinforced Pile Supported Embankments. Heret a numerical analysis was carried out to study the effect of certain factors like pile area, stiffness of the geosynthetic reinforcement, height of the embankment, effect of the soil layer directly below the geogrid which are not considered by other available methods and the results from BS8006 and EBGEO.

5.4. Cases.

The study comprised two cases called case 1 (Thin Embankment) and Case 2 (Thick Embankment).

5.4.1. How to choose the cases.

In British Standards in 1995 (BS8006) consider thick embankment and thin embankment separately. But German Draft Standards did not distinguish embankment variations. To compare with the BS8006, two cases are selected as thick embankment and thin embankment.

5.4.2. Study.

The study comprised two cases called case 1 (Thin Embankment) and Case 2 (Thick Embankment). The axisymmetric unit cell was used to determine the strength of the geogrid. This axisymmetric model was utilized to show the effect of the soil support below the geosynthetic layer.

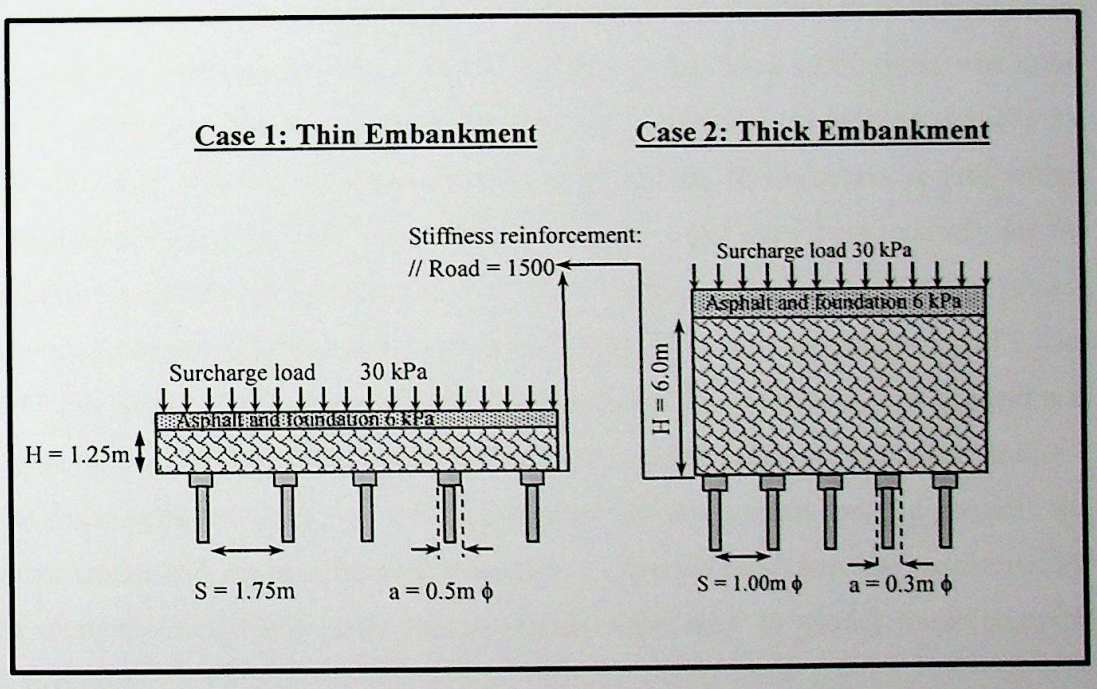

Figure 5.1 Case 1 Thin Embankment Case 2 Thick Embankment

5.4.3. Varieties Studies had to be carried out.

- Embankment Height variation vs. Forces (Axial force, Max.BM and Max.SF) on the Pile Head and Tensile force on the Geogrid parallel to the Road Axis.

- Centre to Centre distance between adjacent Piles variation vs. Forces (Axial force, Max.BM and Max.SF) on the Pile Head and Tensile force on the Geogrid parallel to the Road Axis.
- Pile Area variation vs. Forces (Axial force, Max.BM and Max.SF) on the Pile Head and Tensile force on the Geogrid parallel to the Road Axis.
- Internal Friction Angle variation vs. Force on the Pile Head and Tensile force on the Geogrid parallel to the Road Axis.
- Surcharge Load variation vs. Forces (Axial force, Max.BM and Max.SF) on the Pile Head and Tensile force on the Geogrid parallel to the Road Axis.

5.5. Axisymmetric Models

The piles in the Geosynthetic reinforced pile supported (GRPS) embankments were arranged in a rectangular pattern. A rectangular arrangement of the piles was taken into consideration. For this analysis, one pile was considered. In order to simplify the analysis, each pile was assumed to have its own zone of influence. A pile with a diameter of 0.5m and 0.3m were used for the case 1 and case 2 respectively for the analysis. A review of constructed GRPS embankments indicated that the typical spacing used in many projects is 1.5 to 4.5m (Han, 1999). An average spacing of 1.75m and 1.0m were used for this study for case 1 and case 2 respectively. The geogrid was placed on the top of the pile. These models were used to perform parametric studies. The four important elements involved in this complex system are, the geogrid, the embankment soil, the pile, the foundation soil. A drained condition was considered for the analysis. Simplified constitutive models were used to model these complex components.

5.5.1. Embankment Soil.

Material Properties.

Parameter	Name	Value	Unit
Material Name	Model	Hardening.	-
Type of Material Behavior	Type	Drain	-
Soil unit weight above phreatic level	γ_{Unsat}	20.0	kN/m^3
Soil unit weight below phreatic level	γ_{Sat}	20.0	kN/m^3
Permeability in horizontal direction	K_x	1.0	m/Day
Permeability in Vertical direction	K_y	1.0	m/Day
E_{50}^{ref}		20,000.00	kN/m^2
E_{oed}^{ref}		13,355.00	kN/m^2
E_{ur}^{ref}		80,000.00	kN/m^2
Interface Reduction Factor	R_{inter}	0.9	
Cohesion(Constant)	C_{ref}	1.0	kN/m^2
Power	m	0.5	
Friction Angle	ϕ	37.5	^{0}
$K_{0\,NC}$		0.391	

Table 5-1 Materials Properties Embankment Soil

5.5.1.1. The Hardening Soil Model

The "Hardening Soil Model" was used for the embankment fill. The Hardening Soil model is an advanced model for the simulation of soil behavior. The limiting states of stress in Hardening Soil Model are described by means of the friction angle, the cohesion and the dilatancy angle. However soil stiffness is described by using three different input stiffness: the triaxial loading stiffness, *E50,* the triaxial unloading stiffness, E_{ur} , and the odometer loading stiffness, E_{oed}. *As* average values for soil type. The hardening soil model accounts for stress-dependency of stiffness moduli, this means that all stiffness increase with pressure. Hence all three input stiffnesses relate to a reference stress, being usually taken as 100 kN/m^2.

UNIVERSITY OF MORATUWA LIBRARY SRI LANKA

5.5.2. Pile Concreting.

Material Properties

Parameter	Name	Value	Unit
Material Name	Model	Linear Elastic	-
Type of Material Behavior	Type	Undrain	-
Soil unit weight above phreatic level	γ_{Unsat}	25.0	kN/m^3
Soil unit weight below phreatic level	γ_{Sat}	25.0	kN/m^3
Permeability in horizontal direction	K_x	0	m/Day
Permeability in Vertical direction	K_y	0	m/Day
Young's Modulus (constant)	E_{ref}	2.3×10^7	kN/m^2
Poisson's Ratio	v	0.3	-
Interface Reduction Factor	R_{inter}	1.0	-

Table 5-2 Materials Properties Concrete (Pile)

5.5.2.1. Linear Elastic Model

The "Linear Elastic Model" was used for the Pile Concreting. Soil behavior is highly non-linear and irreversible. The linear elastic model is insufficient to capture the essential features of soil. The use of the linear elastic model may, however, be considered to model massive structures in the soil.

5.5.3. Foundation Soil

Material Properties.

Parameter	Name	Value	Unit
Material Name	Model	Soft soil Creep.	-
Type of Material Behavior	Type	Drain	-
Soil unit weight above phreatic level	γ_{Unsat}	13.0	kN/m^3
Soil unit weight below phreatic level	γ_{Sat}	13.0	kN/m^3
Permeability in horizontal direction	K_x	0.002	m/Day
Permeability in Vertical direction	K_y	0.001	m/Day
Modified Compression Index	λ^*	0.067	
Modified Swelling Index.	K^*	0.009	
Secondary Compression Index.	μ^*	0.0033	
OCR		1.1	
Interface Reduction Factor	R_{inter}	1.0	
Cohesion(Constant)	C_{ref}	0.001	
Poisson's Ratio	v	0.15	kN/m^2
Friction Angle	ϕ	20	^{0}

Table 5-3 Materials Properties Foundation Soil

The "Soft Soil Creep Model" was used for the Foundation Soil.

5.5.3.1. Soft Soil Creep Model

A specific feature of the soft soil is their high degree of compressibility. The "Soft soil model" in Plaxis was used to represent the weak foundation soil. This model is a Cam Clay type model used to simulate the behavior of normally consolidated clay or peat. The most important characteristic of the soft soil model is the stress dependent stiffness, which corresponds to the soft soil behavior. A logarithmic relation between the volumetric strain εv and mean effective stress, p' is assumed. As the model uses volumetric strain instead of void ratio, modified compression index λ^* is used in place of λ (Burland, 1965) (cited in Brinkgreve & Vermeer, 1998).

5.6. Plain strain Model

In order to study the effect of changes of Pile size, Pile spacing, Embankment Height, Traffic load, No. of GR layers and Spacing between GR layers on Pile axial load, Embankment settlement, Max. BM & SF of piles and Max. Tension of piles etc. this model was used. Following table summarizes the variation of each input used.

Case	Pile Dia. (mm)	Pile Spacing (m)	Emb. Height (m)	No.of GR layers	Spacing bet. GR layers (mm)	Traffic Load (kN)
Effect of change of Pile dia.	300 350 400 450 500 550	3	6	3	250	36
Effect of change of Emb. Height	450	3	2 3 4 5 6	3	250	36
Effect of change of GR Spacing	450	3	6	0 1 2 3 4	250	36
	450	3	6	2 3 4	300	36
	450	3	6	2 3 4	400	36
	450	3	6	2 3 4	500	36
Effect of change of Pile	450	1.50 3.00 4.50 6.00	6	3	250	36
Effect of change of Traffic load	450	3.00	6	3	250	25 30 35 40

Table 5-4 Input variation used for Plaxis models

5.6.1. Embankment Soil.

Material Properties.

Parameter	Name	Value	Unit
Material Name	Model	Mohr-Coulomb.	-
Type of Material Behavior	Type	Drain	-
Soil unit weight above phreatic level	γ_{Unsat}	18.0	kN/m^3
Soil unit weight below phreatic level	γ_{Sat}	20.0	kN/m^3
Permeability in horizontal direction	K_x	1.0	m/Day
Permeability in Vertical direction	K_y	1.0	m/Day
E_{ref}		22000	kN/m^2
ν		0.3	-
Interface Reduction Factor	R_{inter}	0.9	
Cohesion(Constant)	C_{ref}	0.8	kN/m^2
Friction Angle	ϕ	31	^{0}
ψ		1	^{0}
$K_{0\,NC}$	0.485		

Table 5-5 Materials Properties Embankment Soil (for plain strain model)

5.6.2. Pile Concreting.

Material Properties

Squire piles were used for modeling purpose. In order to feed the data to the Plaxis 2D model, the properties had to be converted as linear properties. Table 5-6 & Table 5-7 shows the used pile properties. The linear properties vary with pile size and the spacing of the piles.

Plate element was used to model the piles so that the Bending moment and Shear force can be observed.

Model: Elastic

Pile Width. (mm)	Pile spacing (m)	E_c (kN/mm^2)	A_p (mm^2)	I_p (mm^4)	$(EA)_{PSP}$ (kN/m)	$(EI)_{PSP}$ (kNm^2/m)	W (kN/m/m)	Eq. Dia(d)
300	3	28.0	9.00E+04	6.75E+08	8.40E+05	6.30E+03	0.72	0.008
350	3	28.0	1.23E+05	1.25E+09	1.14E+06	1.17E+04	0.98	0.010
400	3	28.0	1.60E+05	2.13E+09	1.49E+06	1.99E+04	1.28	0.013
450	3	28.0	2.03E+05	3.42E+09	1.89E+06	3.19E+04	1.62	0.017
500	3	28.0	2.50E+05	5.21E+09	2.33E+06	4.86E+04	2.00	0.021
550	3	28.0	3.03E+05	7.63E+09	2.82E+06	7.12E+04	2.42	0.025

Table 5-6 Materials Properties of Piles with the variation of pile size (for plain strain model)

Pile Width. (mm)	Pile spacing (m)	E_c (kN/mm^2)	A_p (mm^2)	I_p (mm^4)	$(EA)_{PSP}$ (kN/m)	$(EI)_{PSP}$ (kNm^2/m)	W (kN/m/m)	Eq. Dia(d)
300	1.5	28.0	9.00E+04	6.75E+08	1.68E+06	1.26E+04	1.44	0.008
300	3.0	28.0	9.00E+04	6.75E+08	8.40E+05	6.30E+03	0.72	0.008
300	4.5	28.0	9.00E+04	6.75E+08	5.60E+05	4.20E+03	0.48	0.008
300	6.0	28.0	9.00E+04	6.75E+08	4.20E+05	3.15E+03	0.36	0.008

Table 5-7 Materials Properties of Piles with the variation of pile spacing (for plain strain model)

5.6.3. Foundation Soil

The foundation soil was considered as consisted as three layers. First 8 m depth is peat, second 3m is sand and last three meter is Dense sand. The pile tip is penetrated two meters in to the Sand layer. Table 5-8 to Table 5-10 show the properties used.

Material Properties.

Parameter	Name	Value	Unit
Material Name	Model	Mohr-Coulomb	-
Type of Material Behavior	Type	UnDrained	-
Soil unit weight above phreatic level	γ_{Unsat}	15.0	kN/m^3
Soil unit weight below phreatic level	γ_{Sat}	18.0	kN/m^3
Permeability in horizontal direction	K_x	0.0001	m/Day
Permeability in Vertical direction	K_y	0.0001	m/Day
E_{ref}		3400	kN/m^2
ν		0.33	-
Interface Reduction Factor	R_{inter}	0.9	
Cohesion(Constant)	C_{ref}	4	kN/m^2
Friction Angle	ϕ	22	^{0}
ψ		0	^{0}
$K_{0\ NC}$	0.625		

Table 5-8 Materials Properties of Peat (for plain strain model)

Parameter	Name	Value	Unit
Material Name	Model	Mohr-Coulomb	-
Type of Material Behavior	Type	Drained	-
Soil unit weight above phreatic level	γ_{Unsat}	16.5	kN/m^3
Soil unit weight below phreatic level	γ_{Sat}	20	kN/m^3
Permeability in horizontal direction	K_x	1	m/Day
Permeability in Vertical direction	K_y	1	m/Day
E_{ref}		18000	kN/m^2
ν		0.3	-
Interface Reduction Factor	R_{inter}	0.9	
Cohesion(Constant)	C_{ref}	1	kN/m^2
Friction Angle	ϕ	31	^{0}
ψ		1	^{0}
$K_{0\ NC}$	0.485		

Table 5-9 Materials Properties of Sand (for plain strain model)

Parameter	Name	Value	Unit
Material Name	Model	Mohr-Coulomb	-
Type of Material Behavior	Type	Drained	-
Soil unit weight above phreatic level	γ_{Unsat}	17	kN/m^3
Soil unit weight below phreatic level	γ_{Sat}	21	kN/m^3
Permeability in horizontal direction	K_x	0.5	m/Day
Permeability in Vertical direction	K_y	0.5	m/Day
E_{ref}		20000	kN/m^2
ν		0.3	-
Interface Reduction Factor	R_{inter}	0.9	
Cohesion(Constant)	C_{ref}	2	kN/m^2
Friction Angle	ϕ	33	^{0}
ψ		3	^{0}
$K_{0\,NC}$	0.455		

Table 5-10 Materials Properties of Dense Sand (for plain strain model)

5.7. Methodology

The axisymmetric model helped in estimating the tensile strength in the geogrid. However, in order to study the entire system plane strain models of the entire system need to be developed.

Once the geometry of the model was developed, initial situation and initial stress state should be stated. This was done in the initial conditions part of the input program. The elements that are not active in the initial situation can be deselected. Initial stresses are developed by the K0-procedure. The water conditions can also be specified in the Geometry configuration mode.

Considering the symmetry, only half from the centre of the geometry for plain strain model was developed. However, in order to justify the results, a full geometry was analyzed.

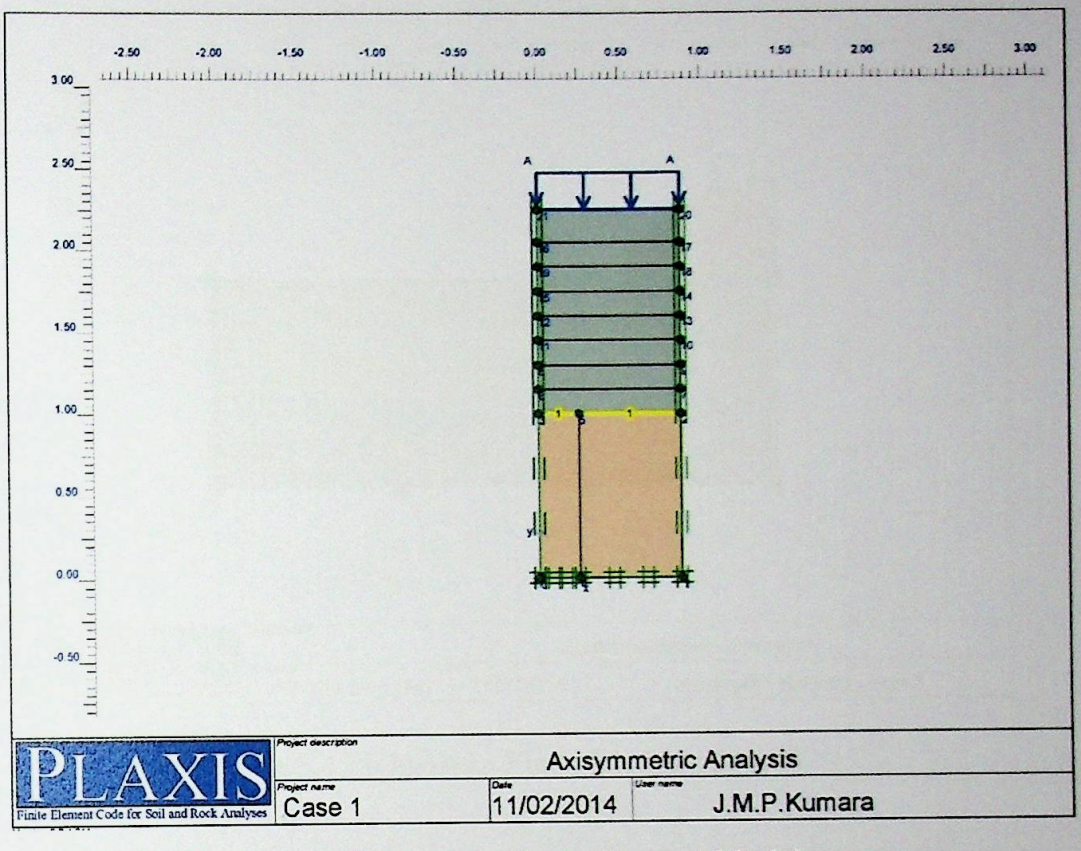

Figure 5.2 Axi-Symmetric Finite Element Model

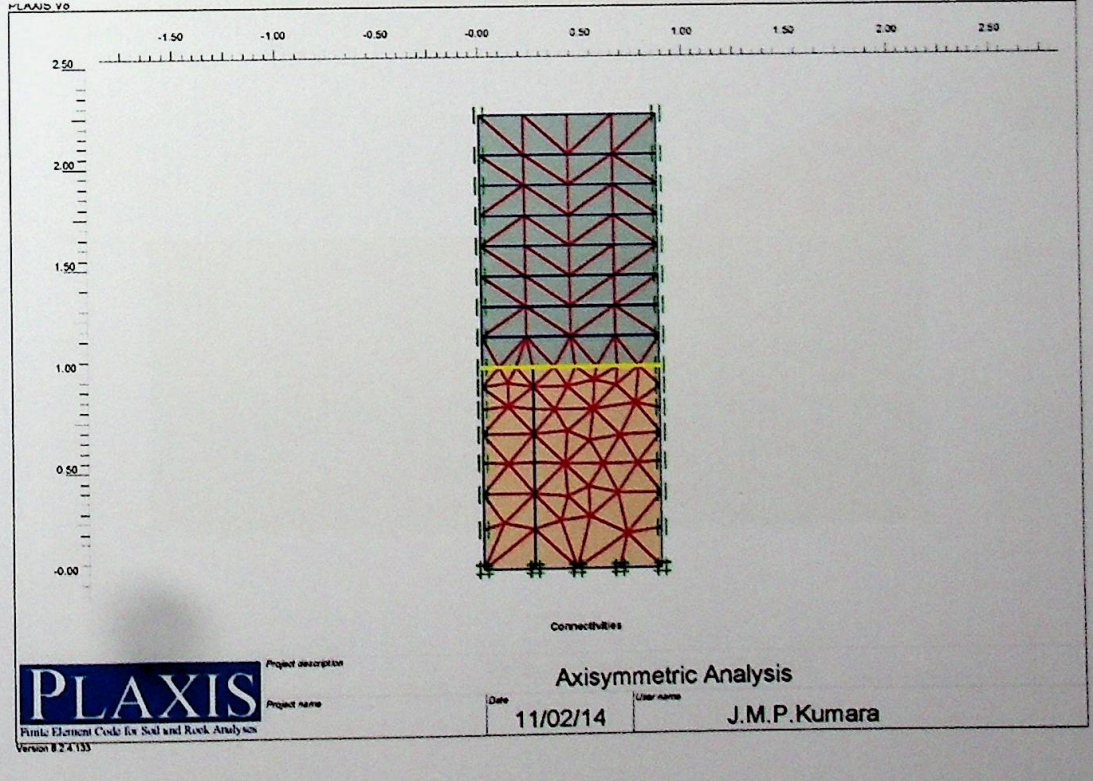

Figure 5.3 Axi-Symmetric Finite Element Model - Connectivity

UNIVERSITY OF MORATUWA
LIBRARY
SRI LANKA

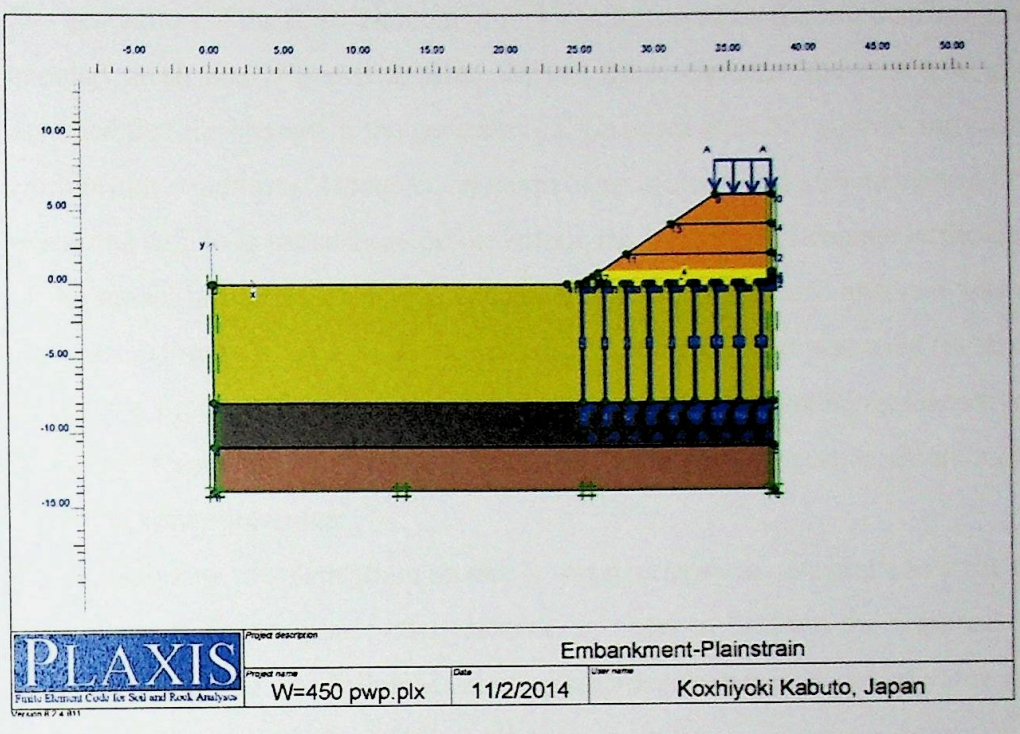

Figure 5.4 Plainstrain Finite Element Model

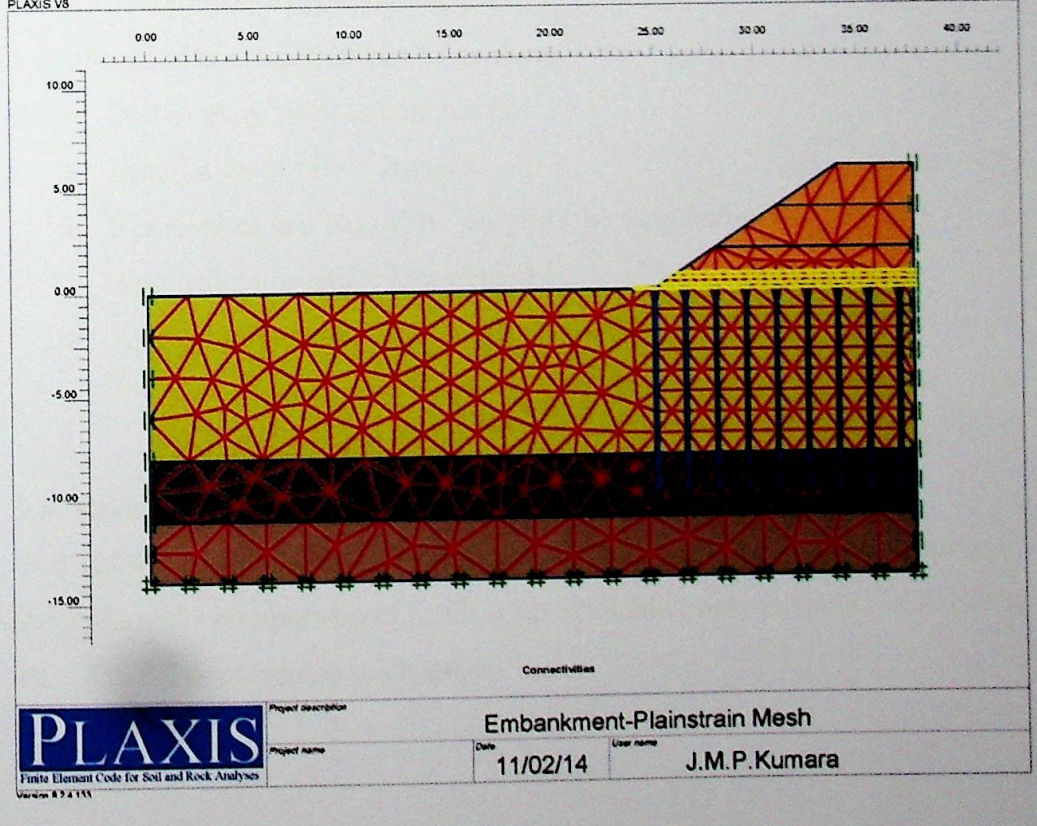

Figure 5.5 Plain Strain Finite Element Model - Connectivities

The generation of the finite element model was followed by the calculations phase. An updated mesh analysis was applied. In the finite element analysis it is generally assumed that the change in the geometry of the mesh does not significantly affect the equilibrium conditions. However, in cases of reinforced soil structures and the cases where the soft soils cause large deformations the influence of change in the geometry of the model has to be taken into consideration. Updated mesh analysis was used in such cases (Figure 5.3 & 5.5). A staged construction procedure was used for simulation of realistic process of construction. This option enabled activating and deactivating of elements, changing geometry configuration, changing properties of materials and changing water pressures.

While analyzing the plain strain model, it was necessary to consider about the time for dissipation of Excess pore water pressure. In order to find out the required time, an iteration procedure was followed. Final excess pore water pressure of value less than $4kN/m^2$ was expected after the final stage.

5.7.1. The phases of construction

The phases of construction can be given as

- Soil in place prior to construction
- Installation of pile + geogrid
- Removal of soil below the geogrid (the void below the geogrid)
- Application of embankment load
- Application of surcharge load

5.8. Results and Comparison.

The results of the study are presented in Appendix 1. The Axisymmetric Model Analysis and a comparison of result from available methods (BS8006 & EBGEO) and PLAXIS 8.2 is presented in chapter 6.

UNIVERSITY OF MORATUWA LIBRARY SRI LANKA

6. COMPARISON OF VARIOUS METHODS

- BS8006 Friction Pile. (STUIT)
- BS8006 End Bearing Pile.(KLEEF)
- German Draft –Standard.(EBGEO)
- PLAXIS 8.2

6.1. Introduction.

Three design models which are BS8006 (STUIT & KLEEF), EBGEO & PLAXIS 2D are considered here. The idea is analysis the reliability of these models, the models are considered mathematical and are validated by means of:

- Numerical calculations –
- Field measuring –
- Laboratory tests.

This report discusses the comparison of the three models with numerical calculations.

6.2. Two Cases

Two cases have been calculated. Case 1 has a thin embankment and case 2 has a thick embankment. The centre to centre distance of the piles and diameter of the piles are different, and other parameters are identical.

For both cases a number of varieties studies has been carried out, where always one parameter is varied whereas the remaining parameters are constant.

6.2.1. Calculations with EBGEO.

The calculations of the forces in the pile head are calculated using the formulas from EBGEO.

6.2.2. Calculations with Plaxis

Characteristics simple Plaxis model: -

- Axial symmetric model therefore
- pile extended in infinitely field,
- No edge impact.
- ground model: Hardening Soil

- Geogrid on the pile head.
- No interface between pile and ground (no interaction)

6.2.3. Calculations with BS8006.

The calculations of the forces in the pile cap are calculated using the formulas from 8.3.3 of BS 8006: 1995

The shape of the pile head is in the middle left. In 8.3.3.6 suggests that the plate a square or a round shape can have: a is the size (or diameter) of the pile cap.

In this report is based on a quadratic equation and square pile head. Compared with the EBGEO calculations, which are based rounded pile head, the surface of the pile head equal. The equivalent pile diameter is calculated by the following formula:

$a_{eq} = \sqrt{(0.25x \pi x D^2)}$

This creates the following dimensions:

- EBGEO., Round pile head ϕ 300mm BS8006 $a_{eq} = 266mm$
- EBGEO., Round pile head ϕ 500mm BS8006 $a_{eq} = 443mm$

In the charts appear in the BS8006 cases sometimes big jumps calculated to be. (Embankment variation). This is because of the distinction that is made between Bs8006 a thin and a thick embankment.

- Thin embankment $0.7x(s-a) \leq H \leq 1.4x(s-a)$
- Thick Embankment $H > 1.4x (s-a)$

The BS8006 formulas for the vertical load on the reinforcement not exclude each other as $H = 1.4 (sa)$.

6.2.4. Case 1 Thin Embankment.

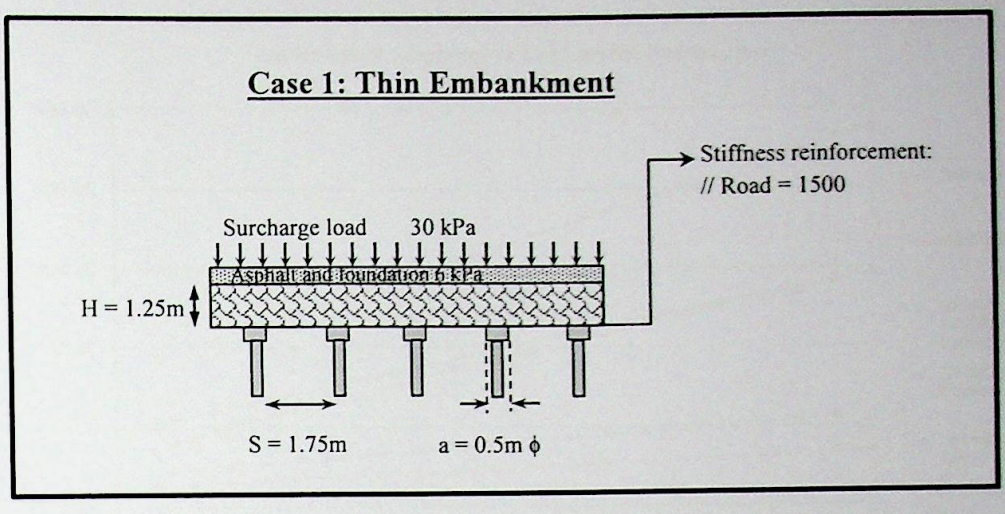

Figure 6.1 Thin Embankment

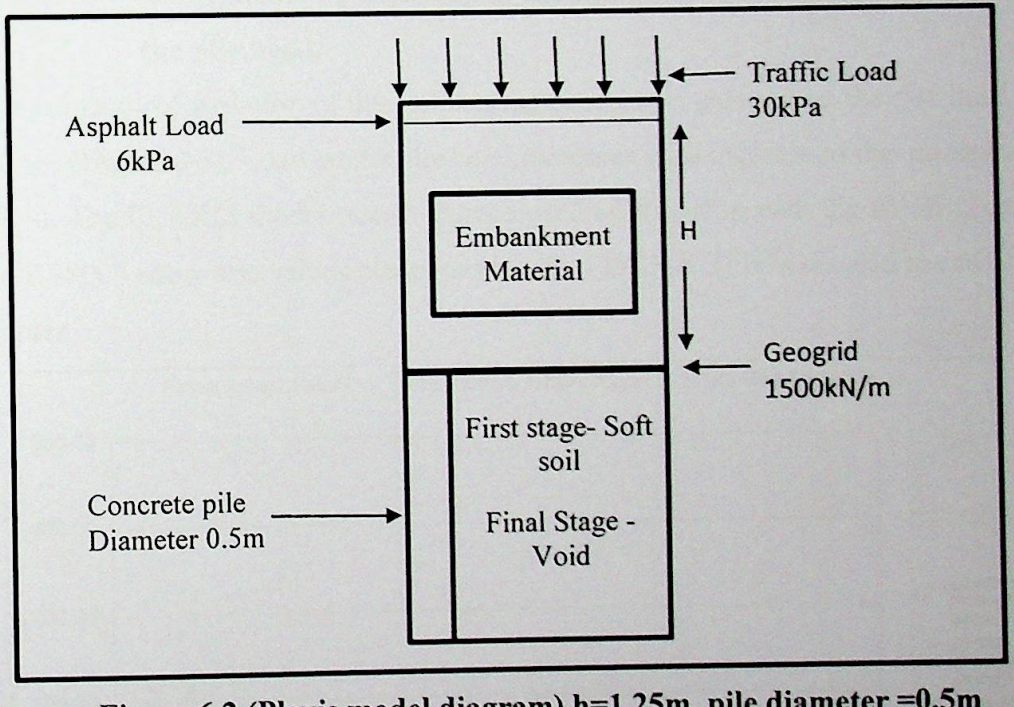

Figure 6.2 (Plaxis model diagram) h=1.25m, pile diameter =0.5m

From Figure 6.2 to 6.12 for case 1 show that a number of varieties studies has been carried out, where always one parameter is varied whereas the remaining parameters are constant. But in all cases Stiffness of the Geogrid kept as constant (1500kN/m).

6.2.4.1. Varieties Studies.

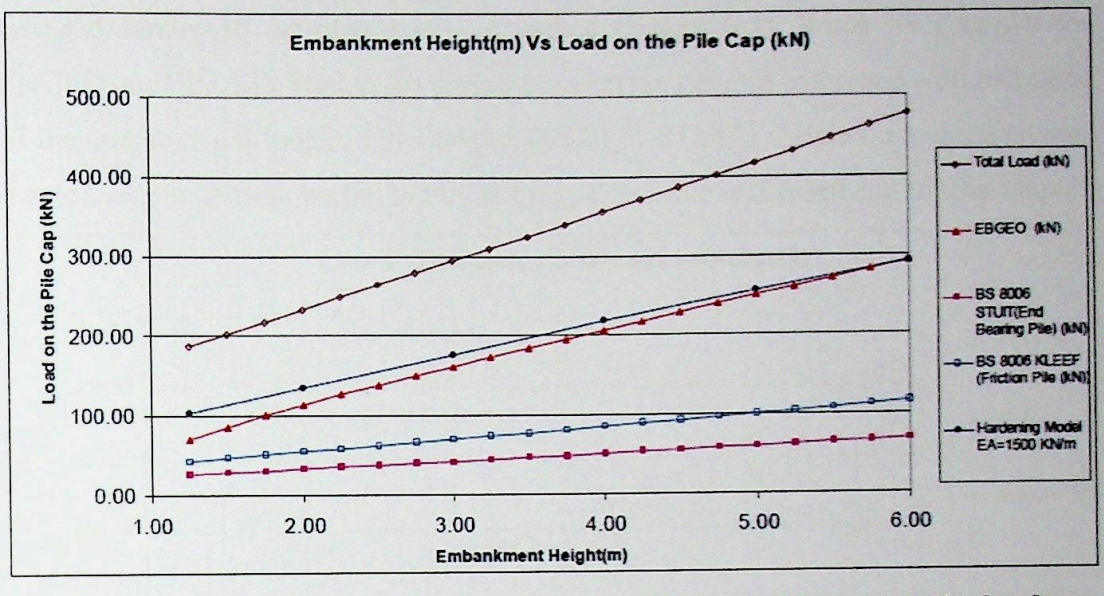

Figure 6.3: The influence of variation of the embankment height on the load on the pile head.

The influence of variation of the embankment height on the load on the pile head was studied (Figure 6-3). Load on the pile head increases with increase of the embankment height. The PLAXIS model results show closed relationship with the EBGEO results and BS8006 show less values compare with the EBGEO. This is disused at end of this chapter.

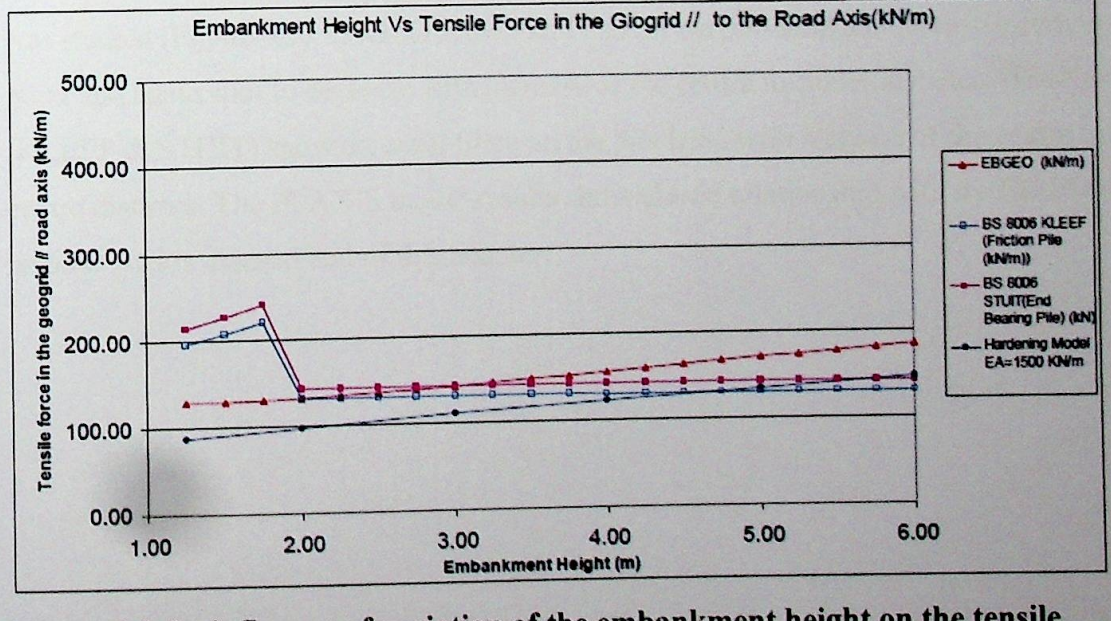

Figure 6.4 the influence of variation of the embankment height on the tensile force on the Geogrid

UNIVERSITY OF MORATUWA LIBRARY SRI LANKA

The influence of variation of the embankment height on the tensile force on the Geogrid parallel to the road axis was studied (Figure 6-4). When we consider the EBGEO and PLAXIS Model, the tensile force on the geogrid increased with increased of the embankment height, but BS8006 (KLEEF, STUIT) showed a sudden change due to the change from partial to full arching. This issue is disused end of this chapter.

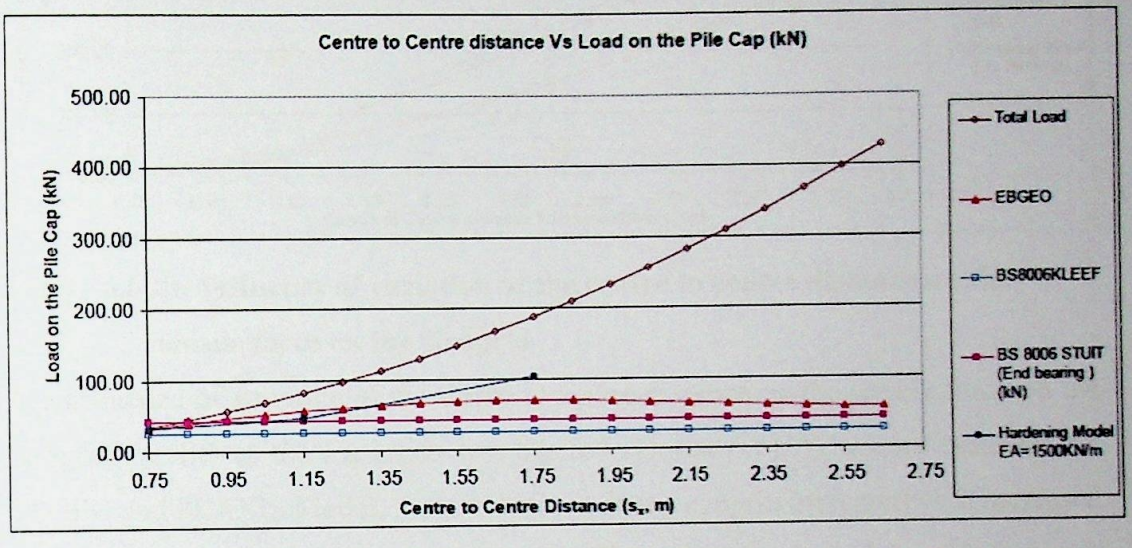

Figure 6.5 the influence of variation of the centre to centre distance on the load on the pile head.

The influence of variation of the centre to centre distance on the load on the pile head was studied (Figure 6.5). EBGEO show that Load on the pile head increases to a certain point and again start to decrease with increase of the centre to centre distance. BS8006 (KLEEF & STUIT) show constant force on the pile head with increase of the centre to centre distance. The PLAXIS model results show closed relationship with the EBGEO results. This is disused end of this chapter.

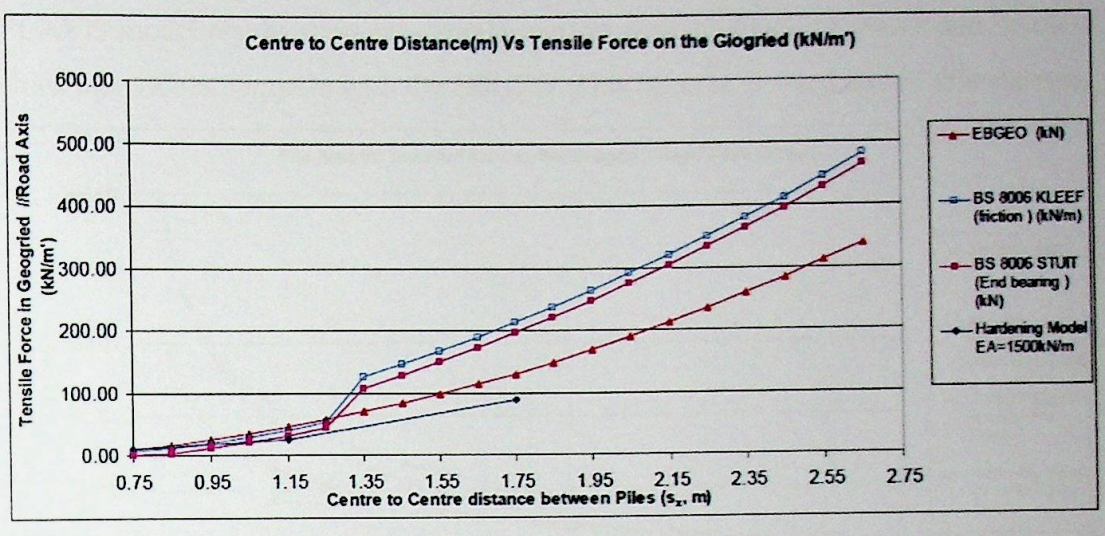

Figure 6.6 the influence of variation of the centre to centre distance on the tensile force on the Geogrid

The influence of variation of the centre to centre distance on the tensile force on the Geogrid parallel to the road axis was studied (Figure 6.6). When we consider the EBGEO and PLAXIS Model, the tensile force on the geogrid increased with increased of the embankment height, but BS8006 (KLEEF, STUIT) showed a sudden change due to the change from partial to full arching. This issue is disused end of this chapter.

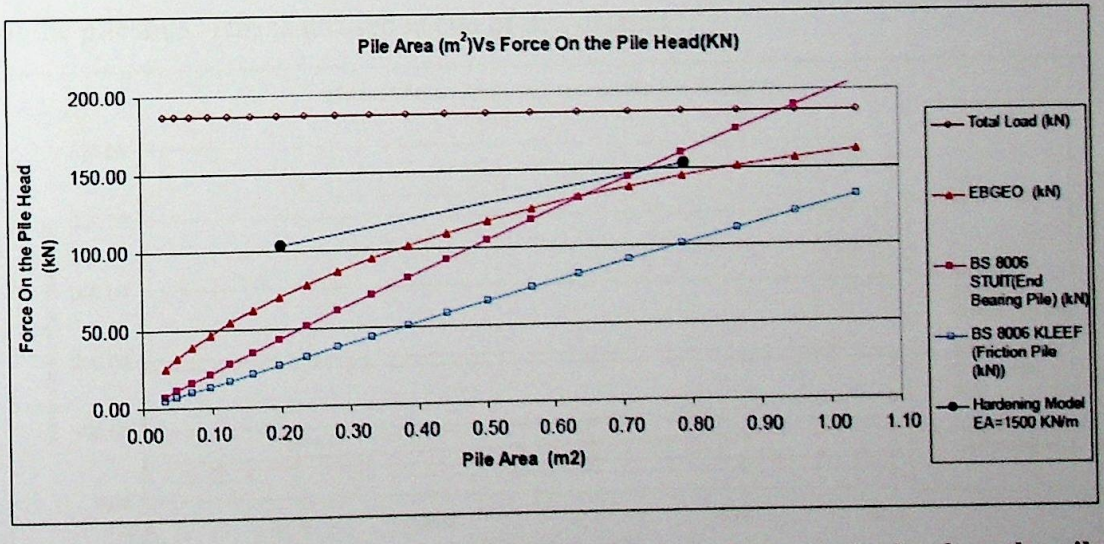

Figure 6.7 The influence of variation of the pile head area on the load on the pile head

The influence of variation of the pile head area on the load on the pile head was studied (Figure 6.7). Load on the pile head increases with increase of the pile head area. The

PLAXIS model results show closed relationship with the EBGEO results and BS8006 show less values compare with the EBGEO. This issue is disused end of this chapter.

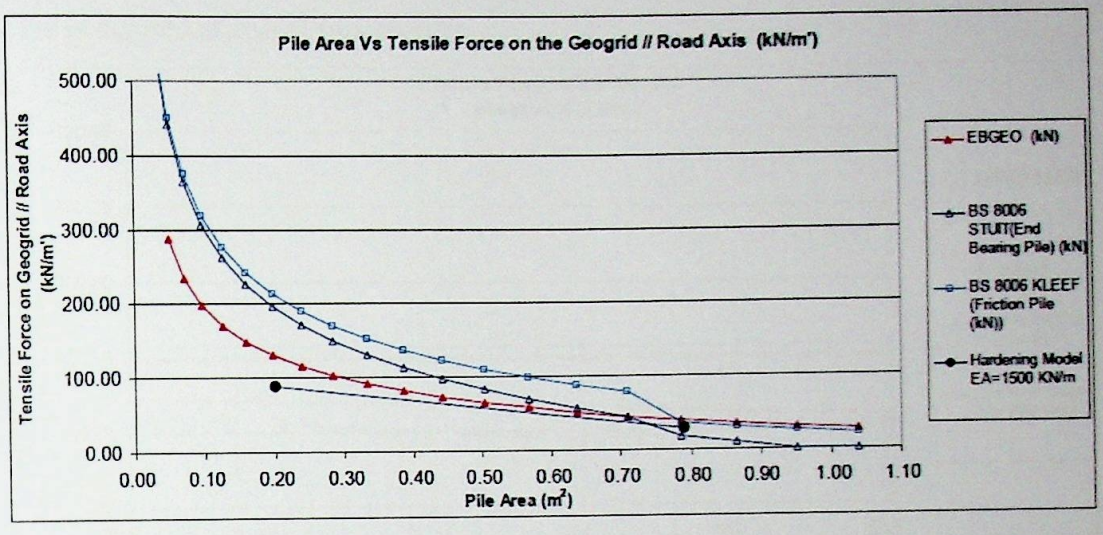

Figure 6.8 The influence of variation of the pile head area on the tensile force on the Geogrid.

The influence of variation of the pile head area on the tensile force on the Geogrid parallel to the road axis was studied (Figure 6.8). When we consider the BS8006, EBGEO and PLAXIS Model, the tensile force on the geogrid decreased with increased of the pile area. This is disused at end of this chapter

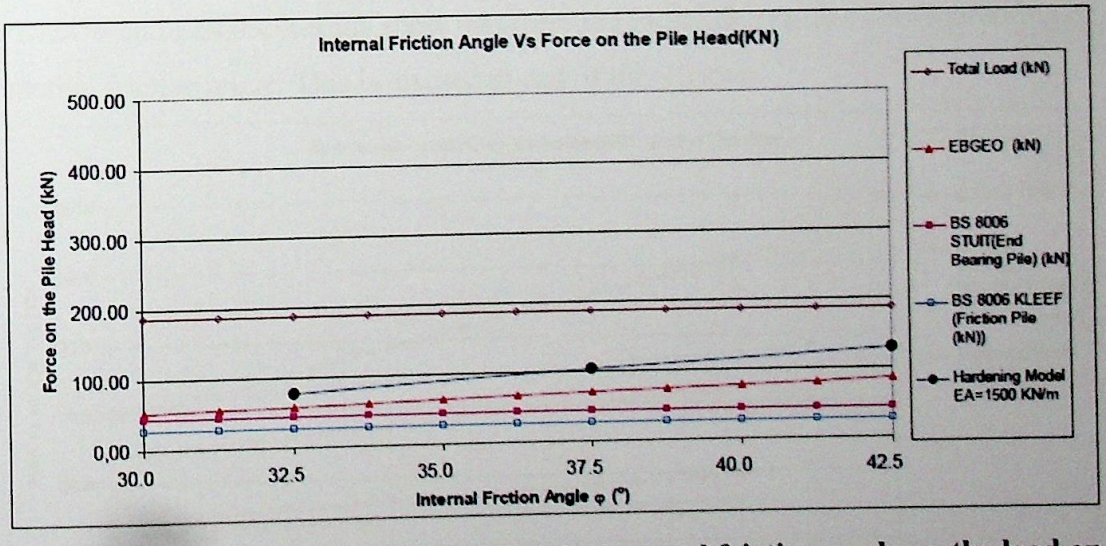

Figure 6.9 The influence of variation of the internal friction angle on the load on the pile head.

The influence of variation of the internal friction angle on the load on the pile head was studied (Figure 6.9). Load on the pile head keep as constant value with increase

of the internal friction angle in BS8006(KLEEF & STUIT) The PLAXIS and EBGEO results show that there are increasing values with increasing of internal friction angle. This is disused at end of this chapter.

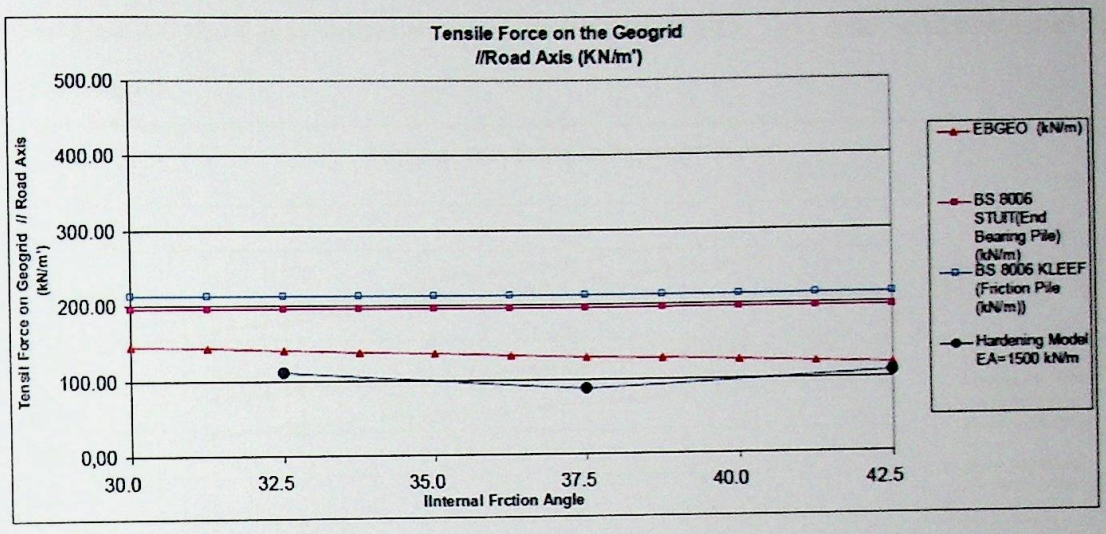

Figure 6.10 The influence of variation of the internal friction angle on the tensile force on the Geogrid

The influence of variation of the internal friction angle on the tensile force on the geogrid head was studied (Figure 6.10). Tensile force on the geogrid keep as constant value with increase of the internal friction angle in BS8006(KLEEF & STUIT) The PLAXIS and EBGEO results show that there are increasing values with increasing of internal friction angle. This is disused at end of this chapter.

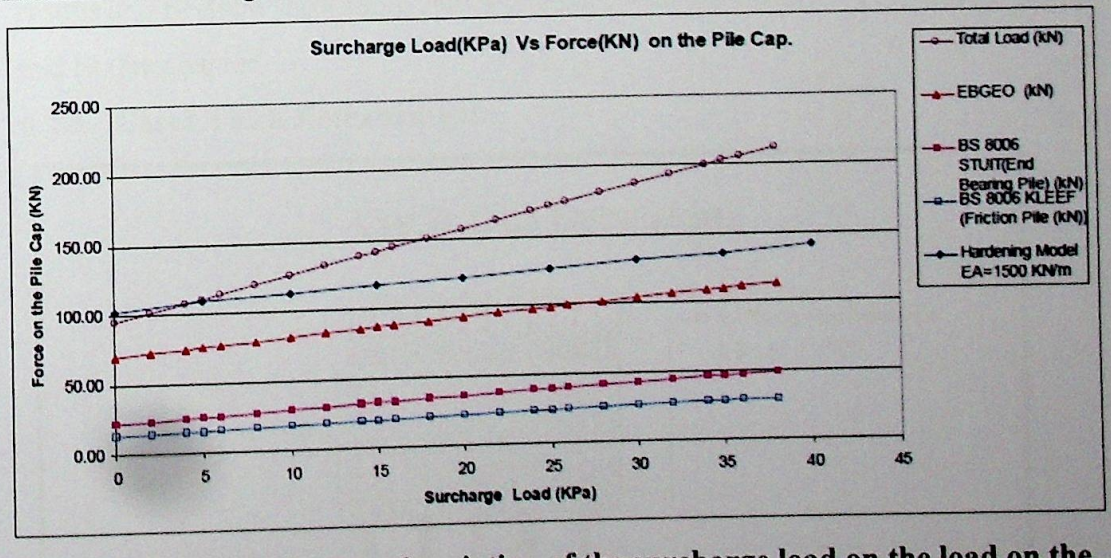

Figure 6.11: The influence of variation of the surcharge load on the load on the pile head.

The influence of variation of the surcharge load on the load on the pile head was studied (Figure 6.11). Load on the pile head increases with increase of the surcharge load. The PLAXIS model results show closed relationship with the EBGEO results and BS8006 show less values compare with the EBGEO. This issue is disused end of this chapter.

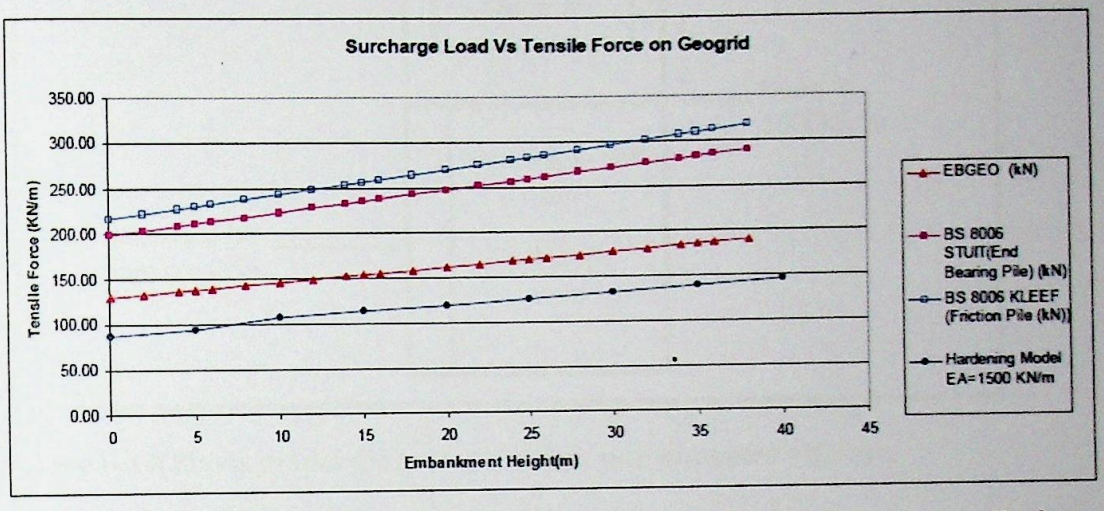

Figure 6.12 The influence of variation of the surcharge load on the tensile force on the geogrid

The influence of variation of the surcharge load on the tensile force on the geogrid was studied (Figure 6.12). Tensile Force on the geogrid increases with increase of the surcharge load. The PLAXIS model results show closed relationship with the EBGEO results and BS8006 show large values compare with the EBGEO. This issue is disused end of this chapter.

6.2.5. Case2 Thick Embankment.

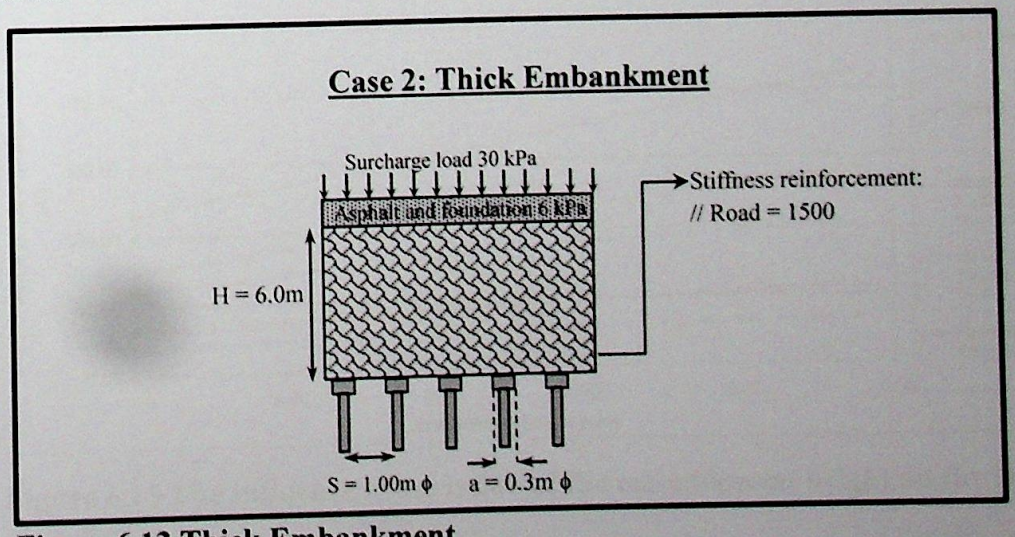

Figure 6.13 Thick Embankment

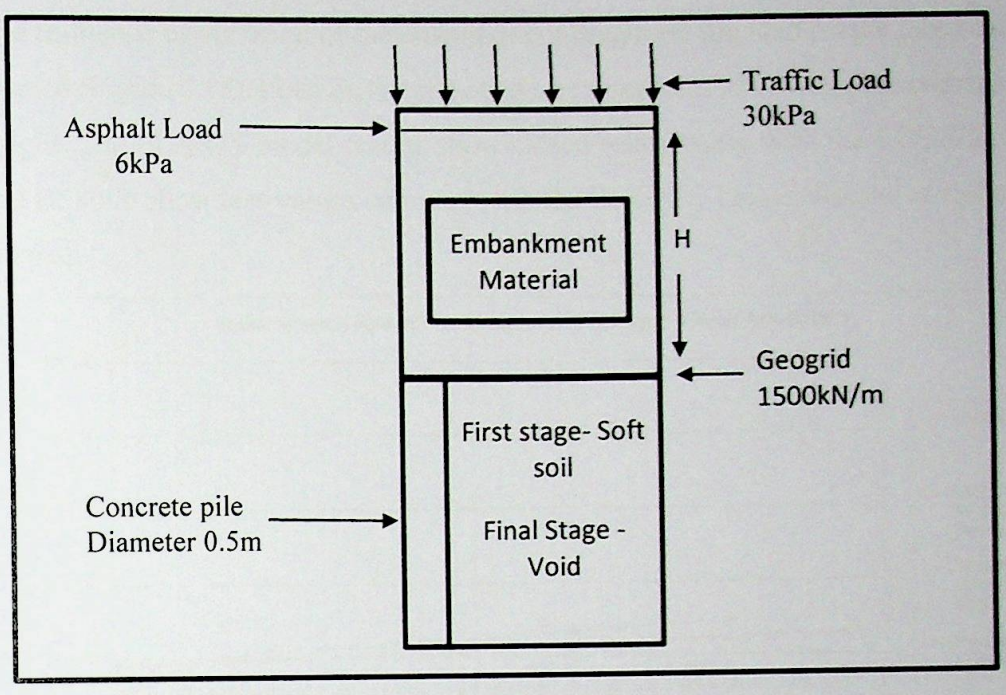

Figure 6.14(Plaxis model diagram) h=6.0m, pile diameter =0.3m

From Figure 6.15 to 6.24 for case 2 show that a number of varieties studies has been carried out, where always one parameter is varied whereas the remaining parameters are constant. But all cases Stiffness of the Geogrid kept as constant (1500kN/m) except variation of geogrid stiffness.

6.2.5.1. Variety of Studies.

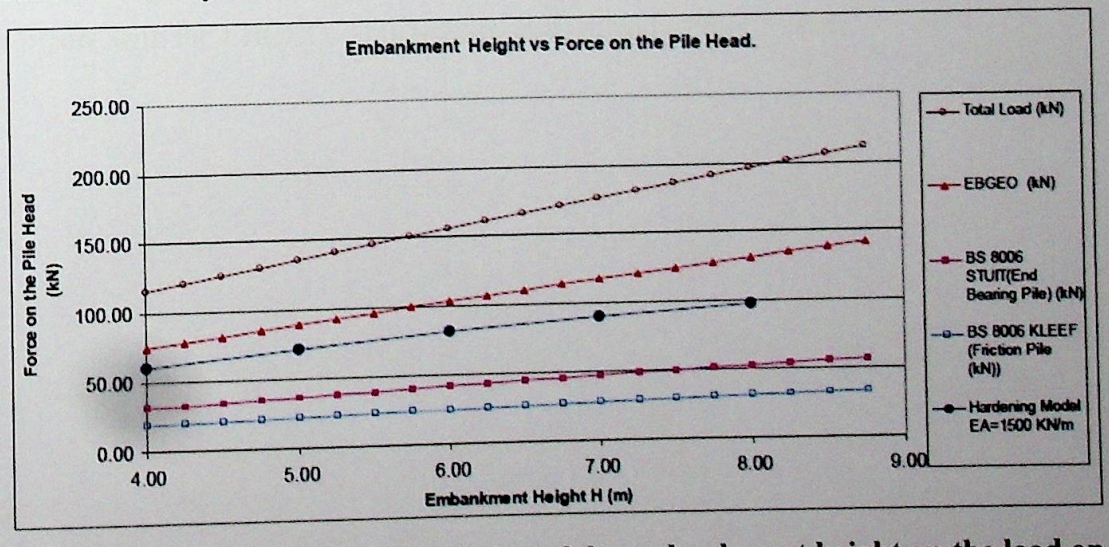

Figure 6.15 The influence of variation of the embankment height on the load on the pile head.

The influence of variation of the embankment height on the load on the pile head was studied (Figure 6.15). Load on the pile head increases with increase of the embankment height. The PLAXIS model results show closed relationship with the EBGEO results and BS8006 show less values compare with the EBGEO. This is disused at end of this chapter.

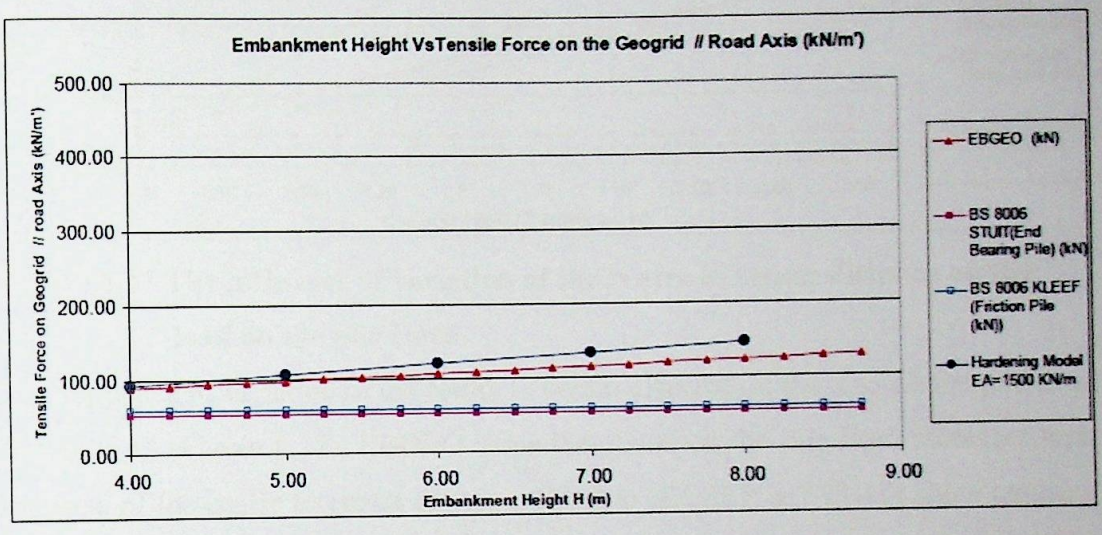

Figure 6.16 The influence of variation of the embankment height on the tensile force on the Geogrid

The influence of variation of the embankment height on the tensile force on the Geogrid parallel to the road axis was studied (Figure 6.16). Tensile force on the Geogrid increases with increase of the embankment height. The PLAXIS model results show closed relationship with the EBGEO results and BS8006 show less values compare with the EBGEO. This issue is disused end of this chapter.

UNIVERSITY OF MORATUWA LIBRARY SRI LANKA

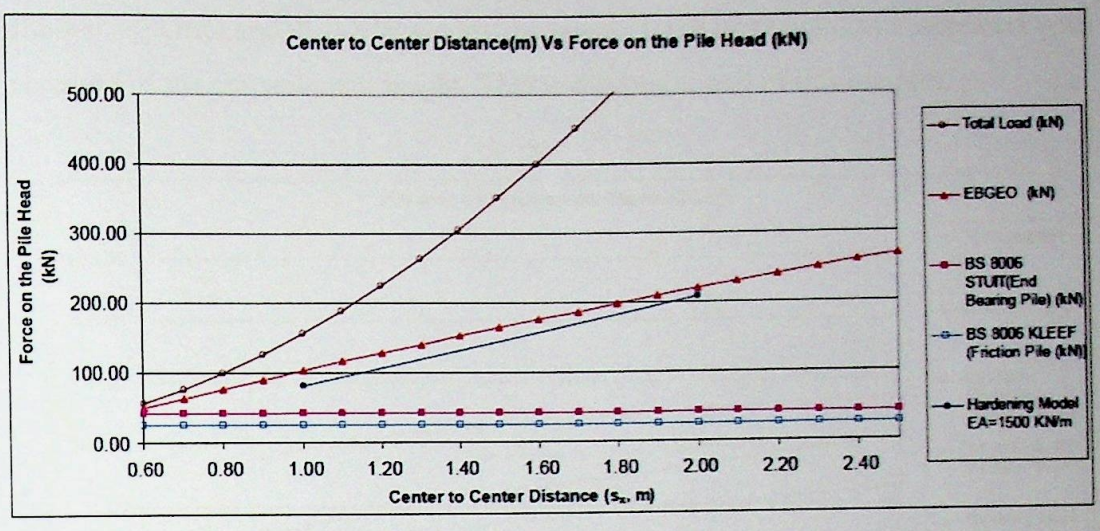

Figure 6.17 The influence of variation of the centre to centre distance on the load on the pile Head

The influence of variation of the centre to centre distance on the load on the pile head was studied (Figure 6.17). EBGEO show that Load on the pile head increases with increase of the centre to centre distance. BS8006 (KLEEF & STUIT) show constant force on the pile head with increase of the centre to centre distance. The PLAXIS model results show closed relationship with the EBGEO results. This is disused end of this chapter.

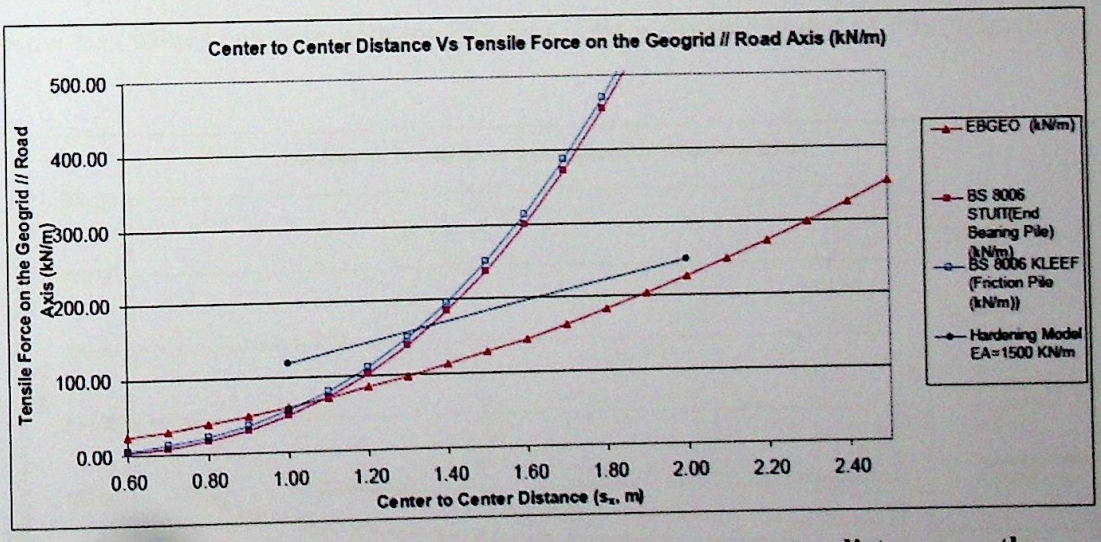

Figure 6.18 The influence of variation of the centre to centre distance on the tensile force on the Geogrid

The influence of variation of the centre to centre distance on the tensile force on the Geogrid parallel to the road axis was studied (Figure 6.18). When we consider the

BS8006, EBGEO and PLAXIS Model, the tensile force on the geogrid increased with increased of the embankment height. This is disused at end of this chapter.

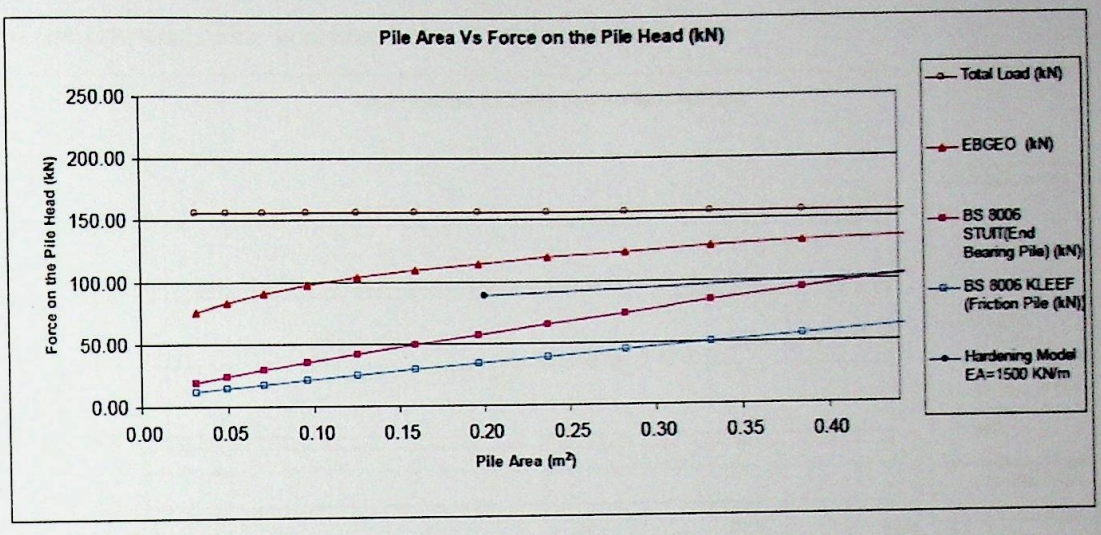

Figure 6.19 The influence of variation of the pile head area on the load on the pile head

The influence of variation of the pile head area on the load on the pile head was studied (Figure 6.19). Load on the pile head increases with increase of the pile head area. The PLAXIS model results show closed relationship with the EBGEO results and BS8006 show less values compare with the EBGEO. This is disused at end of this chapter...

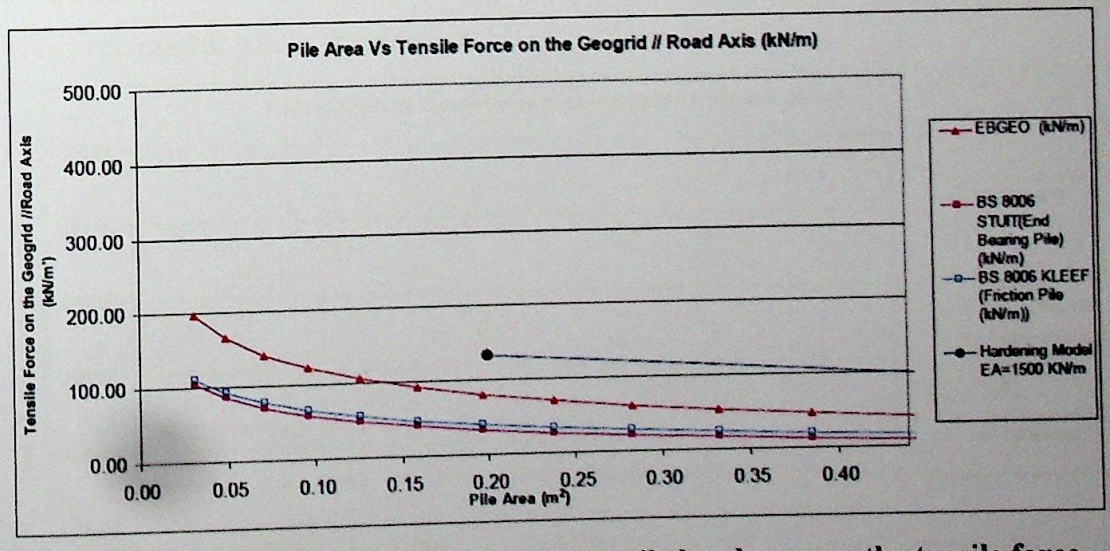

Figure 6.20 The influence of variation of the pile head area on the tensile force on the Geogrid.

The influence of variation of the pile head area on the tensile force on the Geogrid parallel to the road axis was studied (Figure 6.20). When we consider the BS8006, EBGEO and PLAXIS Model, the tensile force on the geogrid decreased with increased of the pile area. This is disused at end of this chapter.

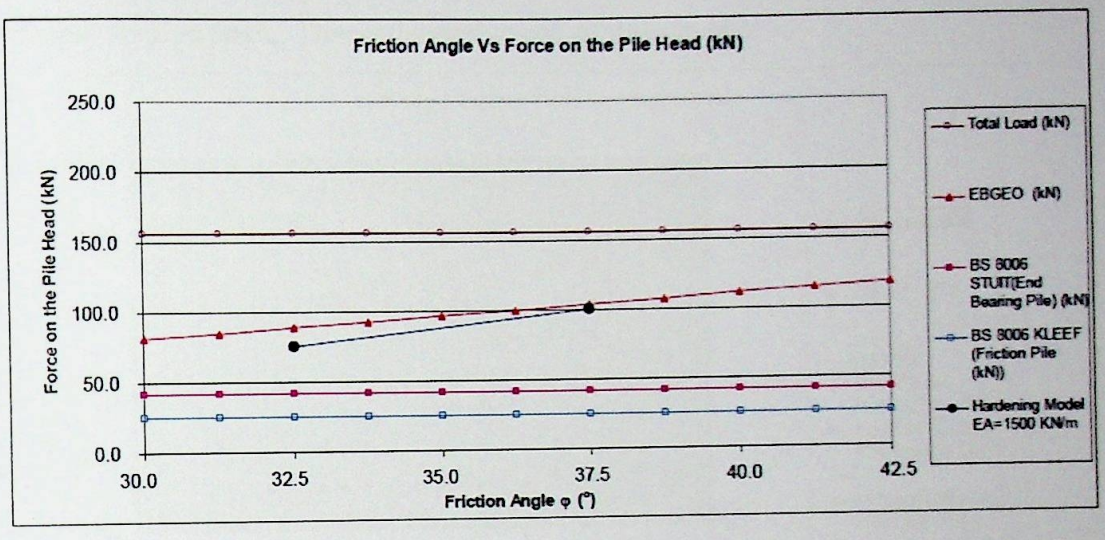

Figure 6.21 The influence of variation of the internal friction angle on the load on the pile head.

The influence of variation of the internal friction angle on the load on the pile head was studied (Figure 6.21). Load on the pile head keep as constant value with increase of the internal friction angle in BS8006(KLEEF & STUIT) The PLAXIS and EBGEO results show that there are increasing values with increasing of internal friction angle. This is disused at end of this chapter.

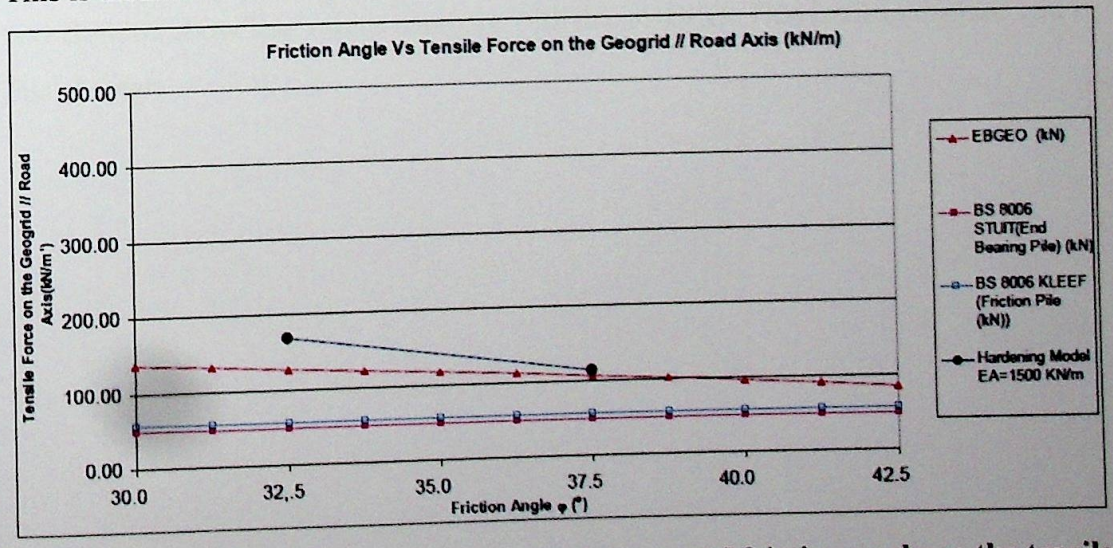

Figure 6.22 The influence of variation of the internal friction angle on the tensile force on the geogrid

The influence of variation of the internal friction angle on the tensile force on the geogrid head was studied (Figure 6.22). Tensile force on the geogrid keep as constant value with increase of the internal friction angle in BS8006(KLEEF & STUIT) The PLAXIS and EBGEO results show that there are increasing values with increasing of internal friction angle. This is disused at end of this chapter.

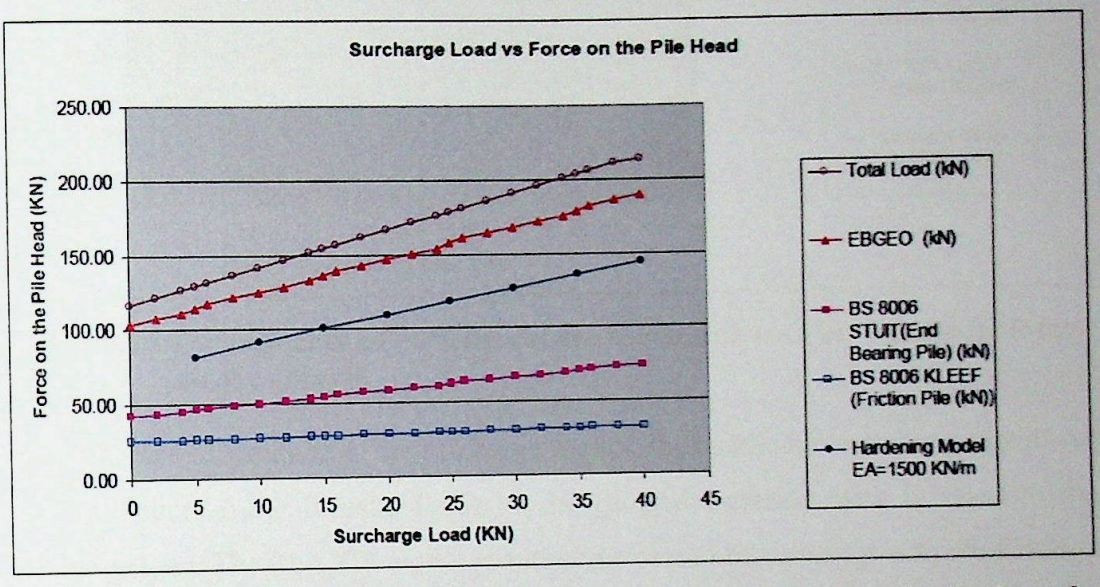

Figure 6.23 The influence of variation of the surcharge load on the load on the pile head.

The influence of variation of the surcharge load on the load on the pile head was studied (Figure 6.23). Load on the pile head increases with increase of the surcharge load. The PLAXIS model results show closed relationship with the EBGEO results and BS8006 show less values compare with the EBGEO. This issue is disused end of this chapter.

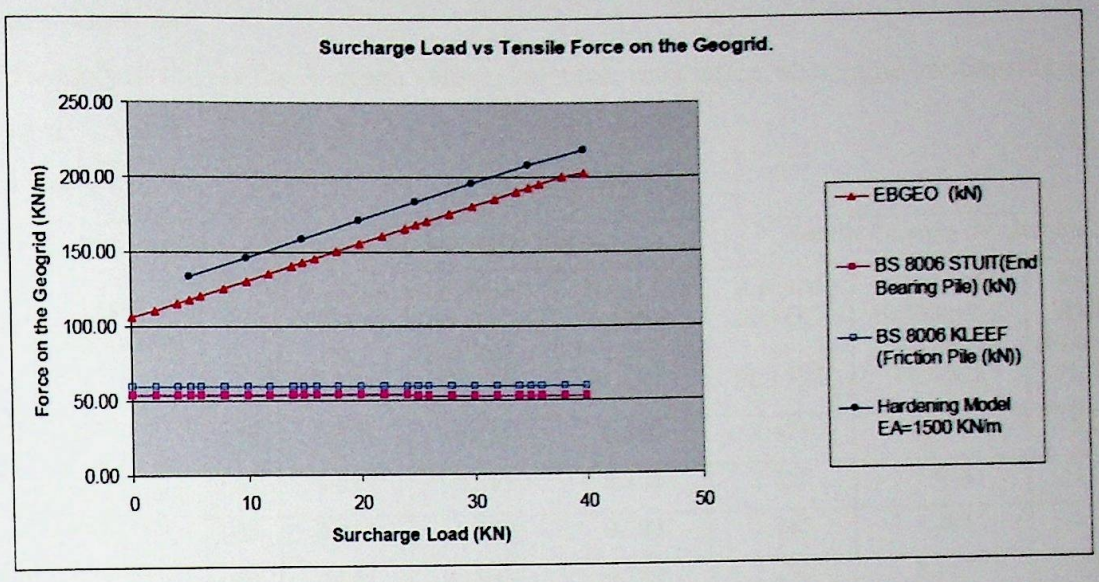

Figure 6.24 The influence of variation of the surcharge load on the tensile force on the geogrid

The influence of variation of the surcharge load on the tensile force on the geogrid was studied (Figure 6.24). Tensile Force on the geogrid increases with increase of the surcharge load. The PLAXIS model results show closed relationship with the EBGEO results and BS8006 show large values compare with the EBGEO. This issue is disused end of this chapter.

6.3. Analysis

To analysis the results Average values, variance, max value, min value are considered here.

Case 1

Load Combination		Force on the Pile			Tensile Force in the Geogrid		
		Ratio of EBEGO to PLAXIS	Ratio of Bs8006(End Bearing) to PLAXIS	Ratio of BS8006 (Friction) to PLAXIS	Ratio of EBEGO to PLAXIS	Ratio of Bs8006(End Bearing) to PLAXIS	Ratio of BS8006 (Friction) to PLAXIS
Embankment Height (m) Variation	1.25	0.678	0.254	0.415	1.479	2.437	2.238
	2.00	0.837	0.243	0.403	1.355	1.478	1.356
	3.00	0.918	0.238	0.397	1.285	1.293	1.184
	4.00	0.945	0.233	0.389	1.270	1.167	1.067
	5.00	0.977	0.233	0.391	1.266	1.065	0.973
	6.00	1.005	0.235	0.395	1.264	0.977	0.892
Surcharge Load (kPa)	5	0.691	0.231	0.141	1.471	2.255	2.457
	10	0.717	0.253	0.155	1.366	2.095	2.284
	15	0.741	0.275	0.168	1.358	2.083	2.272
	20	0.764	0.294	0.180	1.351	2.071	2.260
	25	0.779	0.310	0.190	1.345	2.059	2.248
	30	0.793	0.325	0.199	1.340	2.049	2.237
	35	0.811	0.342	0.209	1.335	2.038	2.226
Centre to Centre distance Variation(m)	0.75	0.935	1.247	0.763	0.979	0.000	0.620
	1.15	1.200	0.925	0.566	1.801	1.246	1.601
Pile Area Variation(m^2)	0.8	0.943	1.040	0.659	1.417	0.597	1.301
Internal Friction Angle Variation	32.5	0.742	0.553	0.339	1.271	1.781	1.939
	42.5	0.655	0.330	0.202	1.100	1.831	1.994
Average		**0.841**	0.420	0.342	**1.336**	1.585	1.730
Variance		**0.020**	0.098	0.033	**0.028**	0.422	0.361
max value		**1.200**	1.247	0.763	**1.801**	2.437	2.457
min Value		**0.655**	0.231	0.141	**0.979**	0.000	0.620
5% high		**0.874**	0.582	0.396	**1.381**	2.277	2.323
5%low		**0.808**	0.259	0.288	**1.291**	0.892	1.138

Table 6-1 Analysis of the results-case1

UNIVERSITY OF MORATUWA LIBRARY SRI LANKA

Case 2

Load Combination.		Force on the Pile			Tensile Force in the Geogrid		
		Ratio of EBEGO to PLAXIS	Ratio of Bs8006 (End Bearing) to PLAXIS	Ratio of BS8006 (Friction) to PLAXIS	Ratio of EBEGO to PLAXIS	Ratio of Bs8006 (End Bearing) to PLAXIS	Ratio of BS8006 (Friction) to PLAXIS
Embankment Height Variation(m)	4	1.240	0.512	0.305	0.965	0.579	0.638
	5	1.251	0.509	0.303	0.918	0.502	0.554
	6	1.268	0.511	0.304	0.883	0.445	0.491
	7	1.300	0.521	0.309	0.859	0.402	0.443
	8	1.350	0.539	0.320	0.839	0.367	0.404
Surcharge Load(kPa)	5	0.917	0.375	0.228	0.883	0.708	0.401
	5	0.925	0.376	0.215	0.893	0.684	0.366
	10	0.931	0.376	0.205	0.901	0.662	0.337
	15	0.936	0.376	0.196	0.909	0.644	0.312
	20	0.940	0.377	0.189	0.915	0.628	0.291
	25	0.944	0.377	0.183	0.920	0.613	0.272
	30	0.948	0.377	0.177	0.925	0.600	0.256
Centre to Centre distance Variation(m)	2.0	1.052	0.199	0.118	0.903	2.611	2.686
Pile Area Variation(m^2)	0.45	1.192	1.341	0.800	0.406	0.000	0.129
Internal Friction Angle Variation	32.5	1.175	0.555	0.329	0.752	0.289	0.332
	37.5	1.177	0.416	0.247	0.739	0.426	0.489
Average		**1.097**	0.484	0.277	**0.851**	0.635	0.525
Variance		**0.026**	0.061	0.023	**0.018**	0.311	0.348
max value		**1.350**	1.341	0.800	**0.965**	2.611	2.686
min Value		**0.917**	0.199	0.118	**0.406**	0.000	0.129
5% high		**1.139**	0.583	0.315	**0.880**	1.145	1.095
5%low		**1.054**	0.384	0.238	**0.822**	0.125	-0.045

Table 6-2 Analysis of results – case2

German Draft Standard shown low variance in case 1 & case 2 in table 6.1 and 6.2 respectively. The values of the tables show that German Draft Standard (EBGEO) gives calculation results that best with PLAXIS 8.2 calculations.

6.4. Discussion.

When we consider the British Standard Code BS8006, there are some fundamental problems.

1) The coefficients presented in BS8006 for the Marston equation distinguish arching on end-bearing piles and on friction piles, which does not agree with the assumption of no support of the soft soil; the equations are not fully 3D and the vertical equilibrium is not generally satisfied: the total load does not equal the sum of the loads on the geosynthetic reinforcement and on the piles. (Van Eekelen et al 2008a)
2) The equations of BS 8006 show several inconsistencies, such as;
   a) Lack of vertical equilibrium for the case of full arching.
   b) The method is based on both 2D and 3D assumptions, which is rather inconsistent.

      When BS 8006 is adapted so that vertical equilibrium is satisfied, and the equations are fully 3D (Van Eekelen and Bezuijen, 2008), the same load distribution is found as in the original BS 8006. However, this adapted approach finally gives lower tensile forces in the geosynthetic reinforcement (GR).
   c) The tensile stress calculated with BS8006 suddenly decreases with increasing embankment Height (H) as shown in figure 6.4. This is caused by the different approaches of full arching and partial arching in BS8006. This is not yet worked out in this thesis.
3) The support of the soft subsoil is considerable and it is worthwhile to calculate its influence on the loading on the GR. Using EBGEO taking into account the support of the soft soil leads to a maximum tensile force in the GR which is smaller than the tensile force without support and in the measured support was even more. However, a permanent long-term presence of this support or counter pressure has to be evaluated very carefully in the stage of design, because e.g. of changes in the ground water level it can decrease significantly (Van Eekelen et al, 2007).

UNIVERSITY OF MORATUWA LIBRARY SRI LANKA

4) Axi- symmetric Model Analysis Plaxis 2D was used for the numerical modeling of the GRPS embankments. In most GRPS embankments, the piles are arranged in a triangular or square grid pattern. A square grid pattern was chosen for the analysis. The ax symmetric model was used to study the impact of varying various factors on the system. A pile having a diameter of 0.5m and 0.3m were selected for the study. Typical spacing between piles in GRPS embankment systems ranges between 1.5 to 4.5m (Han, 1999). A spacing of 1.75 m and 1m were chosen as with respect to the case 1 and case 2. An embankment height of 1.25m was considered for case 1(thin Embankment) and 6m for case2 (Thick Embankment)

5) The effect of certain factors like pile modulus, stiffness of the geosynthetic reinforcement, height of the embankment, effect of the soil layer directly below the geogrid which are not considered by BS 8006 or EBGEO are studied using a finite element program- PLAXIS 2D. The results from BS 8006 and EBGEO are evaluated and compared with the results from PLAXIS. It is found that numerical analysis was able to address many factors that were neglected by BS8006 and EBGEO.

6) The influence of variation of the embankment height on the load on the pile head was studied (Figure 6.3). Load on the pile head increases with increase of the embankment height. The PLAXIS model results show closed relationship with the EBGEO results and BS8006 show less values compare with the EBGEO. The influence of variation of the embankment height on the tensile force on the Geogrid parallel to the road axis was studied (Figure 6.4). When we consider the EBGEO and PLAXIS Model, the tensile force on the geogrid increased with increased of the embankment height, but BS8006 (KLEEF, STUIT) showed a sudden change due to the change from partial to full arching.

7) In classical soil mechanics, we assume that the weight of soil results in a vertical pressure below that soil, in say point *A*. Arching is the phenomenon that the pressure is transferred to stiff parts adjacent to point *A*. With other words: arching

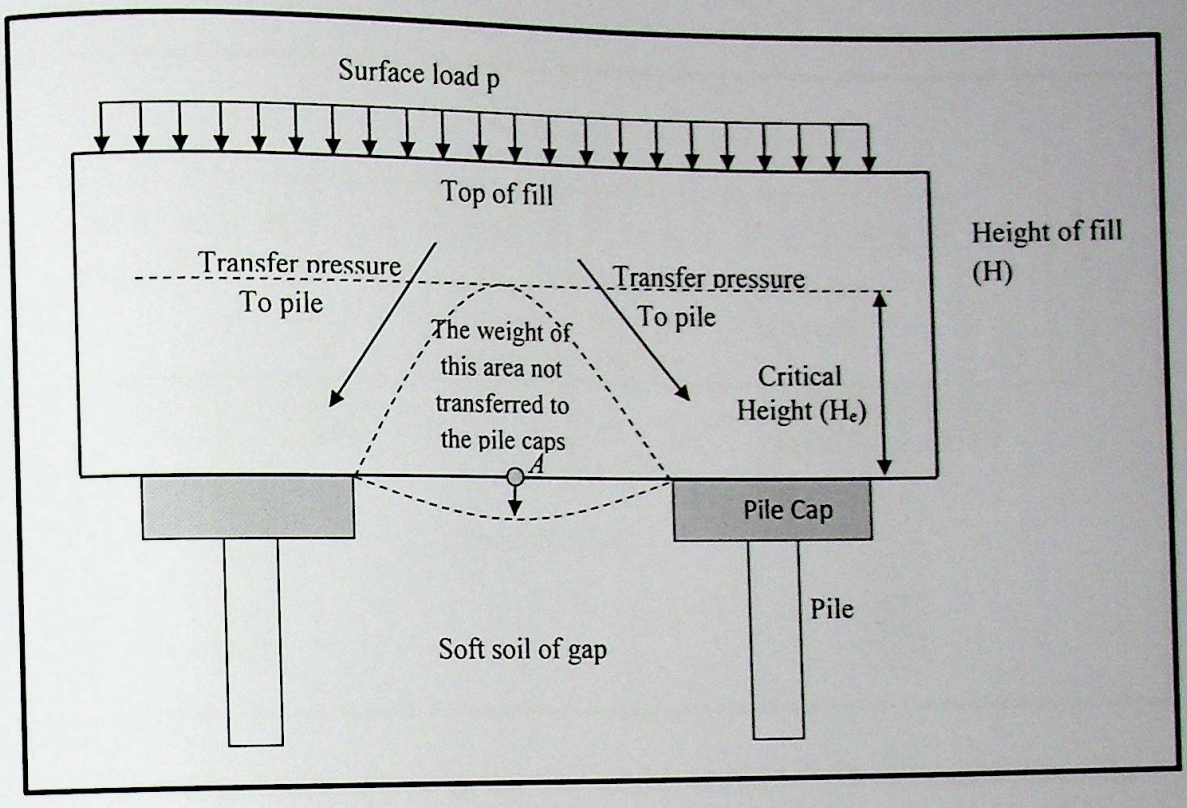

Figure 6.25 Arching: the vertical stress in the soil at point *A* is less than ($\gamma H + p$) (Van Eekelen et al, 2007).

Most theories assume that the weight of the soil above the critical height He and the surface load are both completely transferred to the pile caps (an exception is McKelvey, 1994, see chapter. The soil weight of the area below the 'arch' has to be carried by the subsoil, or the pressures should be transferred to the pile caps by the strength of the area itself, or by some kind of reinforcement in that area. In piled embankments, usually a geogrid is usually applied as reinforcement.

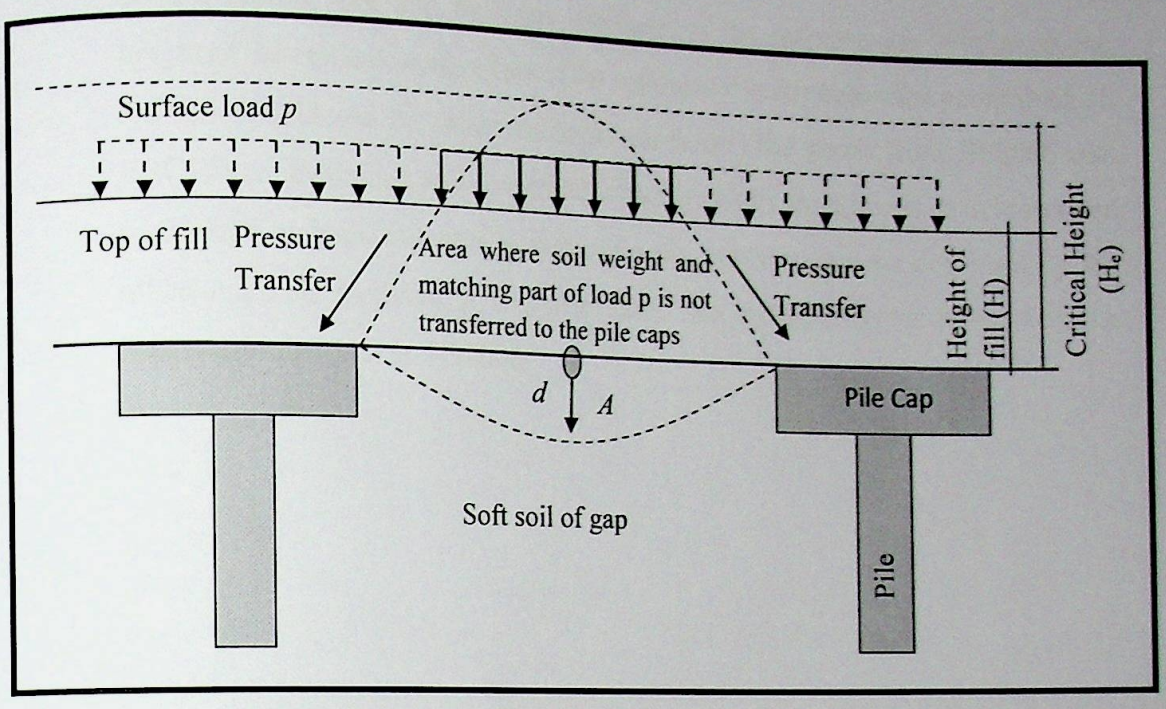

Figure 6.26 Incomplete arching: the height of the fill, H, is smaller than the critical height He. For this case, part of the surface load *p* is not transferred to the pile caps. Therefore, the displacement of point A can be larger than in Figure 3.2(Van Eekelen et al, 2007).

8) Some references make a distinction between the mechanisms in "arching", and they call the "hammock principle" (hangmat principe). A difference between the two situations is that in the "hammock-version", the stress in the reinforcement can be considerably larger than in the arching-version, due to the surface load that is not completely transferred to the pile caps. (Van Eekelen et al, 2007).
9) In this study, we do not make the distinction between arching and hammocks, because in our opinion, in both situation, arching occur, with the only difference that the arching in the second situation is not complete.
10) EBGEO agrees better with the PLAXIS calculations than BS8006. This study attempts to analyze the various methods available today for the design of pile embankment. A numerical study is carried out. The effect of the certain factor like embankment height, center to center distance between piles, pile area, stiffness of the geogrid, internal friction angle in embankment soil and surcharge load are considered here. In Plaxis 8.2 update mesh analysis consider the effect of the

UNIVERSITY OF MORATUWA LIBRARY

certain factors like pile modulus, stiffness of the geosynthetic reinforcement, height of the embankment, effect of the soil layer directly below the geogrid which are not considered by other available methods. The result from BS8006 and EBGEO are evaluated and compared with the results from Plaxis. It is found that numerical analysis was able to address many factors that were neglected by the other available methods. It was also found that EBGEO agrees better with the Plaxis calculation than BS8006.

7. ANALYSIS OF OUTCOMES FROM PLAIN STRESS METHOD

7.1. Introduction

Plain strain analysis was carried out as described before to evaluate the various actions on piles and geo-reinforcement due to changes of some parameters as shown in Table 5-4. Figure 7.1 Shows the basic configuration of the embankment and pile layout used for this theses.

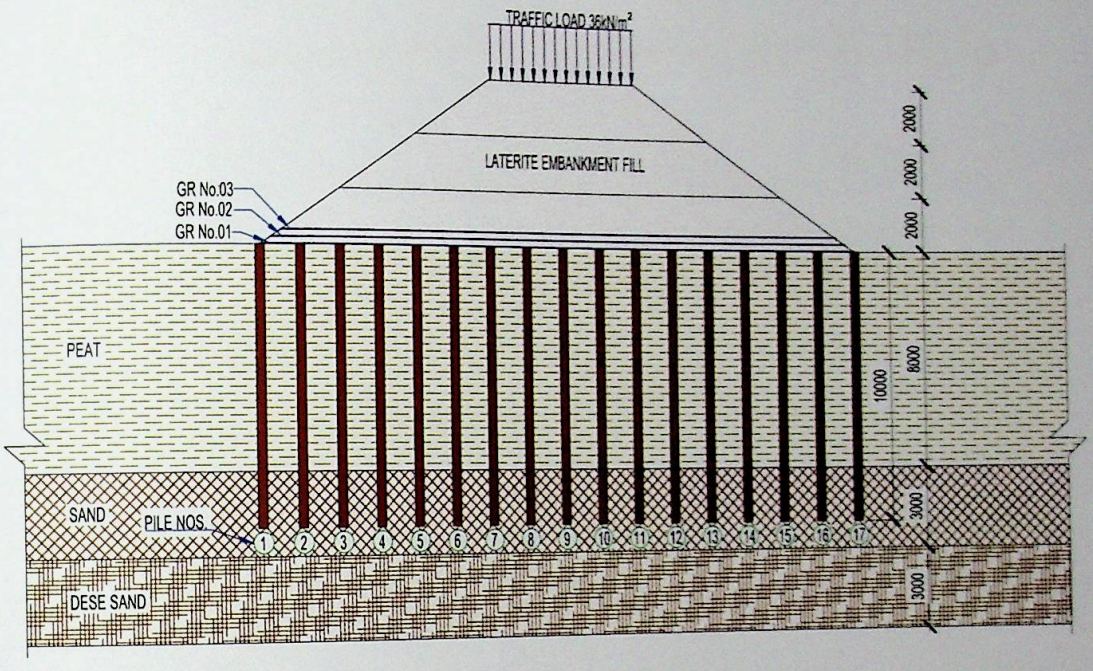

Figure 7.1 Geometry of Embankment used for Plaxis 2D – Plain strain model analysis

Material properties for each element were selected as described in Chapter 5. The piles were spaced at 1.5m intervals during the initial geometry modeling, but some intermediate piles were deactivated in order to increase the pile spacing as required. The loads of piles are presented according to the pile number.

Geo-reinforcement layers (GR) are arranged as shown and numbered starting from bottom.

7.2. Output from Plain strain analysis

7.2.1. Effect of Change of Pile sizes

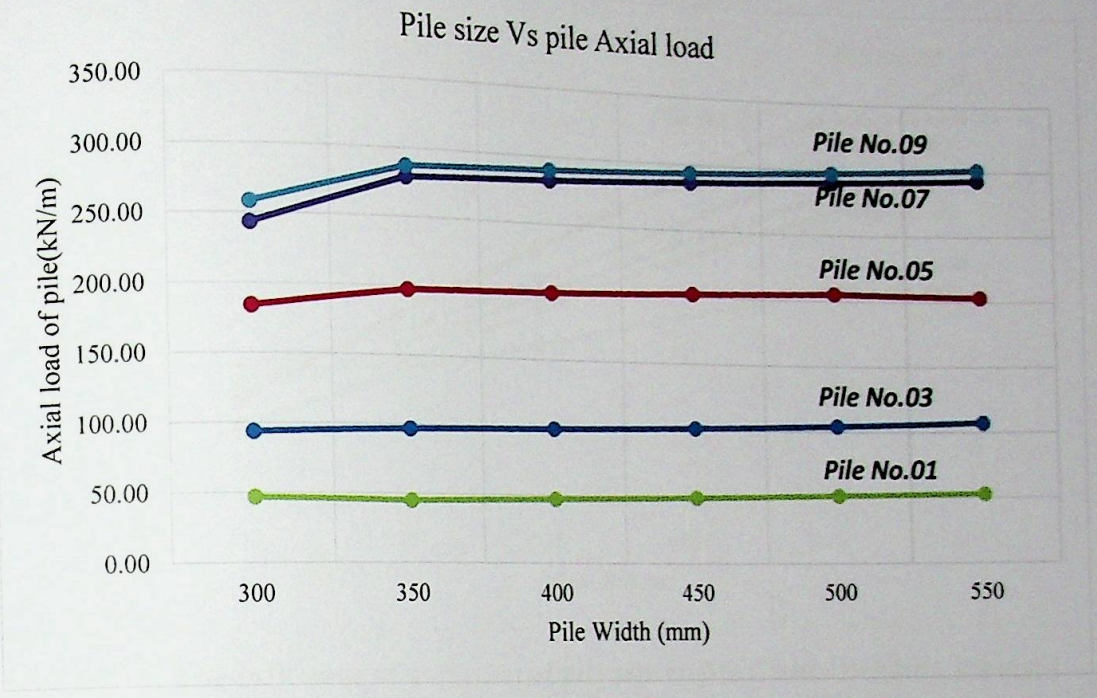

Figure 7.2. The influence of variation of pile size on Axial load on piles

Load on the pile head increases with increase of the pile size. However, the load taken by the pile does not change rapidly after pile size 350x350mm.

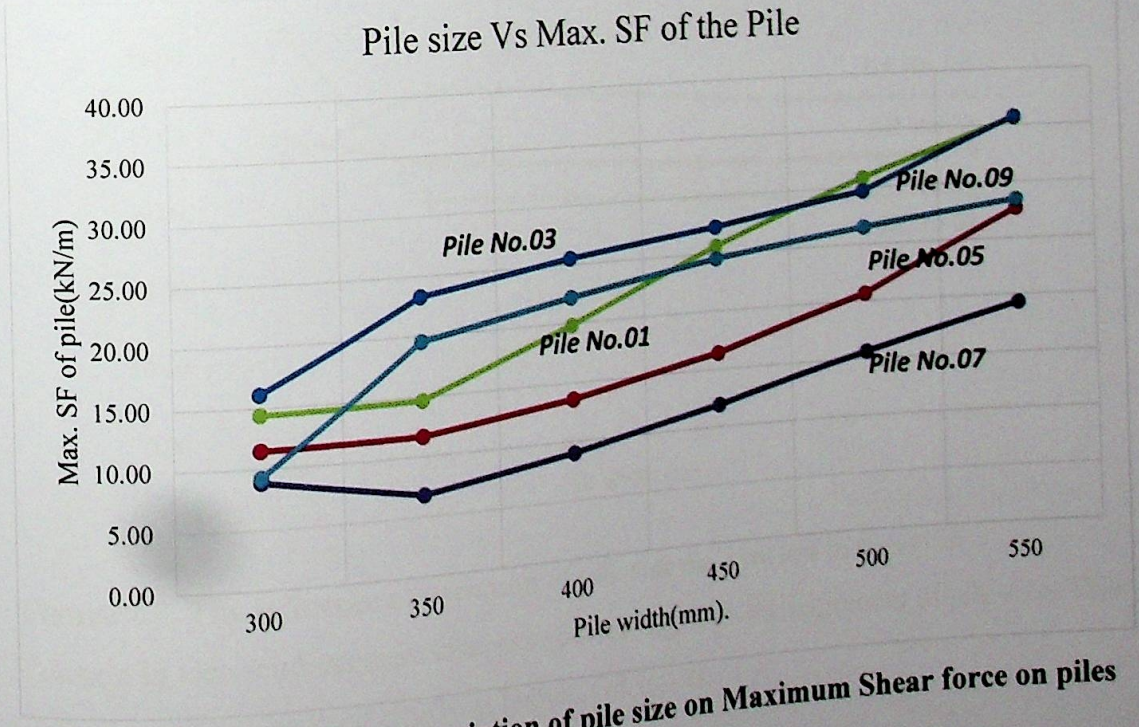

Figure 7.3. The influence of variation of pile size on Maximum Shear force on piles

The maximum Shear Force on a pile increases with the pile size.

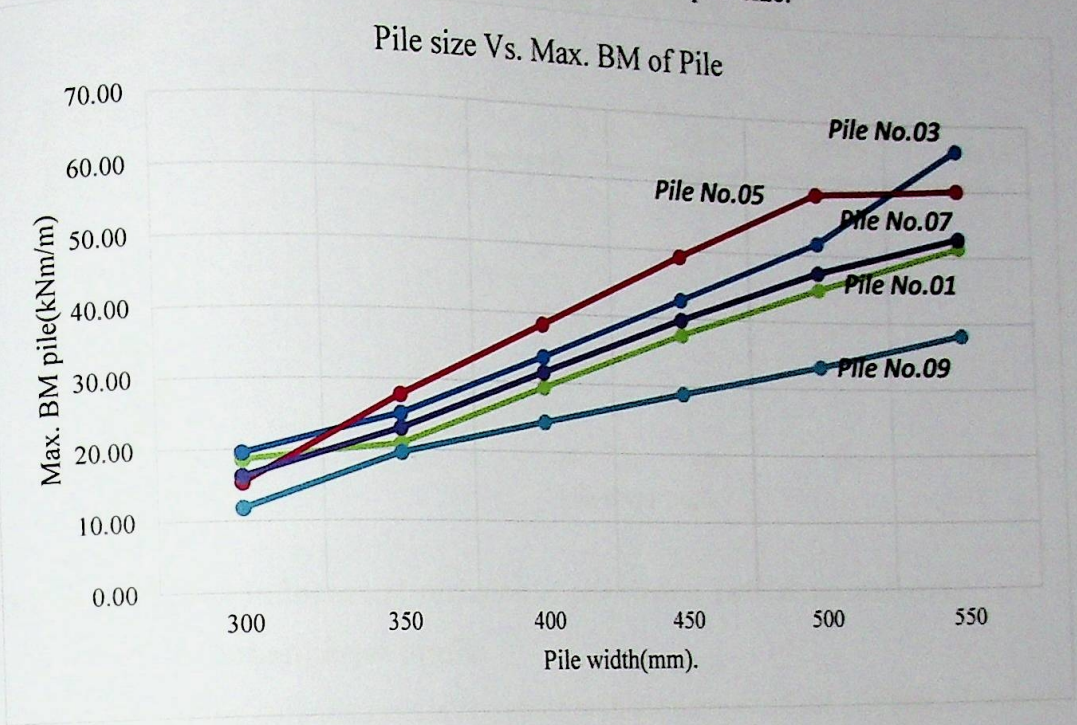

Figure 7.4. The influence of variation of pile size on Maximum Bending Moment on piles

The maximum BM of a pile increase linearly with the increase of the pile size.

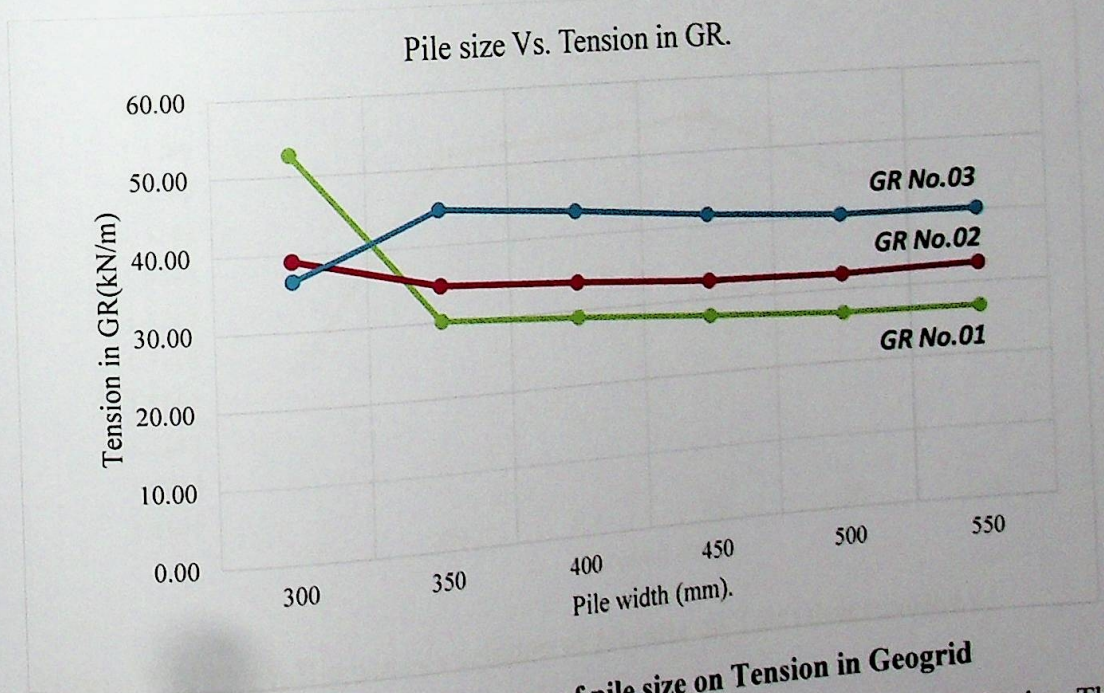

Figure 7.5. The influence of variation of pile size on Tension in Geogrid

Tension in Geo reinforcement layers are decreasing with the increment of pile size. This variation can be observed clearly in bottom GR layers.

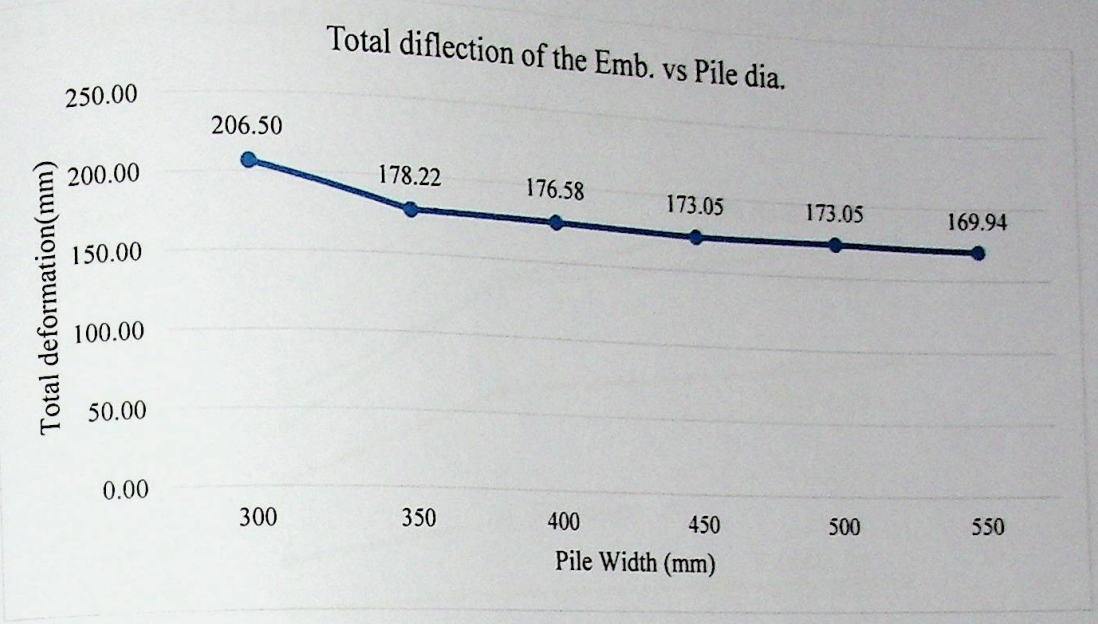

Figure 7.6. The influence of variation of pile size on Total deformation of Embankment profile

Settlement of the embankment is decreased with the increase of the pile size. However, a decrease of rapid lowering of settlement can be observed after the pile size 350x350mm.

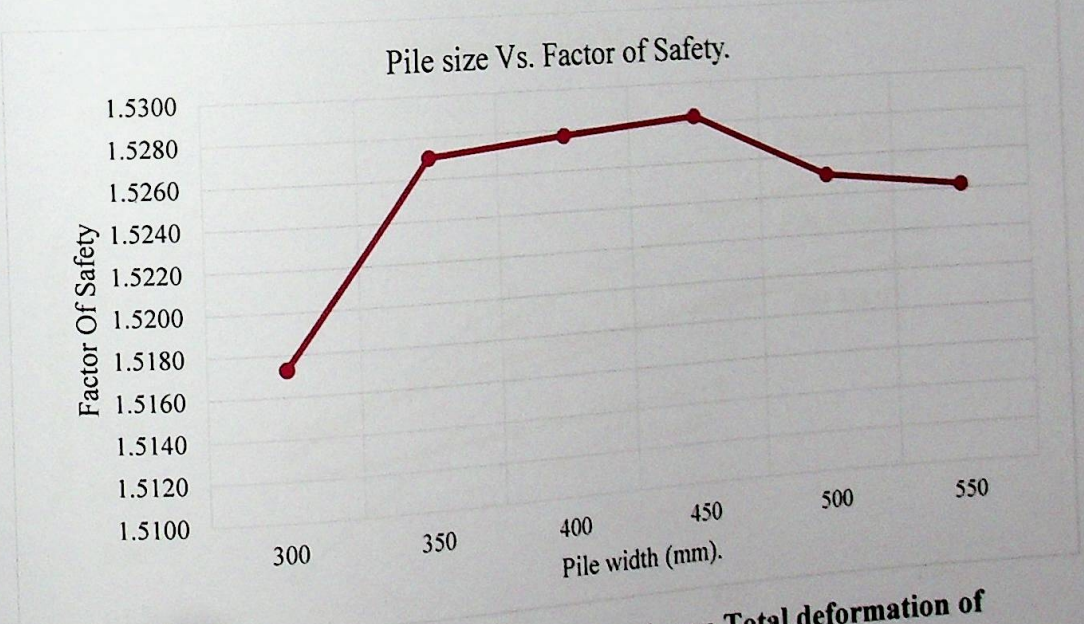

Figure 7.7. The influence of variation of pile size on Total deformation of Embankment profile

FOS of the embankment is increased with size of the pile up to some limit. A highest rate of increment of FOS can be observed up to the pile size of 350x350mm. The FOS starts to reduce after the pile size 450x450mm.

7.2.2. Effect of Change of Pile spacing

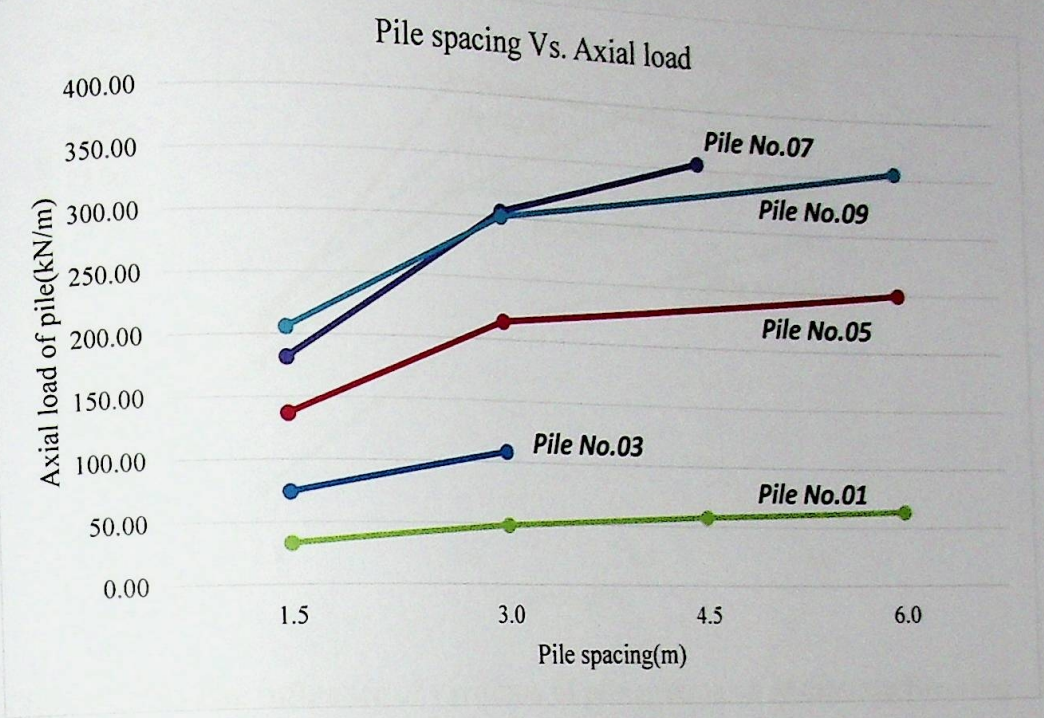

Figure 7.8. The influence of variation of pile size on Axial load on piles

Axial load on the pile increases with the increase of the pile spacing. The rate of the increment reduces after 3.0m spacing.

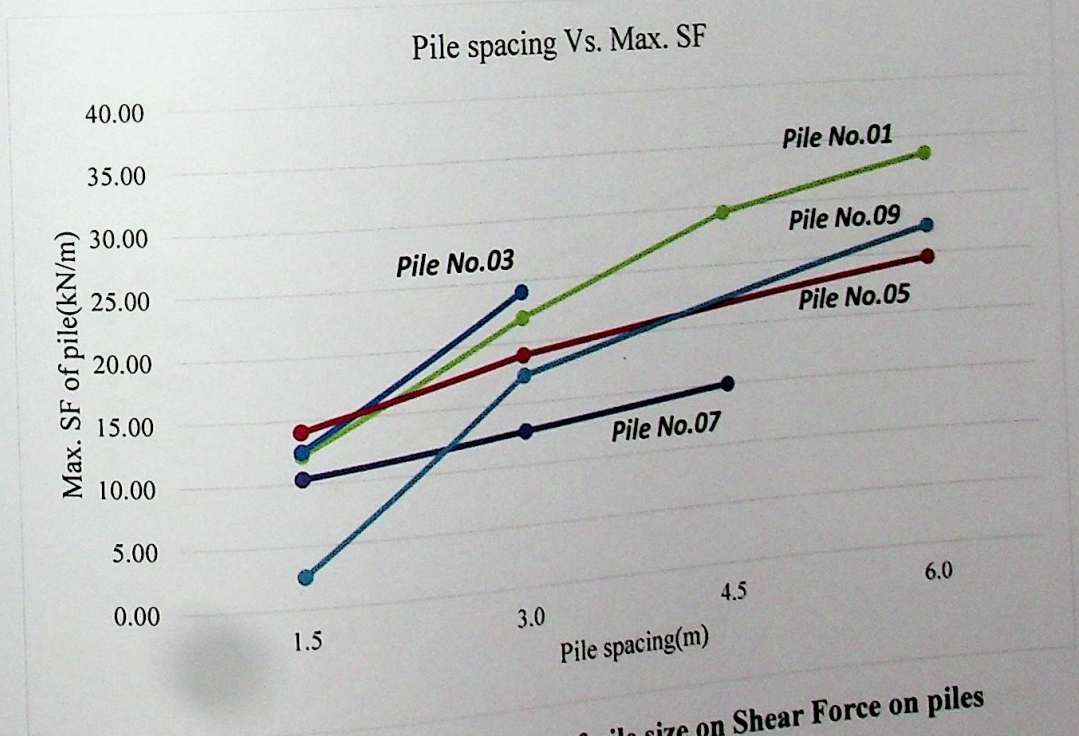

Figure 7.9. The influence of variation of pile size on Shear Force on piles

The maximum shear force on the pile is increased with increase of pile spacing.

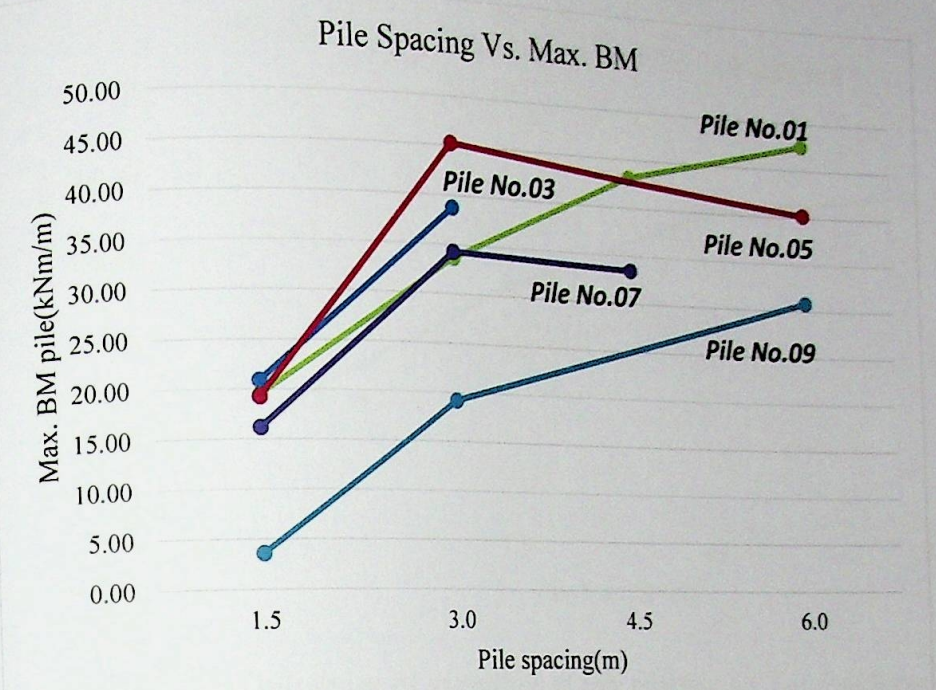

Figure 7.10. The influence of variation of pile spacing on Maximum Bending Moment on piles

The maximum BM of a pile increase with the increase of the pile spacing. However, increment rate changes when the pile spacing exceeds 3.0m.

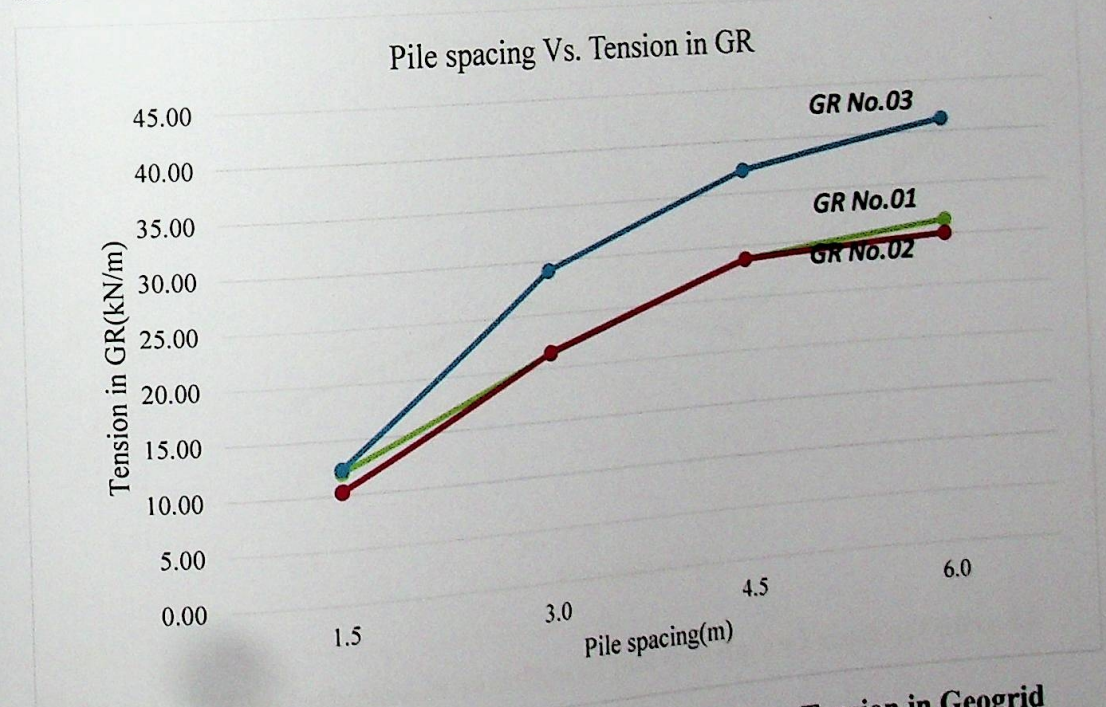

Figure 7.11. The influence of variation of pile spacing on Tension in Geogrid

Tension in Geo reinforcement layers increased with the increment of pile spacing. However, the rate of increment of tension is reduced with increment of pile spacing.

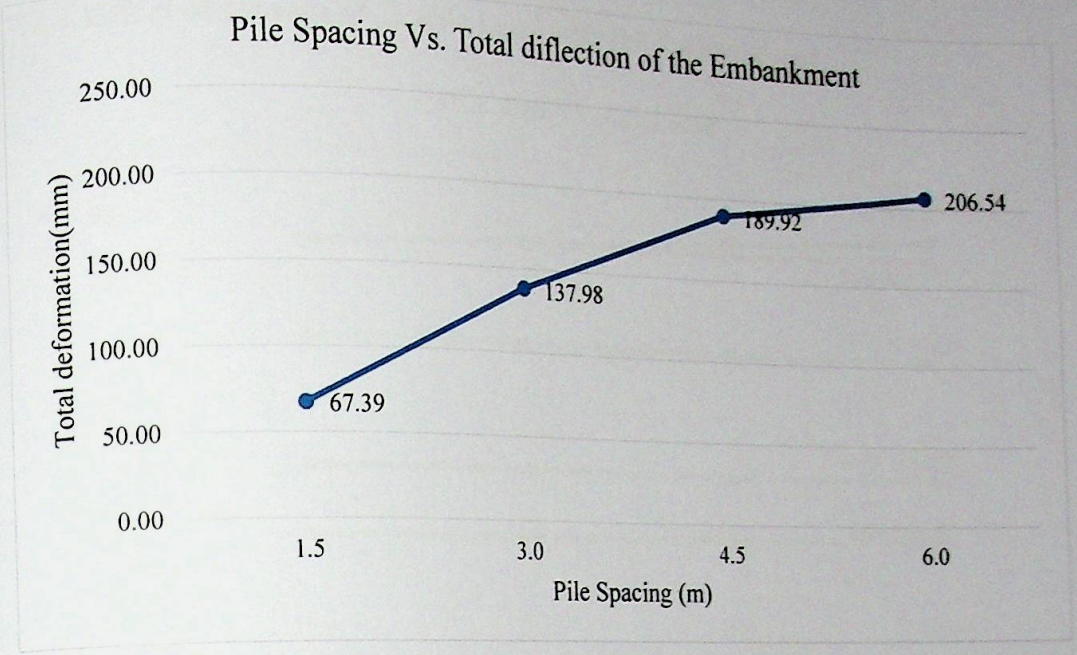

Figure 7.12. The influence of variation of pile spacing on Total deformation of Embankment profile

The amount of settlement of the embankment increases linearly with the increment of spacing between piles.

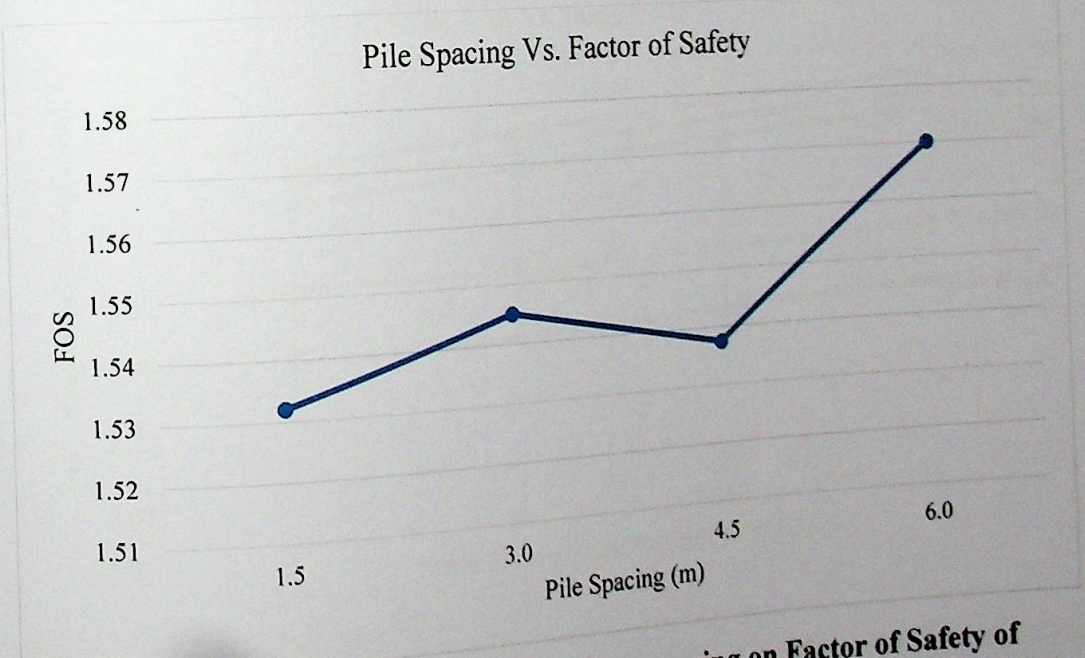

Figure 7.13. The influence of variation of pile spacing on Factor of Safety of Embankment profile

The FOS of the entire embankment section shows increase with the increment of spacing between piles. The possible reasons are discussed at the end of this chapter.

7.2.3. Effect of Change of Traffic Load over the Embankment

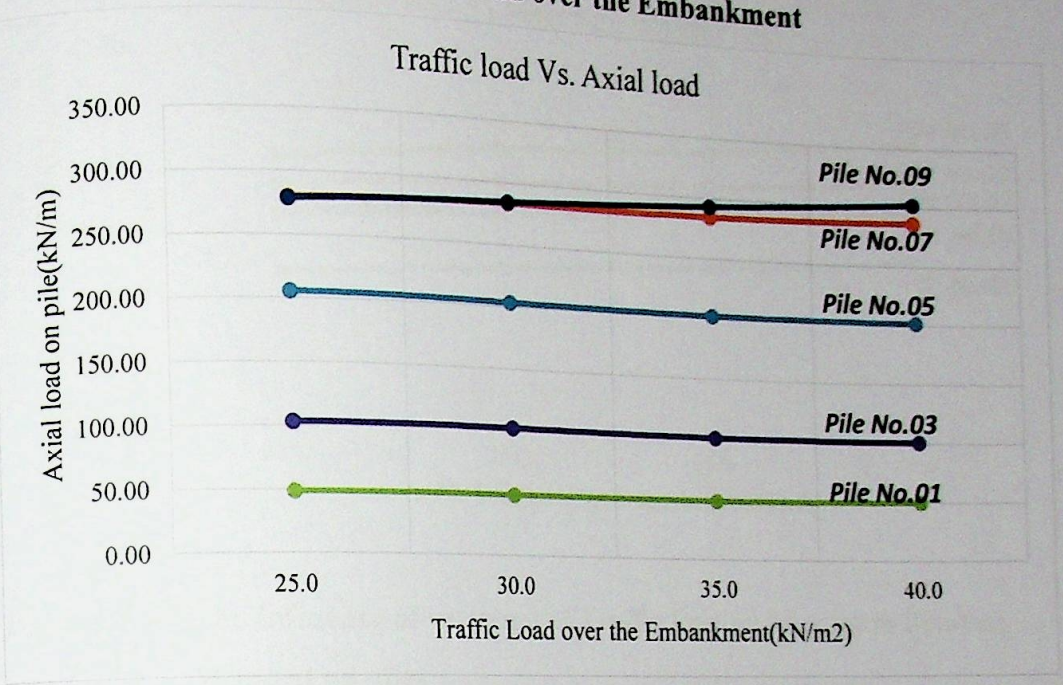

Figure 7.14. The influence of variation of Traffic load on Axial load on piles

The influence of the variation of traffic load on piles is negligible.

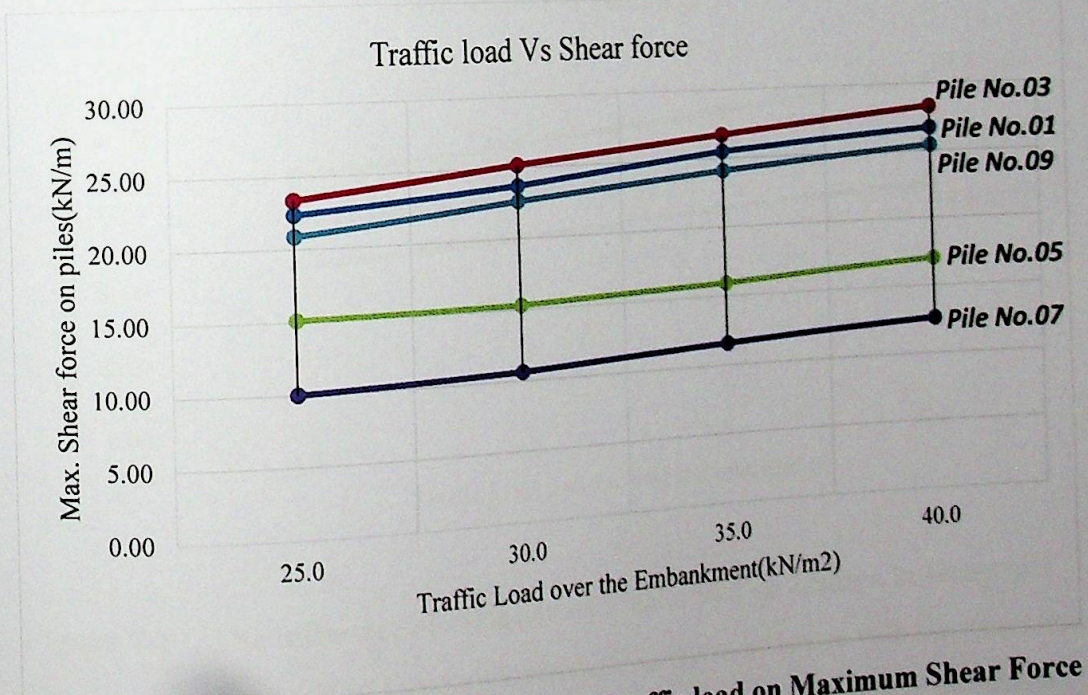

Figure 7.15. The influence of variation of Traffic load on Maximum Shear Force on piles

The maximum shear force on the pile is increased linearly with increase of pile spacing.

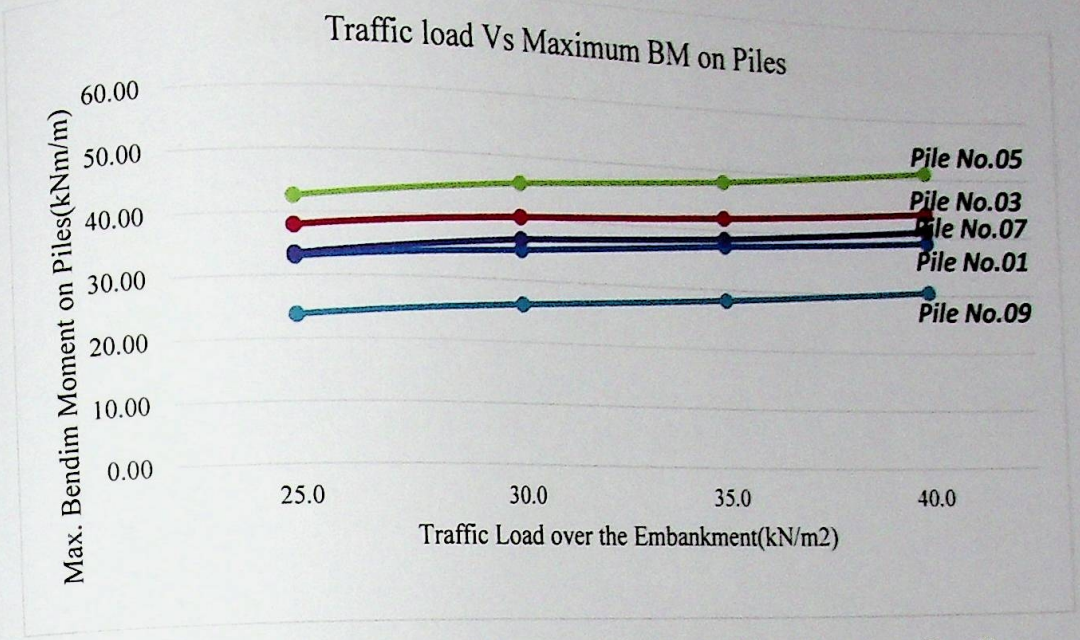

Figure 7.16. The influence of variation of Traffic load on Maximum Bending Moment on piles

The maximum BM in a pile varies linearly with the increment of Traffic load.

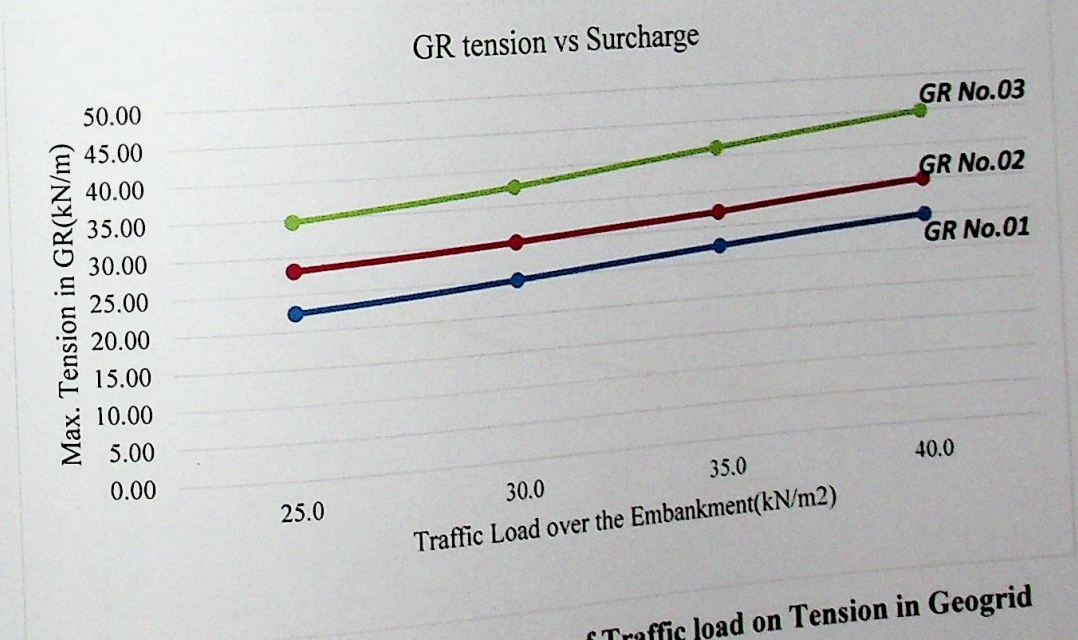

Figure 7.17. The influence of variation of Traffic load on Tension in Geogrid

The maximum tension in Georeinfocement (GR) layers increases with the increment of Traffic load on the piles. The top GR layers take higher component of the tension.

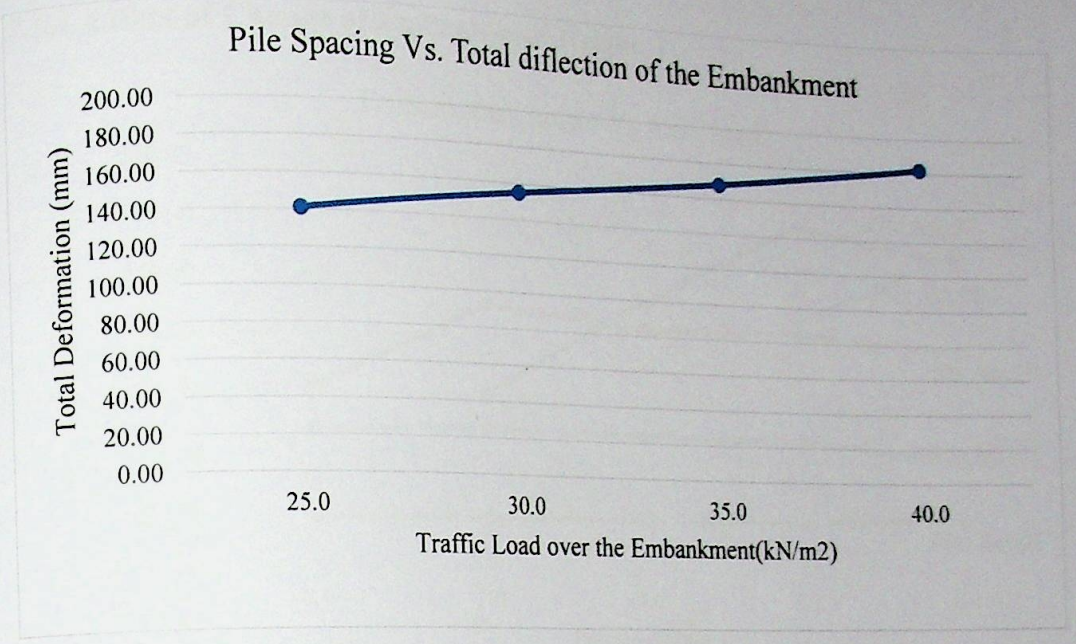

Figure 7.18. The influence of variation of Traffic load on Total deformation of Embankment profile

The amount of settlement of the embankment increases linearly with the increment of spacing between piles. However, the rate of change of affect is a low value.

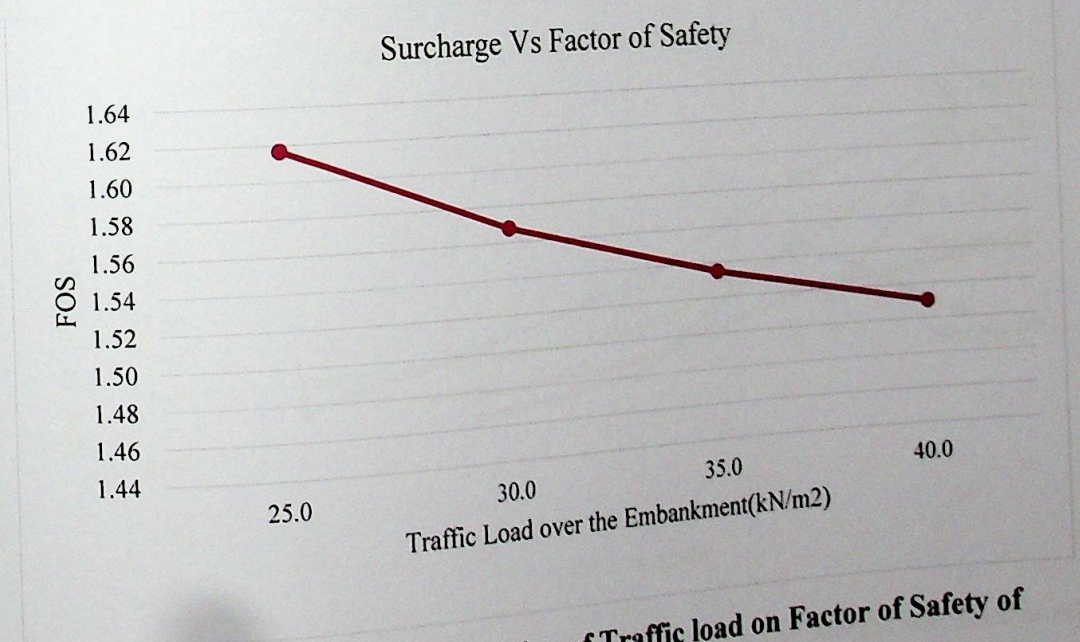

Figure 7.19. The influence of variation of Traffic load on Factor of Safety of Embankment profile

The FOS of the entire embankment section decreases linearly with the increment of traffic load on embankment.

7.2.4. Effect of Change of Embankment Height

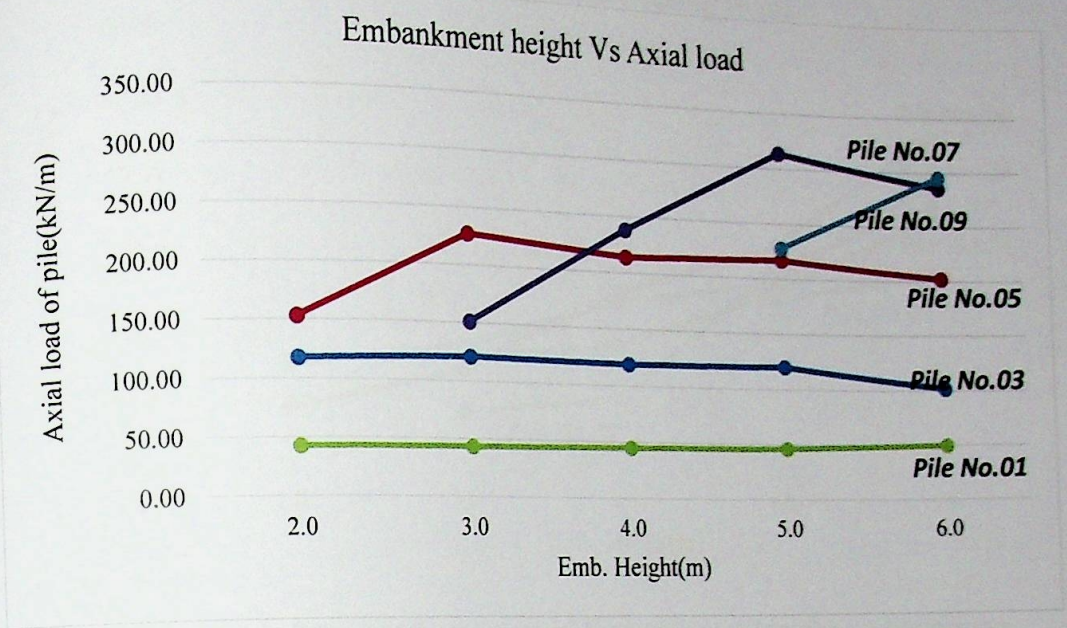

Figure 7.20. The influence of variation of Embankment Height on Axial load on piles

The change of Embankment height make considerable affect only in the middle piles. Axial load of the piles at the toe of the embankment is negligible.

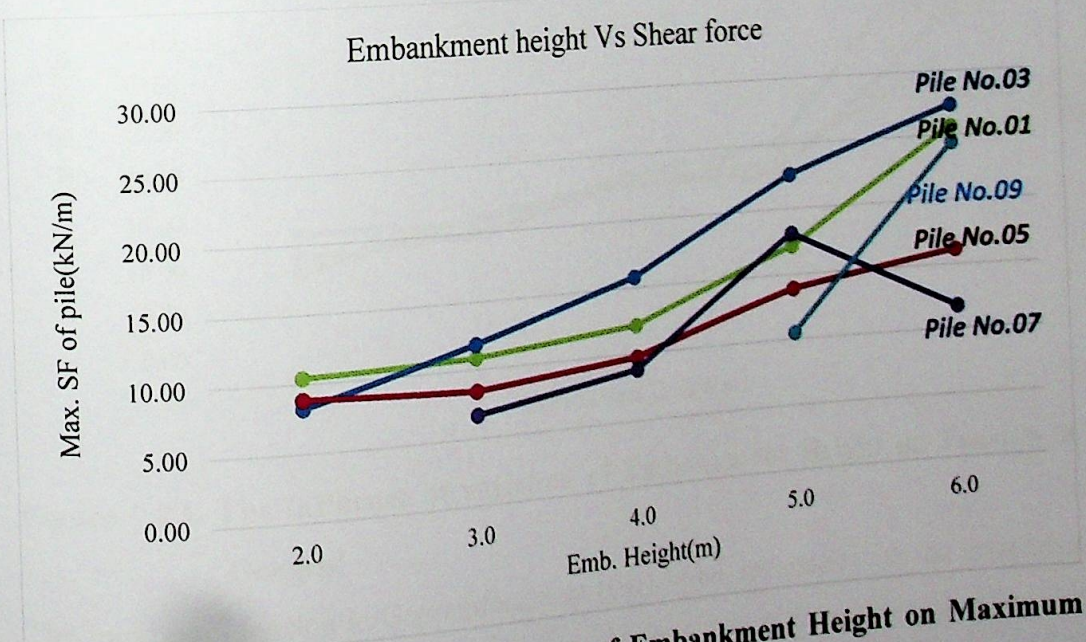

Figure 7.21. The influence of variation of Embankment Height on Maximum Shear Force on piles

The maximum shear force on the piles is increased gradually with the increase of embankment height.

UNIVERSITY OF MORATUWA LIBRARY

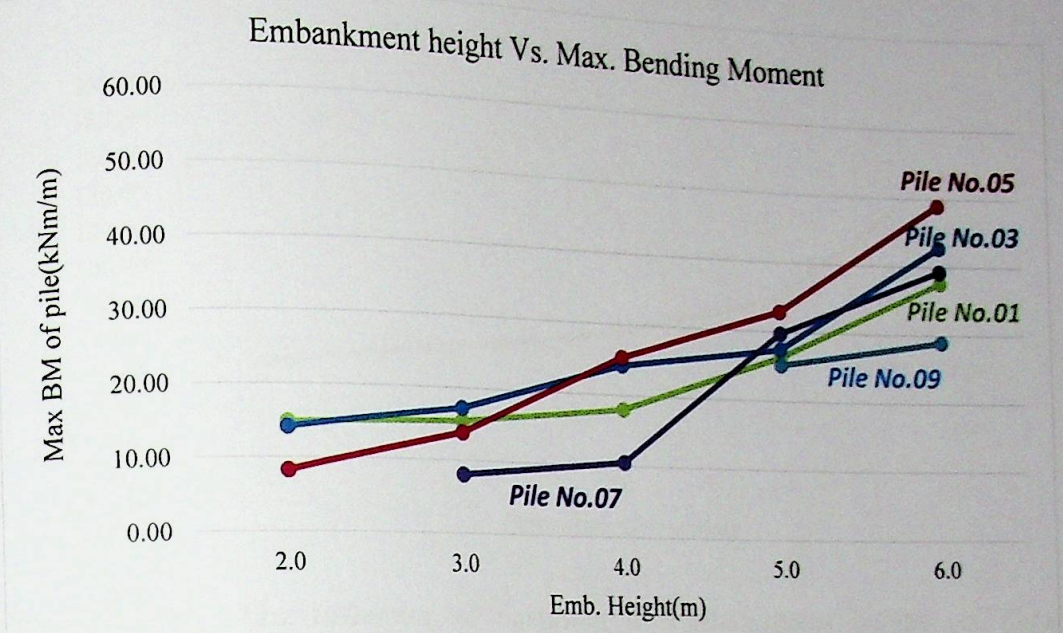

Figure 7.22. The influence of variation of Embankment Height on Maximum Bending Moment on piles

The maximum BM in a pile increase with the increment of Embankment Height.

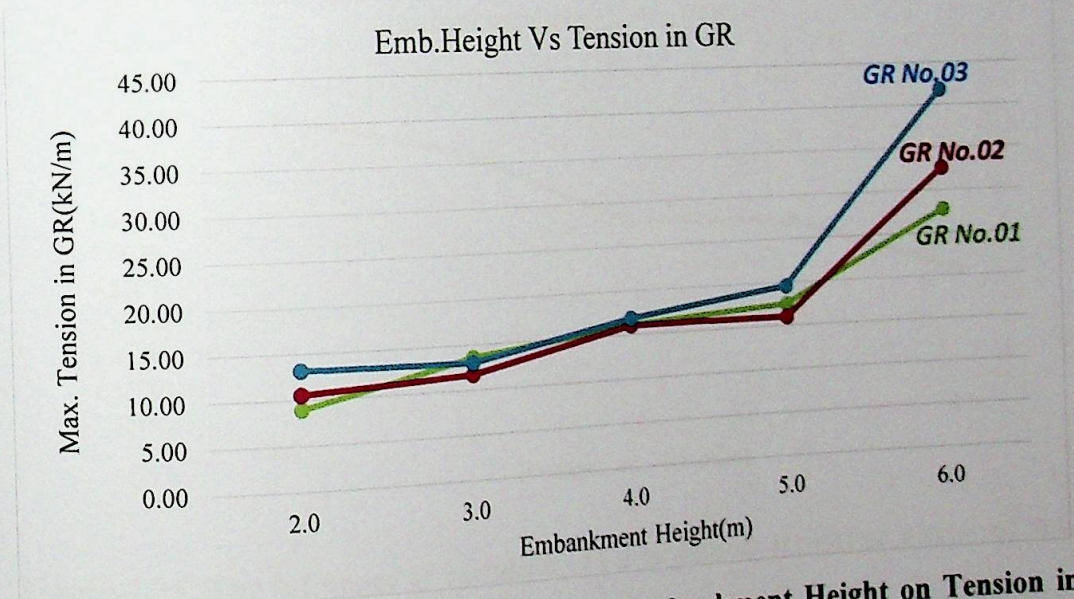

Figure 7.23. The influence of variation of Embankment Height on Tension in Geogrid

The maximum tension in Georeinfocement (GR) layers increases with the increment of embankment height. A rapid increment of tension in GR can be seen when the embankment height exceeded the height 5m.

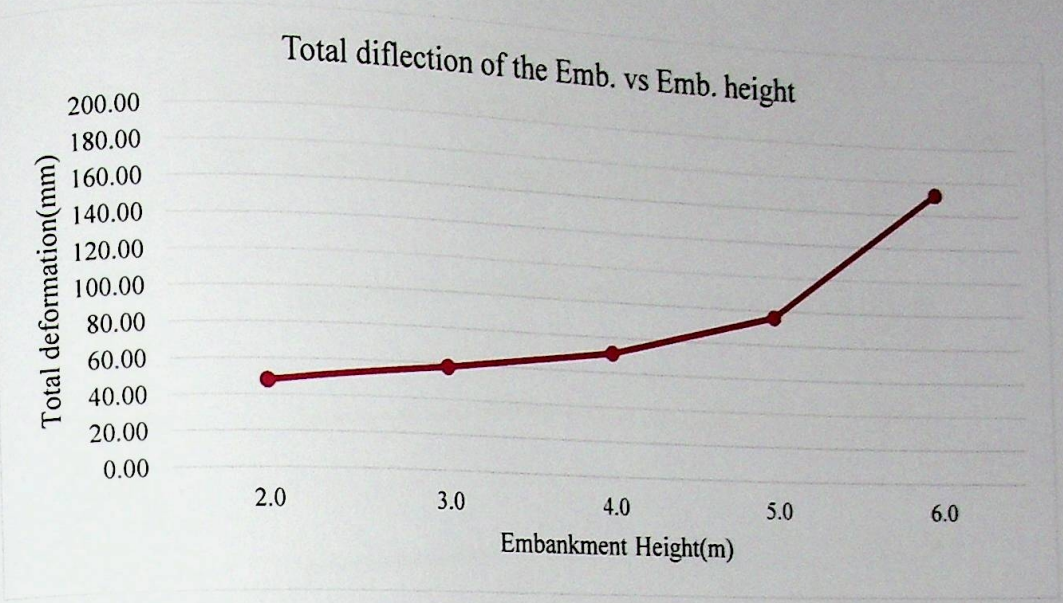

Figure 7.24. The influence of variation of Embankment height on Total deformation of Embankment profile

The settlement of embankment increases gradually with the increase of the height of embankment.

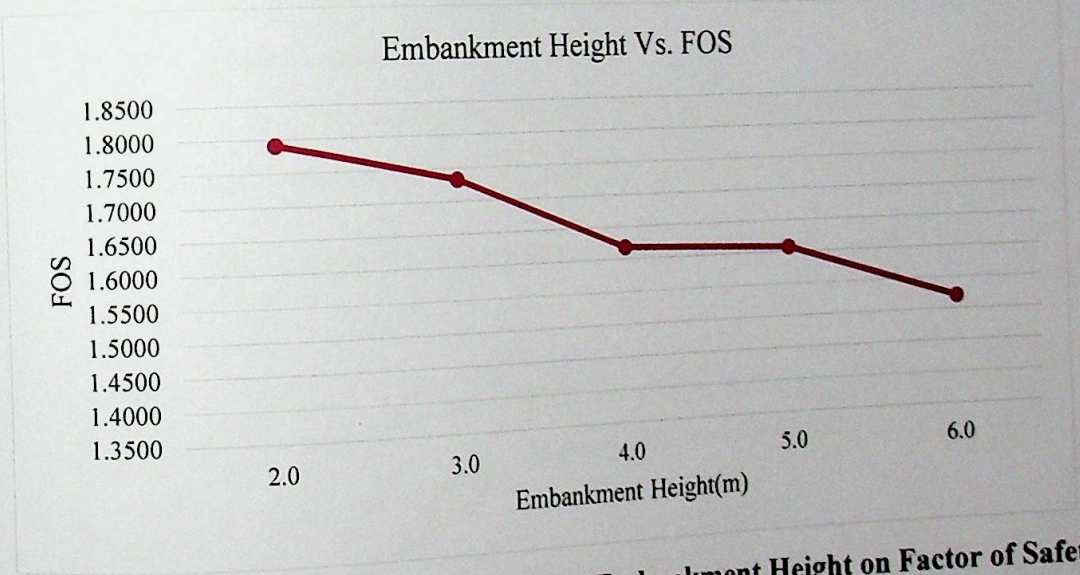

Figure 7.25. The influence of variation of Embankment Height on Factor of Safety of Embankment profile

The FOS of the entire embankment section decreases linearly with the increment of traffic load on embankment.

7.2.5. Effect of Change of Spacing between Geo Reinforcement layers

Three-layered Georeinfocement was considered by varying the space between them.

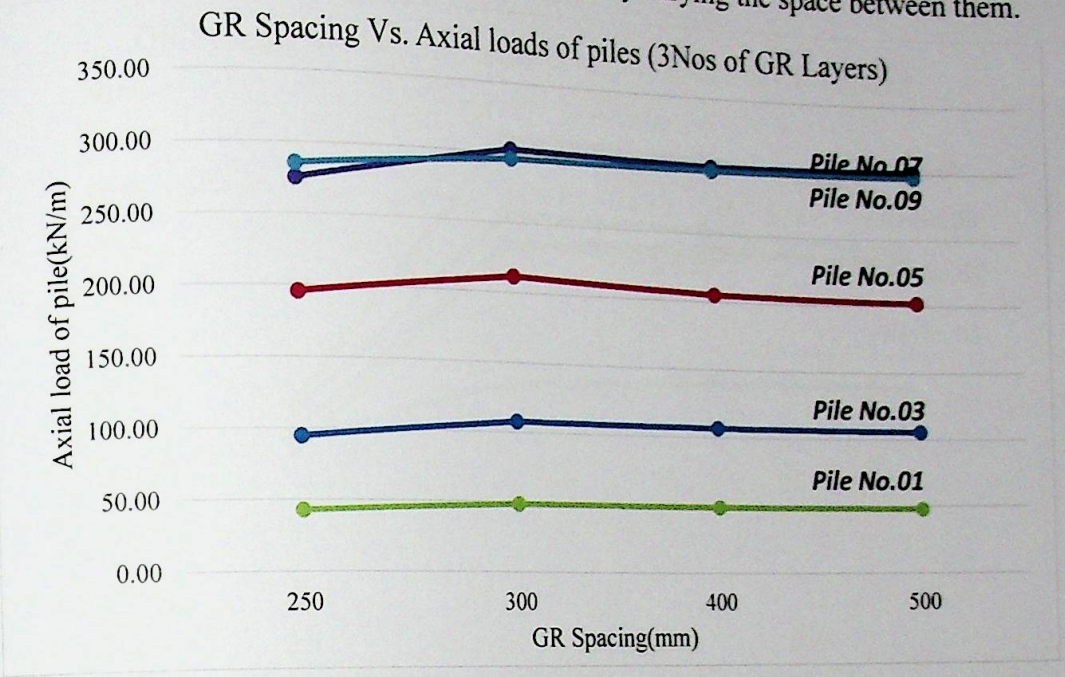

Figure 7.26. The influence of variation of spacing between GR Layers on Axial load on piles

Small increment in axial load can be observed in the space range below 300mm. After that the axial load variation is negligible with the increment of space between GRL.

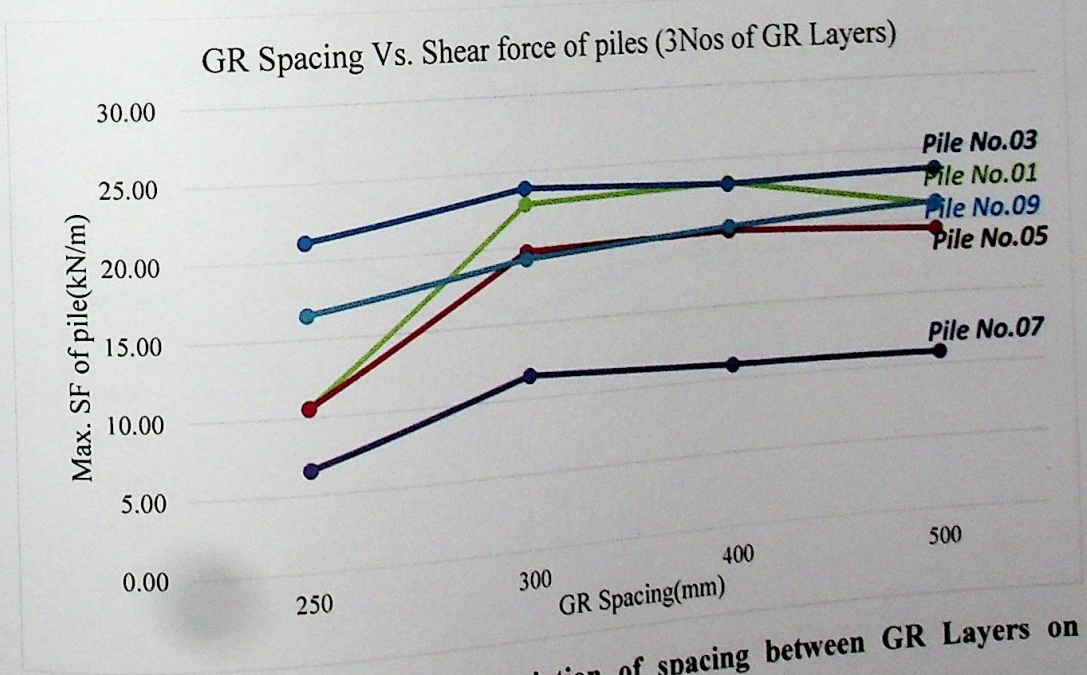

Figure 7.27. The influence of variation of spacing between GR Layers on Maximum Shear Force on piles

An increase in maximum SF in piles can be observed in the space range below 300mm.

UNIVERSITY OF MORATUWA LIBRARY SRI LANKA

After that the variation of SF in piles is negligible with the increase of space between GRL.

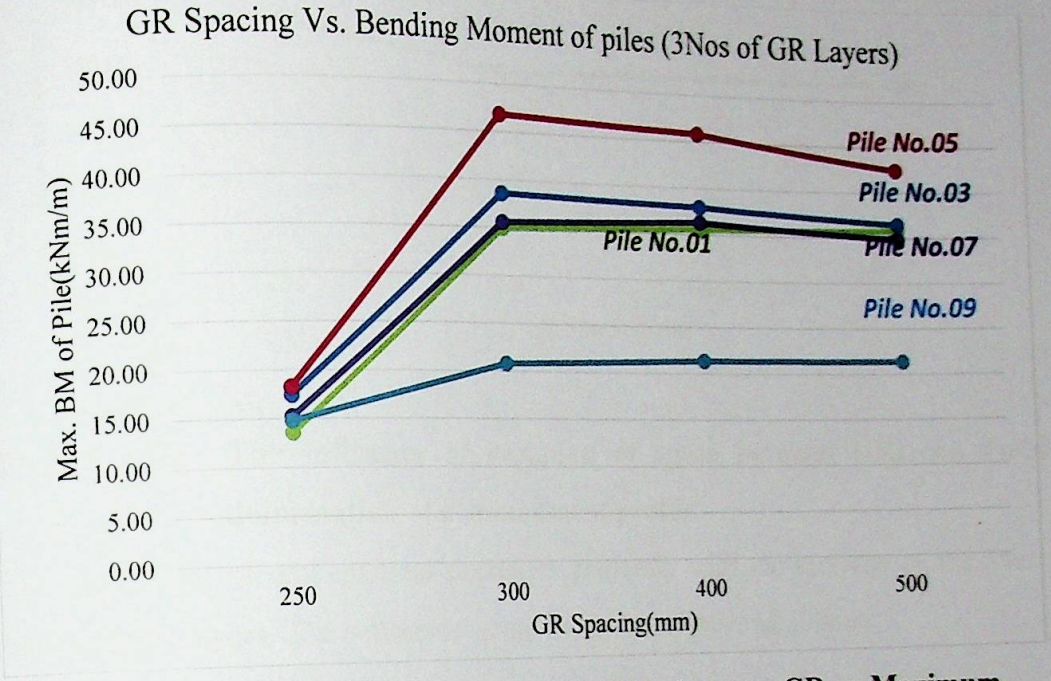

Figure 7.28. The influence of variation of spacing between GR on Maximum Bending Moment on piles

High variation of BM can be observed up to 250mm spacing of GR. Above that, the maximum BM show very small variation.

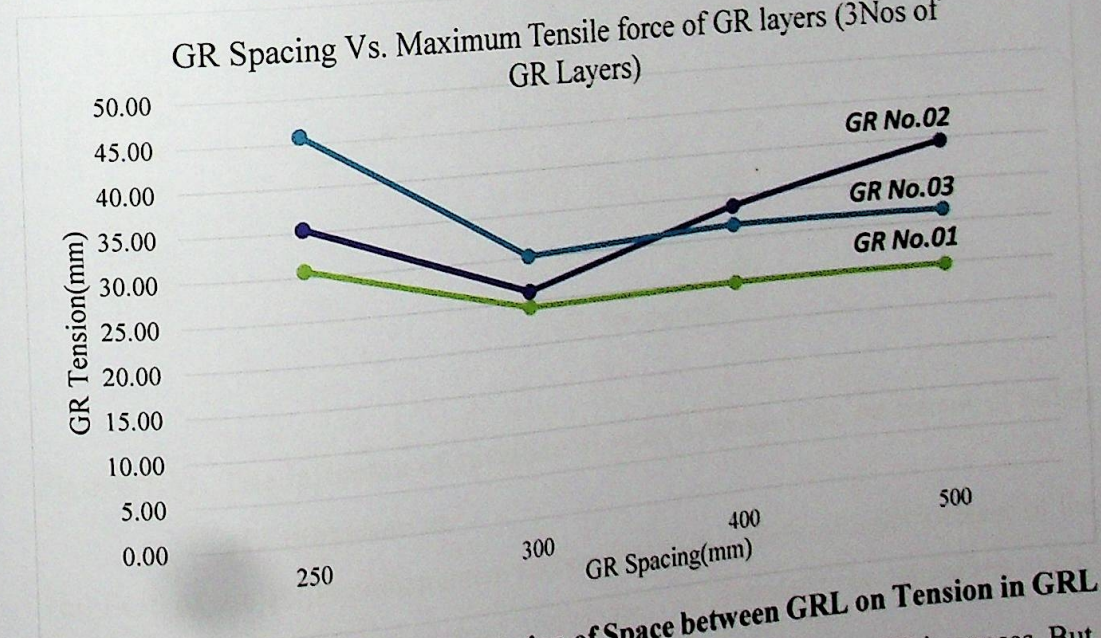

Figure 7.29. The influence of variation of Space between GRL on Tension in GRL

The maximum tension in GR layers decreases when space between GR increases. But, when the space exceed 300mm the tension remains constant.

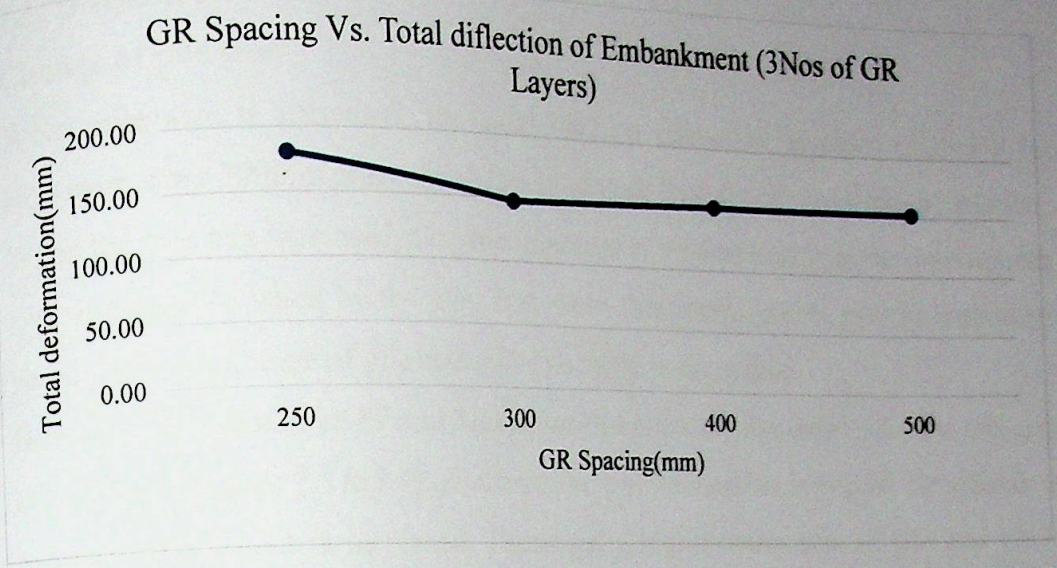

Figure 7.30. The influence of variation of space between GRL on Total deformation of Embankment profile

The settlement of embankment decreases gradually with the increase of the space between GR layers. The settlement remain unchanged beyond 300mm.

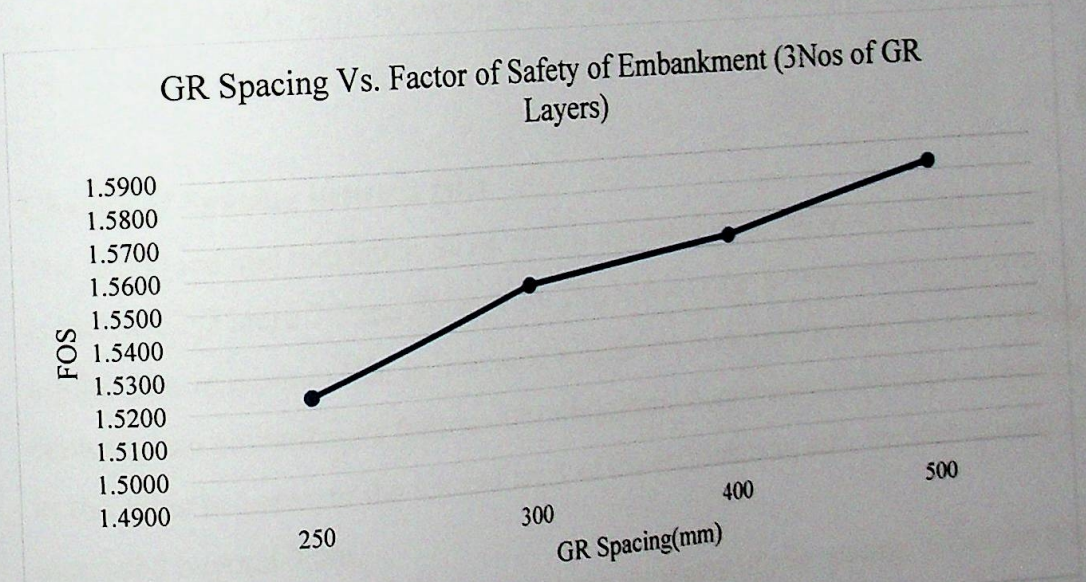

Figure 7.31. The influence of variation of space between GRL on Factor of Safety of Embankment.

The FOS of the entire embankment section increases linearly with the increase of the space between GR layers. However, further analysis is needed to be carried out to find the limit of increase of spacing.

7.3. Discussion.

Change of pile size:

When pile size is increased, the axial load on piles also increased (Figure 7.2). However, after 300mm piles, the variation of axial load doesn't show much variation. When the pile size increased, a lager component of vertical load from the embankment and surcharge is taken by the pile. But, when this component reached its maximum value, further increase of pile size make no sense to the system.

However, the Maximum SF and Maximum BM gradually increased when the pile size is increased (Figure 7.3 & 7.4). As the stiffness of the member increased, the resistance to the displacement is increased. Therefore, a higher component of BM and SF is transferred to the pile. Lesser the pile deflection, lesser the strain in Geo-reinforcement (GR). This leads to a lesser value of tension in GR (Figure 7.5) and subsequently lesser settlement (Figure 7.6) in embankment profile.

The factor of safety (FOS) of embankment increases with the increase of pile size, but not linearly (Figure 7.6). However, all the time FOS stays above the required value 1.5.

Change of Spacing between piles

The axial load and maximum SF on piles is increased when the spacing between piles is increased (Figure 7.7 and Figure 7.8). This is due to the increase of effective area of a pile. The maximum BM is increased only in toe piles (pile no.01) and piles at the center of the embankment (pile no. 09) while some decrement of BM can be observed in the piles in-between the toe and crest of the embankment after the pile spacing is increased beyond 3.0m.

The tension of GR layers increased with the increment of pile spacing. When the pile space is increased, the radius of the soil arch is also increased. Therefore, the soil mass below the arch (which is supported on GR layers) is also increased. But when the pile spacing is beyond 3.0m, as the GR layers start to feel the support of the soil below reducing the rate of increment of tension in GR layers (Figure 7.10). The same phenomenon can be observed for the settlement of embankment (Figure 7.11). The FOS of the embankment also goes up (Figure 7.12) beyond 4.5m spacing due to the same reason as mentioned above.

UNIVERSITY OF MORATUWA LIBRARY SRI LANKA

Effect of traffic load

The increment of traffic load is barely felt by the piles towards the toe (Figure 7.13). The load is dispersed through the embankment height (6.0m) and transferred to the piles. Therefore, the portion of the increment of traffic load is felt by the piles close to the crest of the embankment.

Maximum SF, BM, Tension in GRL and Settlement of the embankment is linearly increased with the increment of traffic load over the embankment (Figure 7.14 to 7.17). The FOS of the embankment reduces with the increment of traffic load. The maximum stress points always emerge above the GR layers. The Figure 7.32 below indicate the possible failure mode for maximum traffic load (40kN/m^2) used for analysis.

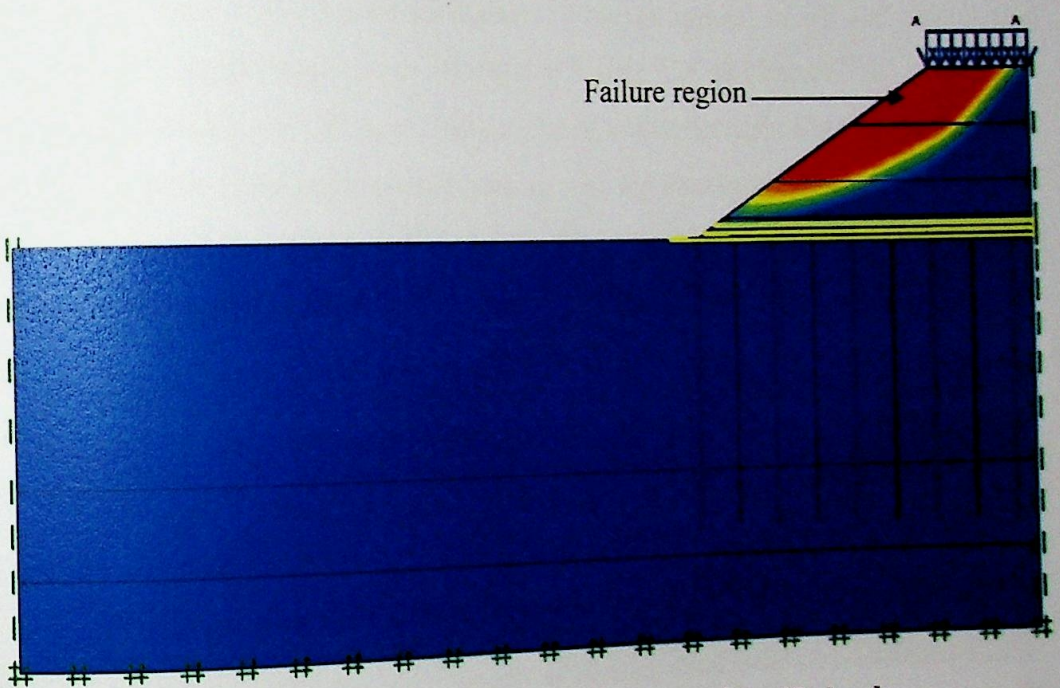

Figure 7.32. The failure mode for 40kN/m^2 traffic load

Change of Embankment Height

The effect on axial load piles due to change of embankment height is mainly felt by the piles away from the toe of the embankment (Figure 7.19). However, Max. SF, BM and Tension in GR layers are increased with the increment of height of embankment (Figure 7.20 – 7.22). Once the soil arching is fully mobilized, the lateral spreading is increased. This leads to develop a higher tensile force in the GRL which can be observed in the Figure 7.22 from Embankment height 5.0m to 6.0m.

The settlement of the embankment rises with the increment of the embankment height (Figure 7.23) while the FOS decreases gradually (Figure 7.24). However, the value of FOS remains above the safe margin even for 6.0m height of embankment.

Change of spacing between GR layers

When the spacing between GR layers are very small the flexibility geo reinforcement mat is high. However, when the spacing is increased GR mat start to act like a rigid beam and transfer more load to piles due to low settlement. The flexible GR mat can transfer some portion of load to the below supporting soil due to higher deflection. This can be clearly observed in Figure 7.25 and Figure 7.29.

Due to the same reasons mentioned above, a higher amount of SF and BM is also transferred to supporting piles as indicated in Figure 7.26 and Figure 7.27.

The tensile force in the GR layers reduces due to low deflection of the GR mat (Figure 7.28). The FOS of the embankment goes up with the increment of space between GR layers (Figure 7.31). The reason for this is due to the higher rigidity of the founding geo-soil mat over the piles.

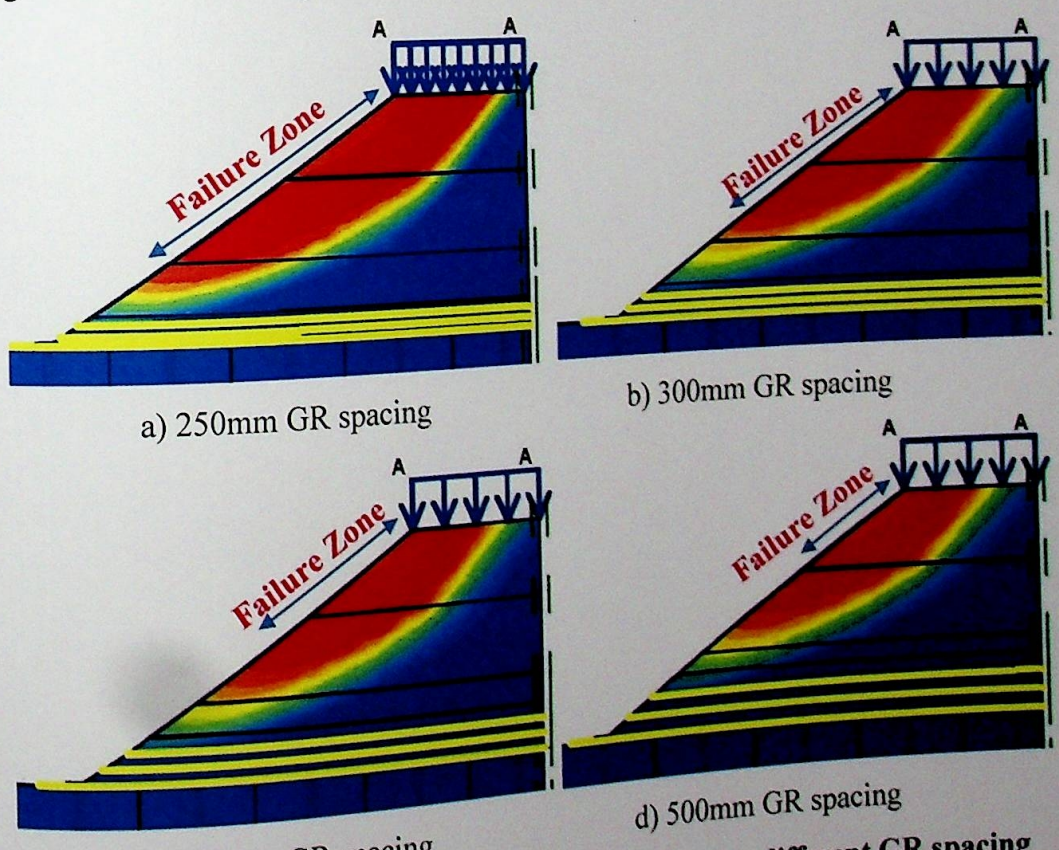

Figure 7.33. The failure modes of embankments having different GR spacing

Figure 7.33 a) to c) shows the variation of zone of failure with the increment of spacing between GR layers (the yellow strips represent the GR layers). The failure region reduces gradually explaining the reasons for increment of FOS with the increase of GR spacing.

8. CONCLUSIONS AND RECOMMENDATIONS

8.1. Conclusions

- By using GRPS Embankment system the differential settlement, lateral moment can be reduced while increasing the slope stability is increased. Reduction of construction time is another advantage over other ground improvement methods.
- Road embankment construction over soft ground, Bridge approaches, Retaining walls and Widening of roads over soft soil are some of the common application of GRPS embankments in Sri Lanka.
- The main aims of this study can be listed as below.
    - Development of finite element models in Plaxis 2D and compare the results with BS8006 and German Draft Standard (EBGEO).
    - Development of graphs for the behavior of Axial load of piles, Maximum SF & BM of piles, Maximum tensile force in the geo reinforcement layers and overall settlement of the embankment due to changes of various factors like pile size, pile spacing, embankment height, number of GR layers, spacing between GR layers and surcharge load etc.
- The finite element study shows that factors like tensile stiffness of the geogrid, the pile Area, the height of the embankment, the position of the geogrid and the properties of the embankment fill affect the GRPS system significantly. However, these effects are not always considered by the other available methods.
- It is very difficult to find an analytical method to evaluate the lateral moment of reinforcement embankments. Chapter 2 of this report discuss some methods used for unreinforced piled embankments. However, focus in this report is on two design procedures for reinforcement embankment on piles namely BS8006 and EBGEO and compare the results with PLAXIS 8.2.
- The Plaxis 8.2 program is equipped with facilities to model several interacting mechanisms in the GRPS system. The stresses and displacement of any point of the system can be evaluated using this finite program. The impact on tensile force in geogrid due to soil resistance provide by the underlying soil can be evaluated. The lateral deformation of piles can be easily studied.

- For the analysis of slope stability, the BS8006 recommend the Bishop Circle method. This method can handle short term stability analysis considering pore water pressures and performing an Undrained analysis. For evaluation of slope stability of a homogenous soil, the friction circle method was found most convenient. However, this method also does not consider the geosynthetic reinforcement.
- According to the Standard Deviation Tables for case 1 and case 2 show that EBGEO gives calculation results that agree best with our Plaxis- 2D calculations
- When compare the currently available methods for analysis of GRPS embankments, the numerical analysis is more reliable. This method considers the effect of numerous variables like the tensile stiffness of the geosynthetic, the pile modulus and the change in height of the embankment on the stress concentration ratio which is neglected by all other methods. The tension in geosynthetic reinforcement in a multi-layer reinforced fill can only be calculated using this method.
- According to the Plain strain model analysis the following conclusions can be derived. These conclusions were made considering optimum combination of axial loads, SF, BM, Tension in GR, Settlement of embankment and FOS of embankment.
    - The most efficient pile size is 350mmx350mm
    - Recommended pile spacing is 3.0 m
    - Efficient GR layer spacing is 300 mm

8.2. Recommendations

- The available methods for analyzing the lateral movement can be used only for non-reinforced embankments. Therefore, it is necessary to develop a method to estimate the lateral moment of GRPS embankments.
- The available methods, BS 8006, EBGEO or any other method does not provide a way to calculate the effect of the resistance provide by the underlying soft soil during the calculation of tension in GR layers. Therefore, more research is required in that area.

UNIVERSITY OF MORATUWA LIBRARY

- A method is needed to be developed to evaluate a multi-layer geo-reinforced embankments.
- A method is needed to be developed for the prior estimation of maximum and differential settlements of the embankment.
- The bending moments of the piles that are generated using the finite element analysis needed to be verified with field data.
- Furthermore, Plaxis calculations are relatively time consuming. It is therefore necessary to have a quick analytical design procedure, at least for the first design calculations for a pile embankment.
- This research shows that EBGEO gives calculation results that agree best with our Plaxis- 2D calculations. According to the Standard Deviation Tables for case 1 and case 2 show that EBGEO gives calculation results that agree best with our Plaxis- 2D calculations.

It is therefore recommended to use this EBGEO design procedure for the first design of a piled embankment. For detail design, Plaxis can be used to check the EBGEO calculations and to calculate the horizontal load on the piles and to check the slope stability of the embankments.

UNIVERSITY OF MORATUWA
LIBRARY

9. APPENDIX 1

9.1. Calculation Example for BS8006 (Friction Pile and End Bearing Pile) and EBGEO.

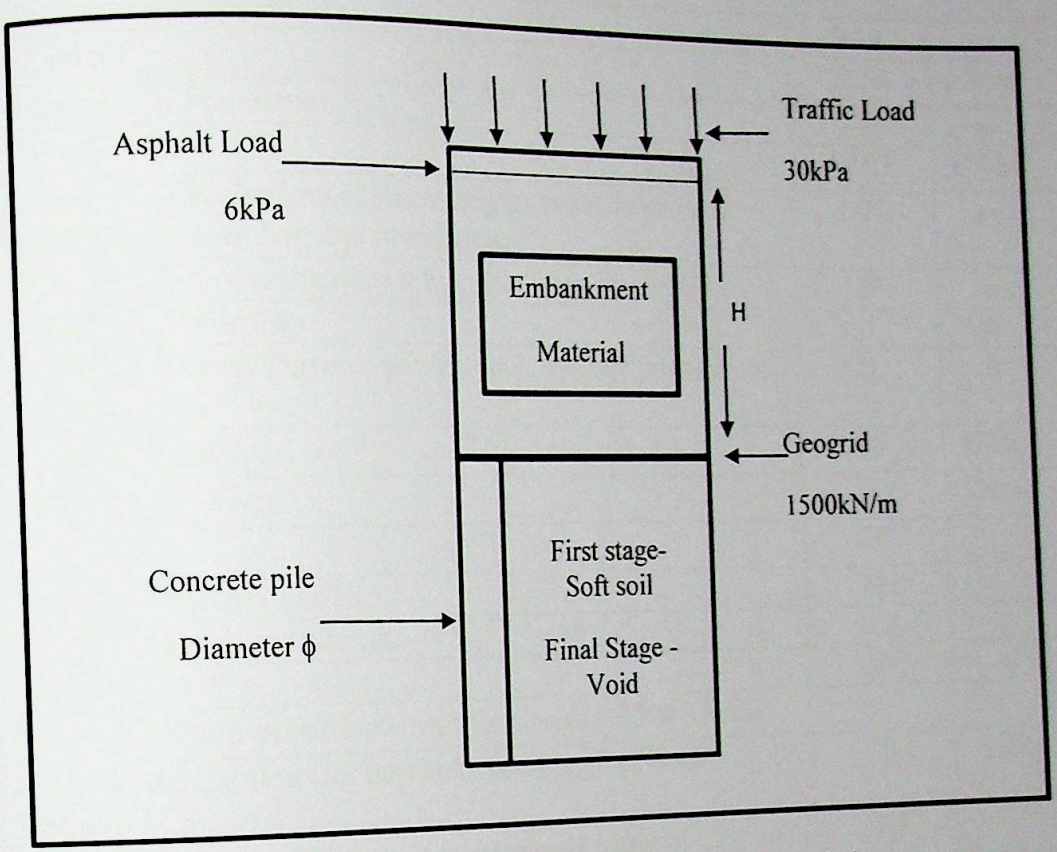

Case1 (Thin Embankment) H=1.25m, Pile Diameter ø =0.5m
Case2 (Thick Embankment) H=6.00m, Pile Diameter ø =0.3m

Figure 9.1 ,Case 1 & 2 Thin and thick Embankment

9.2. BS8006-Friction Pile (KLEEF).

9.2.1. Specimen Calculation

9.2.1.1. Input

Thickness of Asphalt	0.10	m
γ Asphalt	22.56	kN/m^3
Thickness of Foundation	0.21	m
γ Foundation	17.83	kN/m^3
Thickness of Embankment above heights possible phreatic line(Excluding asphalt and foundation)	1.25	m
Thickness part of embankment below heights possible line	0	m
Thickness of Pile Cap	0	m
Z vertical distance between pile cap and (average position) of reinforcement.	0	m
γ Embankment dry.	20	kN/m^3
γ Embankment wet	20	kN/m^3
γ Pile	26	
Pile Cap Circular (Yes/No)	Yes	
Diameter of circular pile cap	0.5	m
Traffic Load P	30	kPa
ζ allowed Strain in reinforcement for Geogrid 1500 KN/m		
Undrained Cohesion (for determination length of slope BS8006) C_u	10	kPa
ϕ'_{cv} angle of internal friction of embankment material	37.5	0
ϕ angle of internal friction of soft soil below embankment.	49.0	0
Assumption of height of area in which the traffic load spread , default 0.5m	0.31	m
Centre to Centre distance piles, δ_x in direction of road axis	1.750	m
Centre to Centre distance piles, δ_y in direction of road axis	1.750	m
Will the Soft soil give support (Yes/No)	No	
Slope of Embankment 1:x	1:5	
Piles are End-Bearing or Friction	Friction	
Calculate with partial factors	No	
Are the piles in square pattern	Yes	
Modulus of sub grade reaction	50	KN/m^3
ζ fracture strain in reinforcement in ultimate limit state	0.12	
Long term strain stiffness of reinforcement in direction of road axis	1500	KN/m
Long term strain stiffness of reinforcement in direction of road axis	4500	KN/m

Table 9-1 BS8006- Friction File (British Standard) Specimen Calculation

UNIVERSITY OF MORATUWA LIBRARY SRI LANKA

9.2.1.2.Summary of equations from BS8006

Parameter	Unit	BS8006 2D approach	BS8006 3D interpretation load on reinforcement*	BS8006 fully 3D**
Load division				
total load on area s*s	kPa	$\sigma'_v = \gamma H + p$		
	kN	$\sigma'_v s^2 = (\gamma H + p)s^2$		
load part directly on piles	kPa	$p'_c = \left(\frac{C_c a}{H}\right)^2 \sigma'_v$		
	kN	$w_c = p'_c a^2$		
Vert. line-load W_T, due to p'_r, on strip geotextile reinforcement between two adjacent pile caps.	kN/m	$W_T = s(\gamma H + p)X$****		$W_T = 0.5(\gamma H + p)\big((s + a)\big)X$
Load part carried by geosynthetic	kPa	$p'_r = \frac{W_T}{s} = (\gamma H + p)X$	$p'_r = \frac{2W_T}{s+a} = \frac{2s(\gamma H + p)}{s+a}X$	$p'_r = \frac{2W_T}{s+a} = (\gamma H + p)X$
	kN	$w_r = p'_r(s^2 - a^2) = (s^2 - a^2)(\gamma H + p)X$	$w_r = p'_r(s^2 - a^2) = (s^2 - a^2)(\gamma H + p)X$	$= (s^2 - a^2)(\gamma H + p)X$
Calculated tensile stress in geotextile reinforcement				
Tensile stress T_{rp} in Geotextile reinforcement	kN/m	$T_{rp} = \frac{W_T(s-a)}{2a}\sqrt{1 + \frac{1}{6\varepsilon}}$		
Calculation factors for comparison with other literature resources				
$E = \frac{w_c}{\sigma'_v s^2} = \frac{p'_c a^2}{\sigma'_v s^2}$	kN/kN	$E = \left(\frac{C_c a}{H}\right)^2 \frac{a^2}{s^2}$		
$1 - E = \frac{w_r}{\sigma'_v s^2} = \frac{p'_r(s^2 - a^2)}{\sigma'_v s^2}$	kN/kN	$1 - E = \frac{(s^2 - a^2)}{s^2}X$ *E+(1-E) = 1*	$1 - E = \frac{2(s-a)}{s}X$ $E + (1 - E) \neq 1$****	$1 - E = \frac{(s^2 - a^2)}{s^2}X$ *E+(1-E) = 1*
Stress Reduction Ratio $SSR = \frac{p'_r}{\sigma'_v}$	kPa/kPa	*X*	$\left(\frac{2s}{s+a}\right)X$****	*X*

* In agreement with Love & Milligan (2008), Stewart (2005) and Russel & Pierpoint (1997)

** Adapted BS 8006

*** Where $X = \frac{s^2 - a^2\left(\frac{C_c a}{H}\right)^2}{s^2 - a^2}$

**** No vertical equilibrium

9.2.1.3.Calculation:

I. Average γ embankment.(BS does not distinguish γ_{wet} and γ_{dry})	=	$(\gamma_{wet} + \gamma_{dry})/2$	20	KN/m³
II. Pile cap is Circular. Therefore BS8006 calculate with square pile capes with equivalent side (a)	=	$\sqrt{\pi} \times \frac{0.5}{2}$	=0.44	m
III. Height of Embankment (H)	=		1.250	m
IV. Centre to Centre distance (s)	=		1.750	m
V. Traffic Load	=		30	KPa
VI. Maximal Vertical settlement between pile caps (Chain rule)	=	(6-0.56)x3xε/8	0.15	m

Table 9-2 Calculation Table1 BS8006 Friction Pile

Influence of Vertical Load

VII. Average vertical stress below embankment due to weight and traffic load ($\sigma'_v = \gamma H + p$)	=	(20x1.25) + (6+3)	61	kPa
VIII. Total weight and traffic load on 1.75m grid surface ($p'_v = \sigma'_v s^2$)	=	61x1.75x1.75	186.82	kN
IX. Arching coefficient conform BS8006, table 28, page 106: distinguish end-bearing piles and friction piles ($C_c = 1.5H/a - 0.07$)	=	$1.5x\frac{1.25}{0.44} - 0.07$	4.16	
X. Vertical Stress on the pile Cap $[p'_c = (C_c a/H)^2 \sigma'_v]$	=	$61x(4.16x0.44/1.25)^2$	132.75	kN/ m²
XI. Vertical Force on the pile cap ($w_c = p'_c a^2$)	=	$132.75x0.44^2$	**26.06**	kN
XII. Vertical force on the reinforcement	=	$61x1.75^2$ -26.0	160.75	kN

Table 9-3 Calculation Table2 BS8006 Friction Pile

XIII. Average vertical load on reinforcement between two adjacent pile caps

$$W_T = \frac{1.75 \times 1 \times 20 \times 1.25 + 1 \times (30 + 6)\left[1.75^2 - 0.44^2\left(\frac{132.75}{61}\right)\right]}{1.75^2 - 0.44^2} = 98.15 kN/m$$

XIV. Stiffness of reinforcement = 1500 kN/m

XV. Strain in reinforcement ε = 0.1422

XVI. Tension stress in reinforcement due to vertical load

$$T_{rp} = \frac{98.15 \times (1.75 - 0.44)}{2 \times 0.44} \sqrt{1 + \frac{1}{6\varepsilon}} = 213.32\ kN/m$$

9.2.1.4. Results. (BS8006-Friction File)

Embankment Height	Force on the Pile Cap (kN)	Tensile Force on the Geogrid parallel to Road Axis (kN/m) Geogrid EA=1500 kN/m
1.25	26.06	213.32
1.50	28.36	226.86
1.75	30.63	240.26
2.00	32.89	143.49
2.25	35.13	143.44
2.50	37.37	143.40
2.75	39.60	143.37
3.00	41.83	143.37
3.25	44.05	143.34
3.50	46.28	143.32
3.75	48.50	143.30
4.00	50.72	143.29
4.25	52.94	143.28
4.50	55.15	143.27
4.75	57.37	143.26
5.00	59.59	143.25
5.25	61.80	143.25
5.50	64.02	143.24
5.75	66.23	143.23
6.00	68.44	143.23

Table 9-4 Result BS8006 Friction Pile

9.3. BS8006-End Bearing (STUIT).

9.3.1. Specimen Calculation.

9.3.1.1. Input.

Piles are End-Bearing or Friction?	End Bearing

9.3.1.2. Calculation:

XVII. Average J embankment. (BS does not distinguish γ_{wet} and γ_{dry})	=	$(\gamma_{wet} + \gamma_{dry})/2$	20	kN/m^3
XVIII. Pile cap is Circular. Therefore BS8006 calculate with square pile capes with equivalent side	=	$\sqrt{\pi} \times \frac{0.5}{2}$	0.44	m
XIX. Height of Embankment (H)	=		6	m
XX. Centre to Centre distance	=		1.75	m
XXI. Traffic Load	=		30	kPa
XXII. Maximal Vertical settlement between pile caps (Chain rule)	=	$(6 - 0.56) \times 3 \times \frac{\varepsilon}{8}$	0.15	m

Table 9-5 Calculation Table 1 End Bearing Pile

Influence of Vertical Load

XXIII. Average vertical stress below embankment due to weight and traffic load (σ'_v)	=	(1.25x6)+6+30	61	kPa
XXIV. Total weight and traffic load on 1.75m grid surface	=	61x1.75x1.75	186.82	kN
XXV. Arching coefficient conform BS8006, table 28, page 106: distinguish end-bearing piles and friction piles (C_c)	=	$1.95x\frac{1.25}{0.44} - 0.18$	5.32	
XXVI. Vertical Stress on the pile Cap	=	$61 \times \left(5.32 \times \frac{0.44}{1.25}\right)^2$	217.02	kN/m^2
XXVII Vertical Force on the pile cap .	=	132.75x0.44^2	**42.61**	kN
XVIII. Vertical force on the reinforcement	=	61x1.75^2 -42.61	144.2	kN

Table 9-6 Calculation Table 2 End Bearing Pile

XXIX. Average vertical load on reinforcement between two adjacent pile caps

$$W_T = \frac{1.75 \times 1 \times 20 \times 1.25 + 1 \times (30+6)\left[1.75^2 - 0.44^2\left(\frac{144.20}{61}\right)\right]}{1.75^2 - 0.44^2} = 88.05 kN/m$$

XIV. Stiffness of reinforcement = 1500 kN/m

XV. Strain in reinforcement ε = 0.1306

XVI. Tension stress in reinforcement due to vertical load

$$T_{rp} = \frac{88.15 \times (1.75 - 0.44)}{2 \times 0.44}\sqrt{1 + \frac{1}{6\varepsilon}} = 195.89\ kN/m$$

9.3.1.2. Results- End Bearing (STUIT)

Embankment Height	Force on the Pile Cap (kN)	Tensile Force on the Geogrid parallel to Road Axis (kN/m) Geogrid EA=1500 kN/m
1.25	42.61	195.89
1.50	46.63	207.81
1.75	50.56	219.69
2.00	54.45	131.62
2.25	58.30	131.48
2.50	62.13	131.36
2.75	65.94	131.28
3.00	69.74	131.21
3.25	73.52	131.12
3.50	77.30	131.07
3.75	81.08	131.03
4.00	84.85	130.98
4.25	88.61	130.94
4.50	92.37	130.92
4.75	96.13	130.88
5.00	99.89	130.85
5.25	103.64	130.83
5.50	107.39	130.81
5.75	111.14	130.78
6.00	114.89	130.76

Table 9-7 Results End Bearing pile

9.4. EBGEO Specimen Calculation

9.4.1. Specimen Calculation

9.4.1.1. Input

Same input as for section **9.3.**

9.4.1.2. Calculation

Starting points	Source: EBGEO	symbol in EBGEO	unit	
Circular pile cap, EBGEO calculates with the diameter	6.9-1	$d = d_{Ers} = \sqrt{4A_s/\pi}$	m	0.500
Height embankment above pile cap		H	m	1.250
C.t.c. distance between adjacent piles // to road axis		S_x	m	1.750
C.t.c. distance between adjacent piles perpendicular on road axis		S_y	m	1.750
C.t.c. distance piles according to EBGEO (diagonal)	Pg 6	$S = \sqrt{S_x^2 + S_y^2}$	m	2.475
height arch	6.9.6.3.2 Pg 13	$h_g = S/2 \; for \; h \geq S/2$ $h_g = h \; for \; h < S/2$	m	1.237
Critical major stress ratio of the embankment material	6.9-5c	$K_{krit} = \tan^2[45^0 + \emptyset' k/2]$	-	4.112
ϕ_{cv} characteristic angle of internal friction of the embankment (partial factor is applied on tan ϕ)		ϕ_k'	°	37.5
specific weight * part factor		γ_k	kN/m³	20.00
Traffic load * part factor		P_w	kN/m²	30.00
Surcharge load of asphalt plus foundation, with factor			kPa	6.00
calculation parameter	6.9-5e	$\lambda_1 = \frac{1}{8}.(s-d)^2$	-	0.488
calculation parameter	6.9-5f	$\lambda_2 = \frac{s^2 + 2.d.s - d^2}{2.s^2}$	-	0.682
calculation parameter	6.9-5d	$x = \frac{d.(K_{krit} - 1)}{\lambda_2.s}$	-	0.922

UNIVERSITY OF MORATUWA LIBRARY SRI LANKA

load distribution in reinforced embankment				
Load on reinforcement between piles due to vertical load				
Characteristic value of the load due to static load	6.9-5a Pg 12	$\sigma_{z0,G,k}$	kN/m²	20.775
Characteristic value of the load due to static and dynamic load	6.9-5b, Pg 12	$\sigma_{z0,G+Q,K}$	kN/m²	40.879
Load on piles due to vertical load				
Surface of influence = Sx * Sy		A_E	m²	3.063
Area pile = $0.25*\pi*d^2$		A_S	m²	0.196
Characteristic load on piles $\sigma_{zs,Gk}$ due to vertical static load	6.9-6a, Pg 18	$\sigma_{zs,G,k}$	kN/m²	180.277
Characteristic load on piles $\sigma_{zs,G+Qk}$ due to vertical static and dynamic loads	6.9-6b, Pg 18	$\sigma_{zs,G+Q,k}$	kN/m²	354.729
Characteristic load on piles $\sigma_{zs,Gk}$ due to vertical static load	6.9-6a, Pg 18	$\sigma_{zs,G,k} \cdot A_S$	kN	35.397
Characteristic load on piles $\sigma_{zs,G+Qk}$ due to vertical static and dynamic loads	6.9-6b, Pg 18	$\sigma_{zs,G+Q,k} * A_S$	kN	69.651

Table 9-8 German Draft Standard (EBEGO) Calculation.

Tensile Force on the Geogrid

Characteristic load in reinforcement				**x direction (// road axis)**
Modulus of subgrade reaction (= Es/tw, is zero when sub soil is not supporting, see sheet "invoer" B25)	6.9-11a	$k_s = \frac{E_{s,k}}{t_w}$	kN/m³	0.00
Long term strain stiffness reinforcement in direction of road axis for 4.5 % strain		$J_{x,t}$ en $J_{y,t}$	kN/m'	1500.00
Equivalent side of pile cap	6.9-9	$b_{Ers} = \frac{1}{2}d.\sqrt{\pi}$	m	0.443

Equivalent length between pile caps	At the bottom of Pg 19	$L_{w,x} = (S_x - b_{Ers.})$ $L_{w,y} = (S_x - b_{Ers.})$	m	1.307
Load surfaces	Pg 20	ALx or ALy	m^2	1.433
Loads due to static loads				
Resulting load on reinforcement piece with width $b_{ErS} = A_{Lx} * \sigma_{zo,G,k}$	Pg 20	$F_{x,(G+Q),k}$ or $F_{y,(G+Q),k}$	kN/m'	58.583
Determination of maximal strain				
Calculation factor $K_{s,k} * L^2_{w,x}/J_{x,\ long\ term}$	fig 6.9-10		-	0.00
Calculation factor $(F_{x,G,k}/b_{Ers.})/J_{x,long\ term}$	fig 6.9-10		-	0.08814
read from figure 6.9-10: maximal strain	fig 6.9-10	$\zeta_{x,(G+Q),k}$ $\zeta_{y,(G+Q),k}$	%	***8.6330***
Determination tension forces (with membrane rule)				
Tension force from membrane phenomenon = max $\zeta_{x,G,k} * J_{x,long\ term}$	fig 6.9-10	$E_{M,(G+Q),k}$	kN/m'	129.496
Load due to spread forces (lateral load)				
Active soil pressure – coefficient according to DIN 4085 (is identical to BS8006 is $\tan^2(45° - \phi'_{cv}/2)$)	DIN 4085	K_{agh}	-	
spread force	6.9-12	$E_{(G+Q),k}$	kN/m'	
Total load in reinforcement		**max Ex,g,k or max Ey,G,k**	kN/m'	**129.496**

Table 9-9 EBGEO Calculation Tensile Force on the Geogrid Results.-EBGEO

LIBRARY
UNIVERSITY OF MORATUWA, SRI LANKA
MORATUWA

9.4.1.3. EBGEO Results

Embankment Height	Force on the Pile Cap (kN)	Tensile Force on the Geogrid parallel to Road Axis (kN/m) Geogrid EA=1500 kN/m
1.25	69.65	129.50
1.50	85.52	129.05
1.75	99.80	129.87
2.00	113.10	131.49
2.25	125.73	133.73
2.50	137.90	136.36
2.75	149.74	139.27
3.00	161.33	142.39
3.25	172.72	145.67
3.50	183.96	149.05
3.75	195.07	152.44
4.00	206.09	155.91
4.25	217.03	159.45
4.50	227.90	163.05
4.75	238.71	166.67
5.00	249.47	170.32
5.25	260.20	174.01
5.50	270.88	177.72
5.75	281.54	181.46
6.00	292.16	185.21

Table 9-10 Results From EBGEO

109272

9.5. PLAXIS 8.2

9.5.1. Specimen Calculation

9.5.1.1. Input (see chapter 5)

9.5.1.2. Results.-Plaxis 8.2

Embankment Height	Force on the Pile Cap (kN)	Tensile Force on the Geogrid parallel to Road Axis (kN/m) Geogrid EA=1500 kN/m
1.25	102.73	87.53
2.00	135.18	97.06
3.00	175.67	110.85
4.00	218.04	122.80
5.00	255.36	134.35
6.00	290.71	146.58

Table 9-11 Results Plaxis 8.2

10. APPENDIX 2 – STRUCTURAL DESIGN OF A PILE

10.1. Code requirements

This chapter discuss an example for Structural design of a reinforced concrete pile. The design of a pile is discussed in several codes and the proposed requirements for the design are varies in each code. Table 10.1 summarizes the requirements of BS 8004, BS 5400 – P 4 and BS 8110.

At present, specific references in UK codes to the design of reinforcement in piles is limited to two documents, BS 8004:1986 "Foundations" and BD 32/88 "Piled Foundations". A summary of the requirements of these codes is given below:

i. BS 8004: 1986 "Foundations"

a) Vertical piles which are axially loaded need not be designed as structural columns unless part of the pile extends above ground level (Cl7.3.3.3). For this latter case, only the upper portion of the pile need be considered as a column down to a point of fixity.

b) All forces acting on the pile are to be determined and the pile reinforced accordingly (Cl7.3.3.4, Cl 7.3.3.6, and Cl7.4.4.3.2). Some or all of the pile length may be unreinforced (Cl 7.4.4.3.2). Pre-cast concrete piles are to be designed to BS 8110 (or CP 116).

c) Where tensile forces are to be resisted by the pile, adequate reinforcement is required to resist the entire tension stresses. The reinforcement should be provided for the full length of the pile or where tensile forces are small, to a depth at which the tensile forces have been fully transmitted to the ground (Cl 7.3.3.7 and Cl 7.4.5.3.2).

d) Minimum spacing of links is given as 150mm (Cl 7.4.4.4.2).

e) For raking piles, loads may be considered as axial with an applied bending force at the top (Cl 7.3.3.5).

f) Durability and protection of reinforcement against corrosion is provided by dense impermeable concrete free from defects (Cl10.4.7). Nominal cover for various exposure conditions should be as BS 8110.

ii. Standard BD 32/88: 1988 "Piled Foundations"

a) This standard applies to both the design of driven and bored piles (Cl 2.1).

b) Pile caps are to be designed to BS 8004 but Cl 3.1 states that the structural design of all concrete elements of the pile is to be to BS 5400 Pt 4.

BS 8110 states that embedded piles need not be designed as columns and piles carrying axial load only need not be reinforced. Some rules are provided regarding calculation of axial forces which may be accommodated without reinforcement but no guidance is given on calculation of shear capacity. Where reinforcement is required, BS 8110 is mentioned for design but is not specifically invoked, except for pre-cast piles. No guidance is given for curtailment of longitudinal steel.

Code/Standard (Date)	Cover to Reinforcement	Longitudinal Reinforcement				Transverse Reinforcement		Crack Control Max Crack Width
		Min. No	Min. Dia.	Max. Spacing	Min %	Max. Spacing	Min. Diameter	
BS 8110 Pt 1 (1985)	75mm (Concrete cast against ground)	4 (Rectangular) 6 (Circular)	12mm	-	Tension 0.8% (Steel) 0.45% (high yield)	12 times Smallest Main bar size	$\frac{1}{4}$ times Largest main Bar size or 6mm	Only checked if $N < 0.2 f_{cu} A_c$ Then max. width = 0.3mm
BS 5400 Pt 1 (1990)	45mm (Buried C30 Concrete)	4 (Rectangular) 6 (Circular)	12mm	300mm	1% or $0.15 N_{fy}$	12 times Smallest Main bar Or 0.74 times effective depth	$\frac{1}{4}$ times Largest main Bar size	0.25mm (Buried concrete) 0.1mm if groundwater pH < 4.5
BS 8004	As BS8110 But add 40mm for concrete cast against ground	----------As BS 8110----------				--------As BS 8110-----		Not mentioned

Table. 10-1 Summary of Code Requirements (Page 123 and Page 124)

UNIVERSITY OF MORATUWA LIBRARY SRI LANKA

Code/Standard (Date)	Permissible Stresses		Maximum Axial Load	
	Concrete	Steel	Without Reinforcement	With Reinforcement
BS 8110 Pt 1 (1985)	Compression $0.67\frac{f_{cu}}{\gamma_m}$ Shear $V_c + 0.6\frac{N.V.h}{A_c.M}$	f_y/γ_m (Tension & Compression)	$0.4\ f_{cu}.A_c$	$0.4\ f_{cu}.A_c + 0.75\ A_{sc}.f_y$
BS 5400 Pt 4 (1990)	Compression $0.67\frac{f_{cu}}{\gamma_m}$ Shear $0.5.\ f_{cu}$ (Triangular Stress Distribution) $0.38\ f_{cu}$ (Uniform Stress Distribution)	Compression $f_y\ /\ (\gamma_m + f_y/2000)$ Tension f_y/γ_m	$0.4\ f_{cu}.\ b.\ d_c$	$0.4\ f_{cu}.\ b.\ d_c + f_{yc}.\ A'_{s1} + f_{s2}.\ A_{s2}$
BS 8004 (1986)	As BS 8110	As BS 8110	As BS 8110	As BS 8110

A_c - area of concrete
A'_{s1} - area of compression
A_{s2} - area of r/f. in other face
A_{sc} – area of vertical reinf. material
b – width of section
d_c – depth of concrete in compression
f_{cu} – characteristic concrete cube strength
f_{s2} - stress in reinf. in other face
f_y - characteristic strength of reinforcement
h – overall depth of section
M – applied design moment
N - applied designed axial load
V – applied design shear
v_c - design concrete shear stress
γ_m - partial safety factor for strength of

Global Reinforcement Design Requirements	BS8004	BS8110	BD 32/88 (BS5400 Pt 4)
o Axial Compression	No guidance Refer to BS 8110	Detailed design rules for structural design (See Table 3.1.1)	Detailed design rules for structural design (See Table 3.1.1)
o Axial Tension	General guidance given on length of pile to be reinforced	- do-	- do-
o Flexure	No guidance Refer to BS 8110	- do-	- do-
o Shear	No guidance Refer to BS 8110	- do-	- do-
o Buckling	Check for Buckling if $C_0 < 20kN/m^2$	No checks required	No checks required
Rules for: o Minimum Reinforcement	No minimum reinforcement required	- do-	- do-
o Links	Minimum spacing 150mm	- do-	- do-
o Calculation of Rebar	Refer to BS8110. Only upper part of pile above ground level to be designed as a column	- do-	- do-
o Cover	As BS8110 plus 40mm	75mm (Concrete cast against ground)	45mm max +40mm in accordance with BS8004 cl 2.4.5
o Crack Control	Not mentioned	Only required for $N<0.2f_{cu}$	0.1mm to 0.25mm depending on exposure conditions
o Durability	Some guidance given	Detailed requirements for concrete design and nominal cover to reinforcement	Detailed requirements for concrete design and nominal cover to reinforcement

Table 10-2: Summary of Current UK Design Codes

This page left intentionally blank.

11. List of References.

1. *Eekelen, Suzanne Van & Bezuyen, Adam (2008a), design of piled embankments, considering the basic starting point of the British Standrad BS8006, to be published in the proceeding of Euro geo 4, September 2008, Edinbourge, paper number 315*
2. *Eekelen, Suzanne Van & Bezuyen, Adam (2008b), Piled embankments in the Netherlands , a full scale test comparing two year of measermunts with design calculations, to be published in the proceedings of Euro geo 4 September 2008, Edinbourgh, Paper Number 264*
3. *Eekelen, Suzanne Van, J M Van, Van, Meindest A , Bezuyen Adam, The Kyotoroad , a full scale test, measurement and calculations, proceeding of ECSMGE, September 2007, Midid , Paper Number 1533-1538*
4. *Geoynthetic Reinforced Pile Supported Embankments by Rutugandha Gangakhedkar, The University of Florida 2004*
5. *Alzamora, D., Wayne, M.H., and Han, J. (2000). "Performance of SRW supported by Geogrids and Jet Grout Columns." Proceedings of sessions of ASCE SpecialtyConference, Amherst, Geotechnical Special Publication No. 94, edited by A.J. Lutenegger and D.J. DeGroot, ASCE, 456-466.*
6. *Brinkgreve, R. B. J., and Vermeer, P.A. (1998). Plaxis - Finite Element Code for Soil And Rock Analysis - Version 7, A.A. Balkema Publishers, Netherlands.*
7. *British Standard 8006 (1995). Design of Embankments with Reinforced Soil Foundations on Poor Ground.* ***Section 8:*** *122-150.*
8. *Gutter, H. H. (2002). "AuGeo Piled Embankment with Fortrac Geogrids Railway Track Rawang -IPOH." OMEGAM Environmental Research Institute, Amsterdam.*
9. *Han, J. (1999). "Design and Construction of Embankments on Geosynthetic Reinforced Platforms Supported by Piles." Invited Speaker, Proceedings, 1999 ASCE/PaDOT Geotechnical Seminar, Hershey, PA.*
10. *Han, J. (2003). "Development of Design Charts for Geosynthetically Reinforced Embankments on Deep Mixed Columns." Interim Report,*

Literature Review, Principal Investigator, funded by the FHWA National Deep Mixing Program, 2002-2003, Widener University, Chester, PA.

11. *Han, J., and Akins, K. (2002). "Use of Geogrid Reinforced and Pile-Supported Earth Structures." Proceedings, International Deep Foundations Congress 2002, Orlando, Geotechnical Special Publication No. 116, edited by O'Neill and Towsend, ASCE, 668-679.*
12. *Han, J., and Gabr, M.A. (2002). "Numerical Analysis of Geosynthetic-Reinforced and Pile- Supported Earth Platforms over Soft Soil." Journal of Geotechnical and Geoenvironmental Engineering, ASCE, 128(1), 44-53.*
13. *Han, J., and Wayne, M.H "Pile-Soil-Geosynthetic Interactions in Geosynthetic Reinforced/Piled Embankments over Soft Soil." Presentation and CD-Rom Paper at 79th Annual TRB meeting.*
14. *Hueng, W., Kuo, C.L.,and Roberts, J. (1998). "Surcharge of Phosphatic Waste Clay with Strip Drains." Proceedings of the Conference American Society of Civil Engineers, Boston, Massachusetts, Geotechnical Special Publication No. 81, edited by A. Maher and D.S. Yang, ASCE, 298-312.*
15. *Kuo, C. L., Heung, W., Tejidor, F.J.,and Roberts, J. (1998). "A Case Study of Timber Pile in-situ soil reinforcement." Proceedings of the Conference American Society of Civil Engineers, Boston, Massachusetts, Geotechnical Special Publication No. 81, edited by A. Maher and D.S. Yang, ASCE, 177-189.*
16. *Li, Y., Aubeny, C., and Briaud, J. (2002). "Geosynthetic Reinforced Pile Supported Embakments." Draft submitted to FHWA, Texas A & M University, College Station.*
17. *Ostensen, A. K., and Bennett, K.D (2002). Geotechnical Report for Slope Stability Repair Concepts. Williams Earth Sciences, Inc., Polk County, Florida.* **1**

UNIVERSITY OF MORATUWA - SRI LANKA * LIBRARY *
RECEIVED
16 SEP 2015
AQ - SECTION

LIBRARY	UOM
20	
20	
20	
20	
20	